Università di Napoli Federico II

Dipartimento di Ingegneria Industriale

Doctorate Thesis

OPTIMAL OPERATION PLANNING OF DISTRIBUTED ENERGY SYSTEMS THROUGH MULTI-OBJECTIVE APPROACH: A NEW SUSTAINABILITY-ORIENTED PATHWAY

Marialaura Di Somma

Tutors

Prof. Nicola Bianco

Dr. Giorgio Graditi - ENEA

March 2016

Università di Napoli Federico II

School of Doctorate in Industrial Engineering

Research Doctorate Program in Mechanical Systems Engineering

XXVIII Cycle

Doctorate Thesis

OPTIMAL OPERATION PLANNING OF DISTRIBUTED ENERGY SYSTEMS THROUGH MULTI-OBJECTIVE APPROACH: A NEW SUSTAINABILITY-ORIENTED PATHWAY

School of Doctorate Coordinator

Prof. Antonio Moccia

Doctorate Program Coordinator

Prof. Fabio Bozza

Tutors

Prof. Nicola Bianco

Dr Giorgio Graditi - ENEA

Candidate

Marialaura Di Somma

To the memory of my father, Antonio.

To the memory of my grandparents, Rita and Raimondo,
two wonderful mentors.

To my mother, Anna, and my sister, Annarita, for their precious support.

And to those who have helped and supported me in any way throughout my education and professional life.

Contents

Acknowledgements

I am most grateful to:

- The institutions where my educational pathway took place, that are the *Dipartimento di Ingegneria Industriale* (*DII*) of the *Università degli Studi di Napoli Federico II*, and the *ENEA Research Center of Portici*.
- The *Department of Electrical and Computer Engineering of University of Connecticut* (USA), where I spent six months as visiting research assistant.
- *Prof. Peter B. Luh* of the Department of Electrical and Computer Engineering of the University of Connecticut to have had the opportunity and the honor to work with him and his research group in the field of optimization of complex energy systems.
- *Dr. Luigi Mongibello* of the ENEA RC Portici, for his precious contribution on my research activity carried out during the doctorate program.
- *Dr. Bing Yan* of the Department of Electrical and Computer Engineering of University of Connecticut for her essential contribution on developing the optimization models, implementing them in CPLEX, and writing "good papers", by always trying to tell a "good story".

Special thanks to my tutors, *Prof. Nicola Bianco* (DII of the Università degli Studi di Napoli Federico II) and *Dr. Giorgio Graditi* (ENEA RC Portici), who gave me the opportunity to develop my doctorate project in these three years.

Finally, a special thank to *Prof. Vincenzo Naso* of the Dipartimento di Ingegneria Industriale of the Università degli Studi di Napoli Federico II. He has been a great source of knowledge and motivation, and his contribution has been a key element in my educational pathway since I was an undergraduate student.

List of Figures

List of Tables

Preface

The energy system is an essential part of nowadays society. The concept of "energy system" commonly refers to the energy-supply chain as the whole system consisting of the energy conversion devices as well as storage units from the energy resources to the final user demands. In the 1900's, energy has been commonly provided by large generation power plants operating in a central location and transmitted to consumers via transmission and distribution networks. In a typical centralized energy system, a large number of end-users is located within a large area.

A Distributed Energy System (DES) can be regarded as the opposite of a centralized energy system, where the term "distributed" illustrates how single energy conversion devices and storage units are integrated into the whole energy system. Therefore, a DES refers to an energy system, where energy is made available close to energy consumers, typically relying on a number of small-scale technologies. In recent years, developing DESs has attracted much interest, since these systems have been recognized as a sustainability-oriented alternative to conventional centralized energy systems. In general, sustainability means an equitable distribution of the limited resources and opportunities in the context of the economy, the society, and the environment, aiming at the well-being of everyone, now and in future, thereby guaranteeing that needs of future generations may be completely satisfied as happens today.

One of the main benefits of DESs is the possibility to integrate different energy resources, including renewable ones, as well as to recover waste heat from power generation plants for thermal purposes. This benefit allows to enhance sustainability of the energy supply through a more efficient use of the energy resources as well as a reduced environmental impact, as compared with conventional energy supply systems. Through an appropriate planning, DESs may exhibit even better performances than a single polygeneration system, such as Combined Cooling Heating and Power systems or conventional energy supply systems.

The optimal planning of DESs is not a trivial task, as integration of different types of energy resources and energy conversion devices as well as storage units may

increase the complexity of the system. Moreover, generally different stakeholders participate in DESs development and management. Hence, objectives can be defined from different perspectives, such as the developers and operators of DESs, or the civil society, ideally represented by the regulator. Some of the DESs planning objectives are naturally conflicting. Consequently, there is not a single planning solution, which can satisfy all the stakeholders. For instance, society interest in sustainable energy supply systems, and with low environmental impacts, might conflict with the economic interest of the developers and operators of DESs. A multi-objective approach helps to identify compromise solutions, which benefit all the stakeholders.

This thesis presents an original tool based on a mathematical programming approach, to attain the optimal operation planning of DESs through multi-objective criteria, by considering both short- and long-run priorities. Multi-objective optimization problems are formulated to find the optimized operation strategies of DESs in order to take into account short-run priorities characterized by the crucial economic factor, as well as long-run priorities in terms of sustainability. This latter is attained through exergy concepts as well as environmental impacts assessments.

Keywords: Distributed energy system, Multi-objective optimization, Mixed Integer Programming Problem, branch-and-cut, Surrogate Lagrangian Relaxation, energy costs, environmental impacts, exergy efficiency, exergy losses.

Marialaura Di Somma,
March 2016

Nomenclature

A	area (m^2)
$\dot{B}$	biomass mass flow rate (kg/h)
B_{cin}	carbon intensity of biomass (kg_{CO_2}/kWh)
c	scaling factor in objective functions
$\dot{C}$	cooling rate (kW)
COP	coefficient of performance
$Cost$	total energy cost ($) - (€)
c_p	specific heat (kJ/ (kg K))
d^k	stepsize at iteration k
DR	maximum ramp-down rate (kW)
ex_{bio}	specific chemical exergy of biomass (kWh/kg)
ex_{NG}	specific chemical exergy of natural gas (kWh/Nm^3)
$\dot{E}$	electricity rate (kW)
E_{cin}	carbon intensity of power grid (kg_{CO_2}/kWh)
Env	environmental impact (kg_{CO_2})
Ex	exergy (kJ)
$\dot{E}x$	exergy rate (kW)
$\dot{E}xloss$	exergy loss rate (kW)
$Exloss_{conv}$	total exergy loss at the energy conversion step (kJ)
f_i	i^{th} objective function
F_{obj}	objective function
F_q	Carnot factor
$\tilde{g}$	surrogate subgradient vectors
$\dot{G}$	natural gas volumetric flow rate (Nm^3/h)
$G(y)$	equality constraints in (2.1)
G_{cin}	carbon intensity of natural gas (kg_{CO_2}/kWh)
$\dot{H}$	heat rate (kW)
H	thermal energy (kWh)

$H(y)$	inequality constraints in (2.1)
$\dot{I}_T$	total solar irradiance (kW/m^2)
L	Lagrangian function
$\widetilde{L}$	surrogate dual value
LHV_{bio}	lower heat value of biomass (kWh/kg)
LHV_{NG}	lower heat value of gas (kWh/Nm^3)
$\dot{m}$	mass flow rate (kg/h)
m	mass (kg)
P_{bio}	biomass price ($/t)
P_{grid}	electricity price (€/kWh) - ($/kWh)
P_{NG}	natural gas price (€/Nm^3) - ($/Nm^3)
q	dual function
$\dot{Q}_{PM,ex}$	heat rate made available by the exhaust gas (kW)
R	generation level of the energy device (kW)
t	time (h)
T	temperature (K)
UR	maximum ramp-up rate (kW)
x	binary decision variable
y	all the decision variables

Greek symbols

Δt	length of the time interval (h)
ε	vector of constraints in (2.4)
ε_{gen}	exergy efficiency of electricity generation
ς	exergy factor
η	efficiency
λ	Lagrangian multipliers
μ_{PM}	percent heat loss rate of the prime mover
ξ	prime mover exhaust gas fraction
φ_{sto}	storage loss fraction
ψ	overall exergy efficiency

ω	weight in the objective functions
Ω	decision variables domain

Superscript/Subscripts

0	reference
abs	absorption chiller
bio	biomass
bioboil	biomass boiler
boil	boiler
BP	bypass
build	building
buy	bought
CCHP	combined cooling, heating and power
CHP	combined heat and power
cold	cold
coll	collector
dem	demand
DHW	domestic hot water
di	directly provided by natural gas
e	electricity
ED	energy device
ex	exhaust gas
grid	power grid
GT	gas turbine
hex	heat exchanger
HP	heat pump
HR	heat recovery
HRB	heat recovery boiler
HTF	heat transfer fluid
in	input
k	iteration
max	maximum
min	minimum

NG	natural gas
out	output
PM	prime mover
r	return
s	supply
SC	space cooling
SH	space heating
solar	solar energy
ST	solar thermal
sto	thermal storage
w	water

Acronyms

CCHP	combined cooling, heating and power
CHP	combined heat and power
DES	distributed energy system
DHW	domestic hot water
GHG	greenhouse gas
HTF	heat transfer fluid
MOLP	multi-objective linear programming
SC	space cooling
SH	space heating

"The need for sustainability and sustainable development has gone beyond being a trend, and rightly so."

Chapter 1

Introduction

1.1. Motivation and Background

In recent years, depletion of fossil energy resources and global warming problems have prompted international awareness about sustainability of energy supply on a worldwide scale. In general, sustainability means an equitable distribution of the limited resources and opportunities in the context of the economy, the society, and the environment [1], aiming at the well-being of everyone, now and in future, thereby guaranteeing that needs of future generations may be completely satisfied as happens today. In the literature, a sustainable energy system has been commonly defined in terms of its energy efficiency, its reliability, and its environmental impacts [2].

In such context, Distributed Energy Systems (DESs) have been recognized as a sustainability-oriented alternative to conventional centralized energy systems [2 - 4]. A DES may consist of small-scale heat and power generation technologies including also renewable ones, and storage units, providing electric and thermal energy to end-users [2]. Figure 1.1 shows a representation of a centralized energy supply system as well as a real DES located at the University of Genova [5]. DESs with an appropriate planning, may exhibit even better performances than a single polygeneration system, such as Combined Cooling Heating and Power (CCHP) systems or conventional centralized energy supply systems. For instance, integration with renewable energy resources may lead to more environmental benefits and more efficient use of energy resources, thereby enhancing sustainability in the energy supply. However, as the penetration increases, many problems become obvious. In addition to the technical,

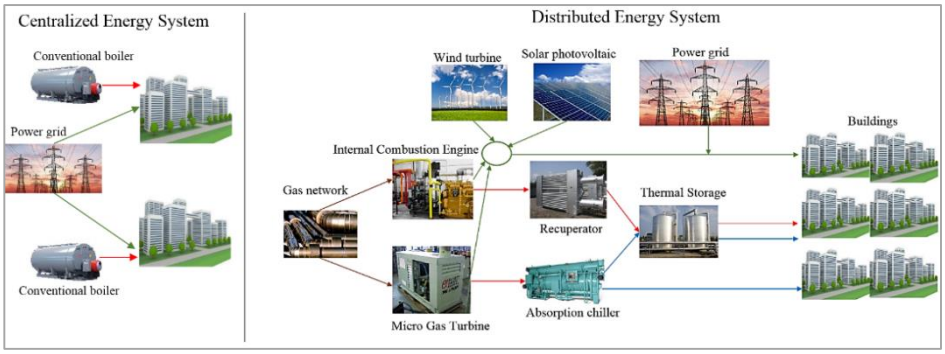

Figure 1.1. Representation of a centralized energy system vs. a distributed energy system.

commercial, and safety issues due to the connection of the energy devices in the distribution networks, the use of renewable energy sources as well as cogeneration and trigeneration systems, usually adds more specific issues related to the actual method used. One of these issues is the unbalance between supply and demand sides. Generally, electrical and thermal demands change with time, whereas the supply of electricity and heat is stable in some situation for certain energy devices involved in the DES.

The operation planning of DESs is not a trivial task, as integration of different types of energy resources and energy conversion devices as well as storage units may increase the complexity of the system. Therefore, for a specific DES involving several energy devices and storage units, the operation planning should be optimized while satisfying the time-varying user demands. Much research has been reported on this topic, and most of which are focused on the optimal operation planning of a specific DES technology (Combined Heat and Power (CHP) system mainly) [6 - 14]. In the context of DESs including several energy devices and energy storage systems, most of the studies in the literature are focused on the operation optimization to reduce energy costs, which is essential in the short run [15, 16].

However, generally different stakeholders participate in DESs development and management. Hence, objectives can be defined from different perspectives, such as the developers and operators of DESs, or the civil society, ideally represented by the regulator. Some of the DESs planning objectives are naturally conflicting. Consequently, there is not a single planning solution, which can satisfy all the

stakeholders. For instance, society interest in sustainable energy supply systems, and with low environmental impacts, might conflict with the economic interest of the developers and operators of DESs. A multi-objective approach helps to identify compromise solutions, which benefit all the stakeholders.

According to the Annex 49 – ECBCS – Low Exergy Systems for High Performance Buildings and Communities [17], application of exergy principles in the context of building energy supply systems can achieve rational use of energy resources by taking into account the different energy quality levels of energy resources as well as those of building demands. The energy demand in buildings for heating and cooling purposes is responsible for more than one third of the final energy consumption in Europe and worldwide [17]. Commonly this energy is provided by different fossil fuel based systems through combustion, which cause greenhouse gas (GHG) emissions, and their reduction is one of the core challenges in fighting climate change. National and international agreements, such as the European 20-20-20-targets and the Kyoto protocol, limit the GHG emissions of industrialized countries for climate protection. While a lot has already been achieved, especially regarding the share of renewables in the electricity supply system, there are still large potentials in the heating and cooling sector for buildings.

Assessments of energy use in buildings are usually based on quantitative considerations based on the First Law of Thermodynamics [17]. Concerning the conservation of energy, the First Law, however, does not take into account the degradation of the energy quality that takes place when high-quality energy resources, such as electricity or fossil fuels, are used to satisfy low-quality thermal demands. Exergy, derived from the Second Law of Thermodynamics, is a measure of the energy quality. It is the maximum amount of work that can be obtained from an energy flow as it comes to the equilibrium with a reference environment [17 - 22], and can be viewed as the potential of a given energy amount. Unlike energy, exergy is not subjected to conservation (except for reversible processes). Rather, exergy is destroyed due to irreversibilities in any real process [23].

Exergy analysis was used for the performance evaluation of single energy systems, e.g., geothermal systems [24 – 26], cogeneration systems [27 – 30], renewable energy sources [31], and heat recovery steam generators [32], with the aim

to find the most rational use of energy. The performances of different options of energy supply systems to meet building demands were evaluated and compared in terms of exergy efficiencies in [33 – 35]. The concept of exergy was introduced to the building environment by Björk et al. [36], Kilkiş [37] and Molinari [38, 39]. In buildings, energy demands are characterized by different energy quality levels. Since the required temperatures for heating and cooling of indoor spaces are low, the exergy analysis shows that the quality of the energy necessary for air conditioning applications is also low (Carnot factor $F_q \approx 7\%$). The production of domestic hot water requires temperature slightly higher than those for air conditioning, and the quality of the energy needed to satisfy this demand is also higher (Carnot factor $F_q \approx 15\%$). For electrical appliances and lighting, the highest quality of energy is needed (Carnot factor $F_q \approx 100\%$).

Exergy analysis may promote the matching of the energy quality levels of supply and demand, by covering if possible low-quality thermal demands with low exergy sources, e.g., solar thermal or waste heat of power generation processes, and electricity demands with high exergy sources, as shown in Figure 1.2.

In this way, sustainability of energy supply is improved by a rational use of the energy resources, thereby reducing the fossil fuels consumption with the related GHG emissions. In detail, there are many advantages in applying exergy principles in the holistic assessment of building energy supply systems. First of all, the environment

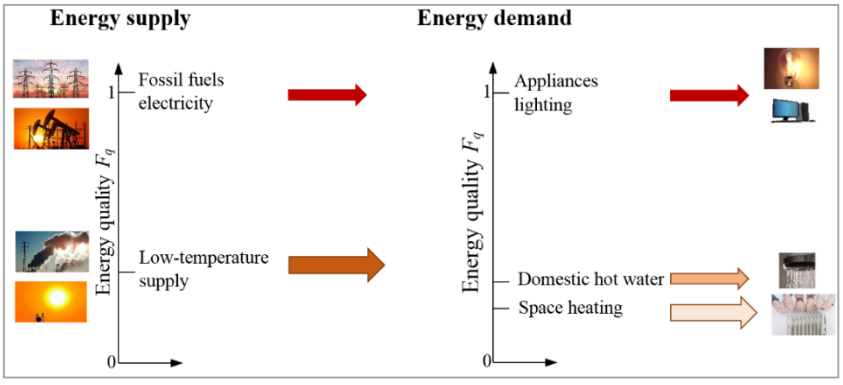

Figure 1.2. Energy supply with sources at different energy quality levels for a typical building with uses at different energy quality levels.

benefits from the exergy principles. The total GHG emissions can be substantially reduced as a result of the reduced use of high-quality energy resources as electricity and fossil fuels to meet low-quality thermal demands. From an economic point of view, high price stability can be expected thanks to the use of locally available, renewable energy sources, or surplus heat from power generation processes. Moreover, a consequent advantage is a lower dependency on foreign fuel supplies. The above mentioned benefits mean long-run sustainability of energy supply, which is the greatest long-run planning objective of the civil society interested in a sustainable future.

As mentioned earlier, in the context of DESs, different energy resources, including renewable ones can be integrated, and low-temperature waste heat from power generation processes can be recovered for thermal purposes. In these applications, DESs, as the smallest units to match the quality levels of supply and demand, provide a unique opportunity to obtain the benefits of exergy analysis in order to improve sustainability of the energy supply.

1.2. Aims and originality

The aim of this thesis is to provide an original tool based on a mathematical programming approach, to attain the optimal operation planning of DESs through multi-objective criteria, by considering both short- and long-run priorities. Multi-objective optimization problems are formulated to find the optimized operation strategies of DESs in order to obtain a rational use of energy resources, while satisfying time-varying user demands. The rational use of energy resources is attained by considering both short- and long-run priorities. The short-run priority is characterized by the economic factor, based on the minimization of the energy costs. The long-run priority is characterized by sustainability of the energy supply. This latter is attained through exergy-based assessments, as well as environmental impact aspects.

The DESs under consideration involve several energy devices, such as Combined Cooling Heating and Power systems or Combined Heat and Power systems, natural gas and biomass boilers, heat pumps, solar thermal plants, which convert a set of

primary energy carriers to satisfy given time-varying user demands. To allow more efficient use of thermal energy, thermal energy storage systems are also included in the DESs configurations. Multi-objective optimization problems are formulated based on the detailed modeling of the energy devices and thermal storage systems, to attain the optimized operation strategies of the DESs, by considering both short- and long-run objectives. The mathematical models proposed aim at providing decision support to planners for selecting the operation strategies of a DES throughout the planning period, based on their short- and long-run priorities.

In order to consider the economic priority crucial in the short-run, and the environmental impacts, essential in the long-run, in the operation planning of DESs, a multi-objective linear programming problem is formulated to obtain the optimized operation strategies to reduce the energy costs and environmental impacts, while satisfying the given time-varying user demands. The economic objective is to minimize the total energy cost, whereas the environmental objective is to minimize the total CO_2 emission. The Pareto frontier, involving the best possible trade-offs between the economic and environmental objectives is obtained by minimizing a weighted sum of the total energy cost and CO_2 emission, by using branch-and-cut.

As mentioned earlier, exergy concepts in the context of DESs facilitate the integration of low temperature energy sources such as solar thermal, and waste heat of power generation processes to meet low-quality thermal demands in buildings. To demonstrate the effectiveness of the exergy analysis in the operation planning of DESs, an innovative exergy-based operation optimization of a DES is presented, through a multi-objective approach for not neglecting the energy costs. A multi-objective linear programming problem is formulated. The economic objective is to minimize the total energy cost. The exergetic objective is to maximize the overall exergy efficiency of the DES, defined as the ratio of the total exergy required to meet the given energy demands to the total primary exergy input to the system. The Pareto frontier, consisting of the best possible trade-offs between the energy costs, essential in the short run, and the overall exergy efficiency crucial in the long run, is obtained by minimizing a weighted sum of the total energy cost and primary exergy input, by using branch-and-cut. Moreover, the influence of the exergy analysis on CO_2 emissions in the optimal operation planning of the DES is also addressed.

The exergy-based operation optimization of a DES is also presented by considering the whole energy-supply chain from energy resources to user demands, through the detailed analysis of the energy system components for conversion, storage, distribution and emission. Instead of considering the overall exergy efficiency, exergy losses are modeled for the system components at the energy conversion step. In order to consider the energy costs as well, a multi-objective optimization problem is formulated to find the optimized operation strategies to reduce the total energy cost and the total exergy loss occurring at the energy conversion step, which accounts for the largest part of the total exergy loss in the whole energy-supply chain. An innovative optimization method based on the Surrogate Lagrangian relaxation combined with branch-and-cut [40 - 42] is used as solution methodology to find the Pareto frontier, by minimizing a weighted sum of the total energy cost and the total exergy loss at the energy conversion step.

Based on the mathematical models proposed, the economic priority, crucial in the short-run, is never neglected, since the optimized operation of DESs allows to reduce the energy costs as compared to conventional energy supply systems. The long-run sustainability is also achieved, since lower environmental impacts as well as higher efficiency in the energy resource use are attained by the optimized operation of DESs, as compared with conventional energy supply systems.

This means to identify compromise solutions, which can satisfy all the stakeholders. On the one hand, there are the developers and operators of DESs, whose greatest interest is the economic factor, on the other hand, there is the civil society, ideally represented by the regulator, whose greatest interest is a sustainable future.

1.3. Organization of the thesis

After the present Introduction (Chapter 1) and before the Conclusions (Chapter 6), the thesis is articulated in the following chapters:

- In Chapter 2, a review on decision-making problems in the context of DESs is presented, focusing the attention on the multi-objective planning, as a new pathway oriented to a sustainable energy decision-making.

- In Chapter 3, a multi-objective optimization problem is presented for the optimal operation planning of a DES, with the aim to find the optimized operation strategies to reduce both the energy cost and the environmental impacts in terms of CO_2 emission.

- In Chapter 4, the exergy analysis is involved in the optimal operation planning of a DES, through a multi-objective approach for not neglecting the energy costs. A multi-objective optimization problem is formulated to find the optimized operation strategies, which reduce the energy cost and increase the overall exergy efficiency. In addition, the influence of the exergy analysis on CO_2 emissions in the optimal operation planning of the DES is also analyzed.

- In Chapter 5, the exergy-based operation planning of a DES is presented through the energy-supply chain from energy resources to user demands. A multi-objective optimization problem is formulated to find the optimized operation strategies of the DES, which reduce the total energy cost and the total exergy loss occurring at the energy conversion step.

Chapters 3, 4 and 5 are based on research reported in papers [43 - 47].

References

[1] World Commission on Environment and Development (WCED). Our common future. Oxford: Oxford University Press, 1987.

[2] Kari A, Arto S. Distributed energy generation and sustainable development. Renewable and Sustainable Energy Reviews 2006;10:539–58.

[3] Akorede MF, Hizam H, Poresmaeil E. Distributed energy resources and benefits to the environment. Renewable and Sustainable Energy Reviews 2010;14:724–34.

[4] Pepermans G, Driesen J, Haesoldoncklx D, Belmans R, D'haeseleer W. Distributed generation: definition, benefits and issues. Energy Policy 2005;33:787–98.

[5] Rivarolo M, Greco A, Massardo AF. Thermo-economic optimization of the impact of renewable generators on poly-generation smart-grids including hot thermal storage. Energy Conversion and Management 2013;65:75-83.

[6] Handschin E, Neise F, Neumann H, Schultz R. Optimal operation of dispersed generation under uncertainty using mathematical programming. International Journal of Electrical Power & Energy Systems 2006;28(9):618–26.

[7] Hawkes AD, Leach MA. Cost-effective operating strategy for residential microcombined heat and power. Energy 2007;32(5):711–23.

[8] Houwing M, Ajah AN, Heijnen PW, Bouwmans I, Herder PM. Uncertainties in the design and operation of distributed energy resources: the case of micro-CHP systems. Energy 2008;33(10):1518–36.

[9] Van Schijndel AWM. Optimal operation of a hospital power plant. Energy and Buildings 2002;34(10):1155–65.

[10] Wakui T, Yokoyama R, Shimizu K. Suitable operational strategy for power interchange operation using multiple residential SOFC (solid oxide fuel cell) cogeneration systems. Energy 2010;35(2):740–50.

[11] Mancarella P, Chicco G. Global and local emission impact assessment of distributed cogeneration systems with partial-load models. Applied Energy 2009;86(10):2096–106.

[12] Kalantar M, Mousavi G SM. Dynamic behavior of a stand-alone hybrid power generation system of wind turbine, microturbine, solar array and battery storage. Applied Energy 2010;87(10):3051-64.

[13] Fumo N, Mago PJ, Chamra LM. Analysis of cooling, heating, and power systems based on site energy consumption. Applied Energy 2009;86(6):928–32.

[14] Wright A, Firth S. The nature of domestic electricity-loads and effects of time averaging on statistics and on-site generation calculations. Applied Energy 2007;84(4):389–403.

[15] Yan B, Luh PB, Sun B, Song C, Dong C, Gan Z, et al. Energy-efficient management of eco-communities. In: Proceedings of IEEE CASE; Madison, USA, 2013 August 17–20.

[16] Guan X, Xu Z, Jia Q. Energy-efficient buildings facilitated by microgrid. IEEE Trans Smart Grid 2011;1:466–73.

[17] ECBCS – Annex 49 – Low Exergy Systems for High Performance Buildings and Communities, homepage. Available: http://www.ecbcs.org/annexes/annex49.htm.

[18] Szargut J. International progress in second law analysis. Energy 1980;5:709–18.

[19] Szargut J, Morris DR, Stewerd FR. Exergy analysis of thermal, chemical and metallurgical processes. New York: Hemisphere; 1988.

[20] Moran MJ. Availability Analysis: a guide to efficient energy use. revised ed. New York: ASME; 1990.

[21] Kotas YJ. The exergy method for thermal plant analysis. reprint ed. Malabar, FL: Krieger; 1995.

[22] Edgerton RH. Available energy and environmental economics. Toronto: D.C. Heath; 1992.

[23] Rosen MA, Dinçer I, Kanoglu M. Role of exergy in increasing efficiency and sustainability and reducing environmental impact. Energy Policy 2008;36:128–37.

[24] Hepbasli A. A review on energetic, exergetic and exergoeconomic aspects of geothermal district heating system (GDHSs). Energy Conversion and Management 2010;51:2041–61.

[25] Hepbasli A, Akdemir O. Energy and exergy analysis of a ground source (geothermal) heat pump system. Energy Conversion and Management 2004;45:737–53.

[26] Esen H, Inalli M, Esen M, Pihtili K. Energy and exergy analysis of a groundcoupled heat pump system with two horizontal ground heat exchangers. Building and Environment 2007;42(10):3606–15.

[27] Fryda L. Integrated CHP with auto thermal biomass gasification and SOFCMGT. Energy Conversion and Management 2008;49:281–90.

[28] Abusoglu A, Kanoglu M. First and second law analysis of diesel engine powered cogeneration systems. Energy Conversion and Management 2008;49:2026–31.

[29] Gonçalves P, Angrisani G, Rosselli C, Gaspar AR, Da Silva MG. Comparative energy and exergy performance assessments of a microcogenerator unit in different electricity mix scenarios. Energy Conversion and Management 2013;73:195–206.

[30] Açikkalp E, Aras H, Hepblaski A. Advanced exergy analysis of an electricity generating facility using by natural gas. Energy Conversion and Management 2014;82:146–53.

[31] Koroneos C, Spachos T, Moussiopoulos N. Exergy analysis of renewable energy sources. Renewable Energy 2003;28:295–310.

[32] Kaviri AG, Jaafar MNM, Lazim TM, Barzegaravval H. Exergoenvironmental optimization of heat recovery steam generators in combined cycle power plant through energy and exergy analysis. Energy Conversion and Management 2013;67:27–33.

[33] Kranzl L, Müller A, Kalt G. The trade-off between exergy-output and capital costs: the example of bioenergy utilization paths. In: 11th Symposium Energy Innovation, Graz, Austria, 2010 February 10–12.

[34] Tolga Balta A, Dincer I, Hepbasli A. Performance and sustainability assessment of energy options for building HVAC applications. Energy and Buildingd 2010;42:1320–8.

[35] Angelotti A, Caputo P. Energy and exergy analysis of heating and cooling systems in the italian context. In: Proceedings of Climamed, Genova, Italy, 2007, 5–7 September, 843–54.

[36] Björk F, Kilkiş Ş, Molinari M. Energy quality management and low energy architecture. In: ASES National Solar Conference, North Carolina, USA; 2011.

[37] Kilkiş Ş. A rational exergy management model for curbing building CO_2 emission. ASHRAE 2007;113:113–23.

[38] Molinari M. Exergy and parametric analysis: methods and concepts for a sustainable built environment. Stockolm, Sweden: Royale Institute of Technology; 2012.

[39] Molinari M. Exergy Analysis in Buildings: a complementary approach to energy analysis, Stockolm. Sweden: KTH- Stockolm; 2009.

[40] Bragin MA, Luh PB, Yan JH, Yu N, Stern GA. Convergence of the Surrogate Lagrangian Relaxation Method, Journal of Optimization Theory and Applications 2015;164(1):173-201.

[41] Bragin MA, Luh PB, Yan JH, Yu N, Stern GA. Surrogate Lagrangian relaxation and branch-and-cut for unit commitment with combined cycle units, in Proceedings of the IEEE Power and Energy Society, General Meeting, National Harbor, Maryland, 2014.

[42] Bragin MA, Luh PB, Yan JH, Yu N, Stern GA. Novel exploitation of convex hull invariance for solving unit commitment by using surrogate Lagrangian relaxation and branch-and-cut, in Proceedings of the IEEE Power and Energy Society, General Meeting, Denver, Colorado, 2015.

[43] Di Somma M, Yan B, Bianco N, Luh PB, Graditi G, Mongibello L, Naso V. Multi-objective operation optimization of a Distributed Energy System for a large-scale utility customer (2016). Applied Thermal Engineering (In press). DOI: 10.1016/j.applthermaleng.2016.02.027.

[44] Di Somma M, Yan B, Luh PB, Bragin MA, Bianco N , Graditi G, Mongibello L, Naso V. Exergy-efficient management of energy districts. In Proceedings of: Intelligent Control and Automation (WCICA), 11th World Congress 2014;2675-2680. IEEE.

[45] Di Somma M, Yan B, Bianco N, Luh PB, Graditi G, Mongibello L, Naso V. Operation optimization of a distributed energy system considering energy costs and exergy efficiency. Energy Conversion and Management, 103, 739-751.

[46] Di Somma M, Yan B, Bianco N, Luh PB, Graditi G, Mongibello L, Naso V. Influence of energy quality management on CO_2 emissions in operation optimization of a distributed energy system. In Proceedings of: Clean Electrical Power (ICCEP), International Conference 2015; 297-304. IEEE.

[47] Yan B, Di Somma M, Bianco N, Luh PB, Graditi G, Mongibello L, Naso V. Exergy-based operation optimization of a distributed energy system through the energy-supply chain. Accepted for publication in Applied Thermal Engineering. DOI: 10.1016/j.applthermaleng.2016.02.029.

Measuring sustainability of the energy supply is a major issue as well as a driving force of the discussion on sustainability development."

Chapter 2

Review on decision-making problems for planning of Distributed Energy Systems

2.1. Introduction

Energy systems play an essential role in the economic and social development of a country, and in the life quality of people [1, 2]. With the increasing of energy demand on a worldwide scale, depletion of fossil fuels, and growing environment protection awareness derived by the latest Climate Conference COP21, improving the efficiency of energy resource use has become one of the key challenges. The IEA's World Energy Outlook 2013 [3] predicts that the global energy demand is projected to grow significantly over the next decades, especially in emerging economies. The global primary energy demand predicted in 2035 is shown in Figure 2.1.a), whereas the share of global energy consumption growth is shown in Figure 2.1.b). This scenario forecasts a significant growth in the global energy demand, especially in the context of emerging economies, which are expected to account for more than 90% of the global net energy demand growth by 2035 [3]. Figure 2.2 shows the global primary energy consumption by sources in the periods 1987-2011 and 2011-2035 [3]. Despite the use of renewables is expected to increase in the next decades, fossil fuels, such as natural gas and coal, are expected to continue supplying most of the energy used worldwide. The use of fossil fuels is dramatically related to greenhouse gas emissions. Climate scientists have observed that CO_2 concentrations in the atmosphere have been increasing significantly over the past century, compared

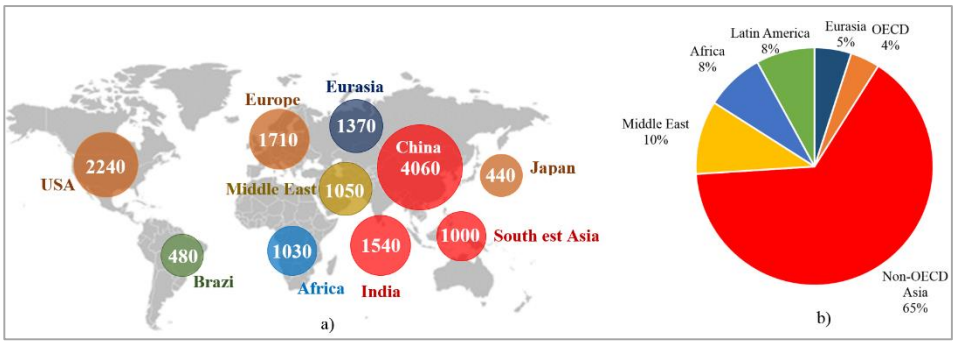

Figure 2.1. Representation of a) global primary energy demand predicted in 2035 (Mtoe) b) share of global energy consumption growth in the period 2012-2035 Elaborated by data from [3].

to the pre-industrial era (about 280 parts per million, or ppm) [4]. The 2014 concentration of CO_2 equal to 397 ppm was about 40% higher than in the mid-1800s, with an average growth of 2 ppm/year in the last ten years. The growing global energy demand from fossil fuels plays a key role in the upward trend of CO_2 emissions and the related global warming problems. Figure 2.3 shows the trend in global CO_2 emission from fossil fuel combustion from 1870 to 2013. It can be noted that since the Industrial Revolution, annual CO_2 emissions have dramatically increased from near zero to over 32 $GtCO_2$ in 2013.

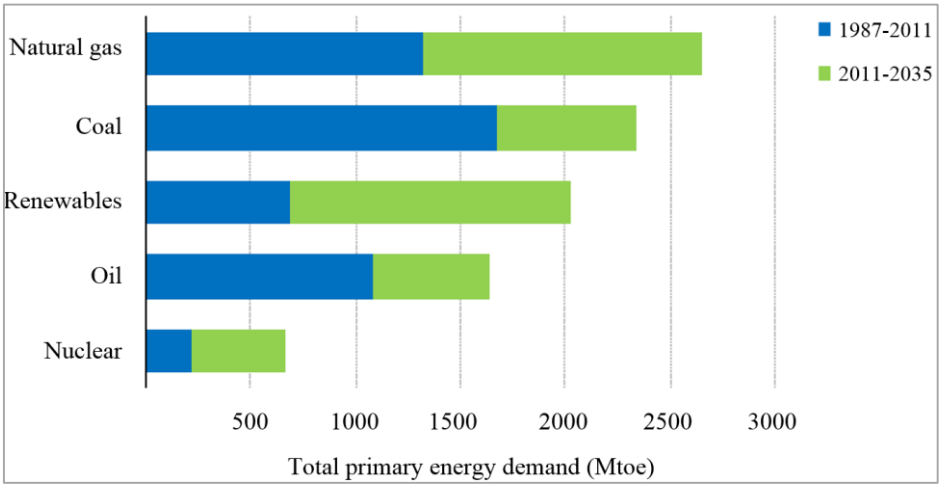

Figure 2.2. Global primary energy consumption by source in the period 1987-2035 [3]

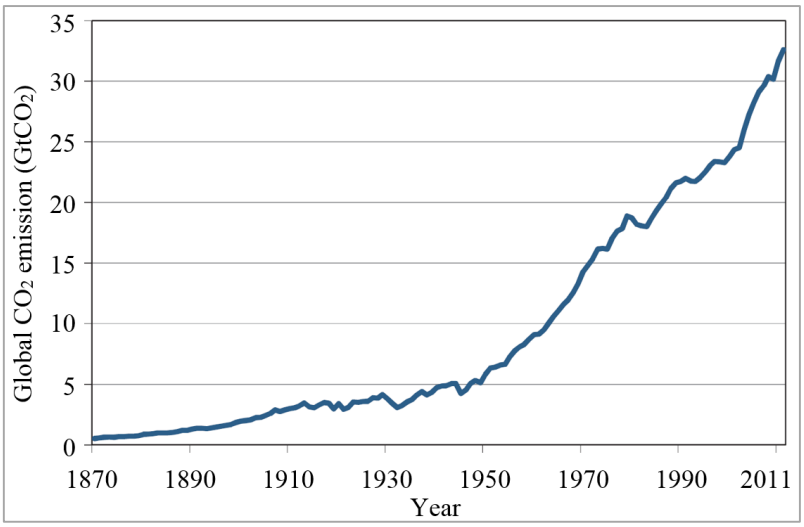

Figure 2.3. Trend of global CO_2 emissions from fossil fuel combustion [4]

The building sector is responsible of more than one third of the global energy demand [5]. Moreover, it is responsible of 15% of the total direct energy-related CO_2 emissions from final energy consumers, but if indirect upstream emissions attributable to electricity and heat consumption are also taken into account, it is responsible of 26% of the global CO_2 emissions [6]. Figure 2.4 shows the global annual per capita final energy use in the building sector in 1990 and 2013 for the several regions in the world, highlighting the growth rate achieved in two decades [6]. The global building energy use may double to triple by mid-century, due to several key trends, such as the migration to cities, the increasing levels of wealth, the growing number of appliances and equipment used. All these factors will contribute to increase significantly the energy demand in the building sector in the next decades. This means that buildings are collectively a major contributor to the above mentioned energy related problems. Based on this background, energy conservation in the building sector has attracted much interest in the last decades. Usually, the energy - saving activities in the building sector have been focused on the improvement of building energy performance, by increasing the energy efficiency in the building stock.

However, besides the reduction of energy consumption in the demand side, it is

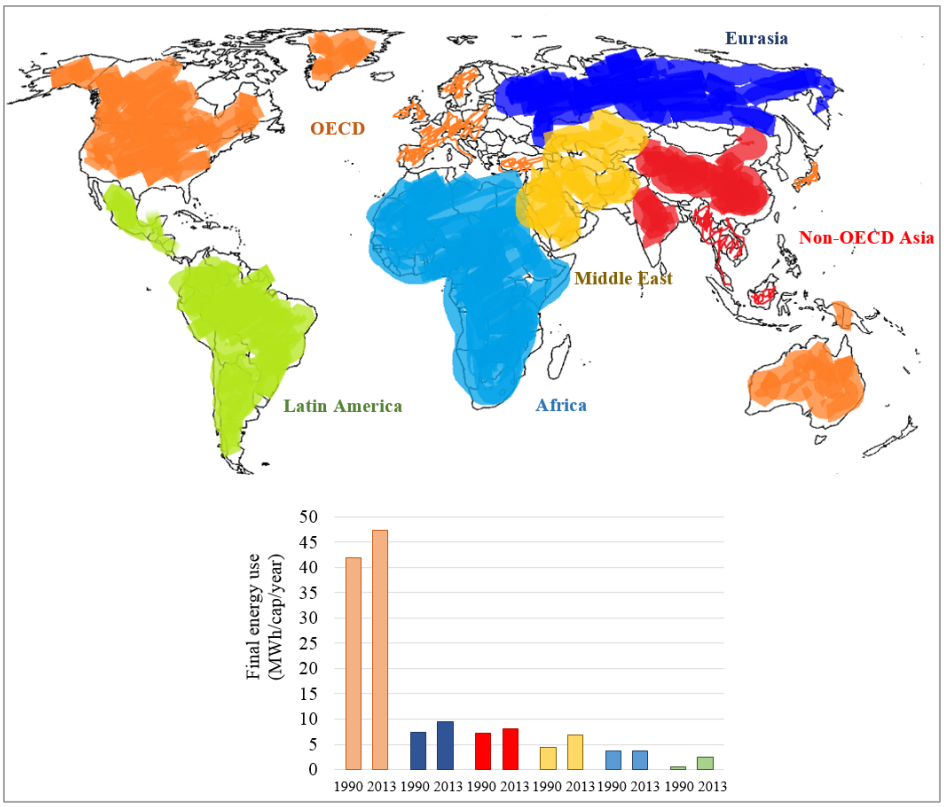

Figure 2.4. Global annual per capita final energy use of building sector in 1990 and 2013. Elaborated by data from [6].

essential to achieve energy conservation in the supply side [7]. Several new government policies have been adopted to encourage the introduction of energy efficiency measures and technical changes, as well as the use of renewable energy sources in the context of building energy supply, with the aim to increase its sustainability [8 - 10]. In such context, interest in developing Distributed Energy Systems (DESs) has been intensifying, since they have been recognized as a sustainability-oriented alternative to conventional energy supply systems [11 - 14]. A DES refers to an energy system where energy is made available close to energy consumers, typically relying on a number of small-scale heat and power technologies [11]. One of the main benefits of DESs is the possibility to integrate different energy resources, including renewable ones, as well as to recover waste heat from power

generation plants for thermal purposes [12 - 14]. This benefit allows to enhance sustainability of the energy supply through a more efficient use of the energy resources as well as a reduced environmental impact as compared with conventional energy supply systems. However, there are many barriers to the spread of these systems. One of which is the lack of a plan and evaluation method for the final decision-making about system selection, taking into account the optimal design and operation planning. Earlier on, building energy supply systems have been selected mainly on the cost-benefit analysis. With the increase of the energy-related problems, the single criteria decision framework has appeared no longer sufficient. This is because it is necessary to take into account several sustainability-related aspects. In the sustainability assessment of energy supply systems, the set of priorities include functional requirements, costs, possibilities and risks. Thus, the evaluation of complex systems depends on a number of parameters, such as economic, technological, environmental, etc. In order to deal with such a difficult problem, a multi-objective approach is usually employed. As one of the major parts of the decision-making process, it provides a flexible idea, which is able to handle and bring together a wide range of variables appraised in different ways, thereby offering valid assistance to decision makers.

In this chapter, a comprehensive review on decision-making problems for planning of DESs is presented. Firstly, the key concepts of optimization problems in the context of DESs, and of single- and multi-objective optimization approaches are presented in Section 2.2. A literature review on the main current research on the optimal planning of DESs is discussed in Section 2.3, whereas Section 2.4 focuses on the prospects of the spread of DESs.

2.2. Decision-making problems for planning of Distributed Energy Systems

As a complex decision-making problem, the optimal planning of DESs is challenging, due to the integration of multiple energy devices and energy storage systems, which convert and store a set of energy carriers with complicated interactions among them to satisfy the user demands. Figure 2.5 shows the typical configuration of a DES, where several energy devices convert a set of input energy sources, including renewable ones, to satisfy the buildings demands [15]. The optimal

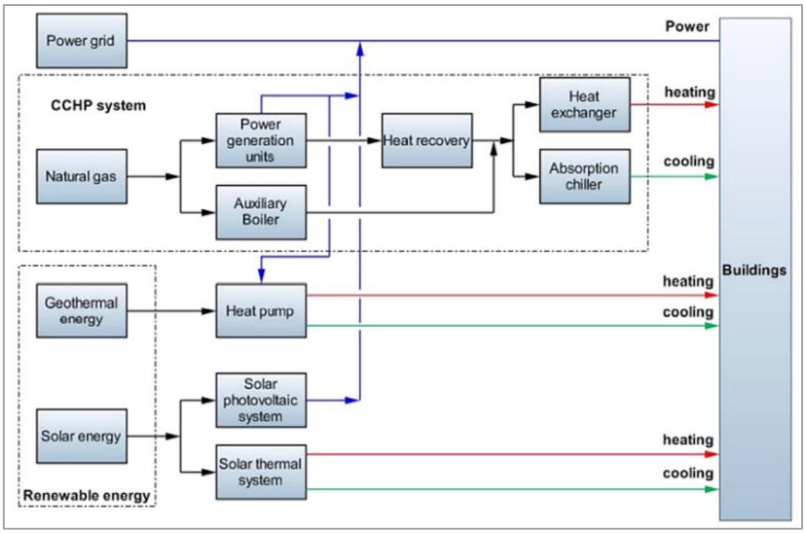

Figure 2.5. Typical configuration of a DES [15].

planning of DESs refers to the structured process of optimizing the design in terms of types and sizes of the technologies involved and/or their location in order to achieve one or more objectives, subjected to a set of constraints. Besides the optimal design, the optimal planning of DESs may also refer to the structured process of optimizing the operation strategies of the technologies involved, in order to achieve one or more objectives, subjected to a set of constraints.

In the following, the key concepts of optimization problems are presented in Subsection 2.2.1. The single- and multi-objective optimization approaches for the optimal planning of DESs are presented in Subsection 2.2.2.

2.2.1. Key concepts of optimization problems for planning of Distributed Energy Systems

A general representation of the optimization problem for the planning of DESs can be formally expressed as [16]:

$$\begin{aligned} &\min F_{obj}(y) = \min ([f_1(y), f_2(y), \ldots, f_m(y)]) \\ &\text{s.t.} \\ &y \in \Omega \\ &G(y) = 0 \\ &H(y) \leq 0 \end{aligned} \tag{2.1}$$

where f_i is the i^{th} objective function; m is the number of objective functions; y is the decision variables vector (e.g., sizes, generation levels of technologies, etc.); Ω is the decision variables domain; $G(y)$ are the equality constraints (e.g., energy balances to satisfy the user demands); $H(y)$ are the inequality constraints (e.g., capacity constraints of energy devices and energy storage).

In general, these optimization problems are mixed-integer programming problems, which may contain both integer and continuous variables. When integer variables are restricted to the values 0 and 1, they are referred to as binary decision variables, and can be used to model yes/no decisions, such as the involvement or not of a certain technology in the DES. On the other hand, continuous decision variables may assume any value between the lower and upper bounds, and can be used, for instance, to model the generation level of a certain technology, once fixed its capacity constraint.

Moreover, these programming problems can be linear or nonlinear. A linear programming problem is characterized by objective functions which are linear in the decision variables, as well as by constraints which are linear equalities or linear inequalities in the decision variables [17]. Mixed-integer linear programming problems are usually difficult to solve because a set of decision variables are restricted to integer values. Branch-and-cut is the most common method used to solve mixed-integer linear optimization problems. In the method, all integrality requirements on variables are first relaxed, and the relaxed problem can be efficiently solved by using a linear programming method. If the values of all integer decision variables turn out to be integers, the solution of the relaxed problem is optimal to the original problem. If not, the convex hull (the smallest convex set that contains all feasible integer solutions in the Euclidean space) is needed since once it is obtained, all integer decision variables of the linear programming solution are integers and optimal to the original problem. The process of obtaining the convex hull, however, is problem dependent, and can itself be NP hard (nondetermistic polynomial-time hard). Valid cuts that do not cut off any feasible integer solutions are added, trying to obtain the convex hull first. If the convex hull cannot be obtained, low-efficient branching operations may then be needed on the variables whose values in the optimal relaxed solution violate their integrality requirements. The objective value of

the current optimal relaxed solution is a lower bound, and can be used to quantify the quality of a feasible solution.

A nonlinear programming problem includes at least one nonlinear function in the decision variables, which could be the objective function or some or all the constraints. Nonlinear mixed-integer programming problems combine the difficulties of solving combinatorial problems with the complexity of nonlinear (and non-convex) objectives and constraints [18]. Usually, the complexity of this optimization task is dealt by using two different approaches. The first is to apply simplifying assumptions to the problem formulation, such as linearization of the objective function and/or the constraints. In this way, it is possible to solve the optimization problem by using traditional mathematical programming methods, for which powerful programming methods are available (e.g., Linear Programming). The second approach is based on the use of heuristic optimization techniques, such as Evolutionary Algorithms. There are three main groups of Evolutionary Algorithms: Genetic Algorithms (GA), Evolutionary Strategies (ES) and Evolutionary Programming (EP). These algorithms are based on stochastic search by using groups of potential solutions. The best performing solutions are iteratively chosen, and combined (GA) or modified (ES, EP) to find better solutions, until a stopping criterion is met.

2.2.2. Single- and Multi-objective planning of Distributed Energy Systems

In the context of the optimal planning of DESs, a single-objective approach is often practical from the point of view of developers and operators of DESs, whose greatest interest is the economic factor. The developer of a DES can obtain information about the most promising configuration, in terms of types and sizes of the technologies, and/or their location, to minimize the total cost, in terms of investment, operation and maintenance and energy costs. On the other hand, once fixed the DES configuration, the operator of the DES can obtain information about the operation strategies to minimize the total energy costs.

However, generally different stakeholders participate in DESs development and management. Hence, objective planning can be formulated from different perspectives, such as developers and operator of DESs, or the civil society, ideally represented by the regulator [16]. Some of the DESs planning objectives are naturally

conflicting. For instance, society interest in sustainable energy supply systems, and with low environmental impacts, might conflict with the economic interest of the developers and operators of DESs. Consequently, there is not a single planning solution, which can satisfy all the stakeholders. A multi-objective approach helps to identify compromise solutions, which benefit all the stakeholders. Moreover, multi-objective approaches applied to the optimal planning of DESs can provide valuable information about the correlation between the benefits and impacts of DES integration, thereby supporting the decision-making process [19]. From a high-level perspective, a multi-objective analysis of DESs integration can help to promote incentives and policies to encourage the DESs development, which ensure benefits and minimize the related negative impacts.

In the following, the key concepts of multi-objective optimization are discussed, and the main types of multi-objective optimization methods are introduced.

When an optimization problem has a single objective function, the definition of "best solution" is one-dimensional, and there is only a single best solution, or none, if any. Conversely, a multi-objective optimization problem does not have a single optimal solution, but a set of optimal solutions. In this case, the multidimensional concept of dominance is used to determine if one solution is better than other solutions. A solution *a* is said to dominate a solution *b* if the following two conditions are true [20]:

- *a* is no worse than *b* in all objectives;
- *a* is better than *b* in at least one objective.

In this case, *b* is said to be dominated by *a*, or alternatively, *a* is said to be non-dominated by *b.* A dominated solution is also said to be sub-optimal. The solution of the multi-objective optimization problem is characterized by the set of non-dominated solutions, known as Pareto set. In terms of their objective functions, the Pareto set is referred as to the Pareto frontier, whose graphics for three dimensions is a surface, whereas when only two objectives are involved, it degenerates to a trade-off curve, consisting of the range of optimal choices available for planners. A solution belongs to the Pareto frontier, if no improvement is possible in one objective, without losing in any other objective. An example of Pareto frontier with the key concepts mentioned above is shown in Figure 2.6. The general flow-chart of the multi-

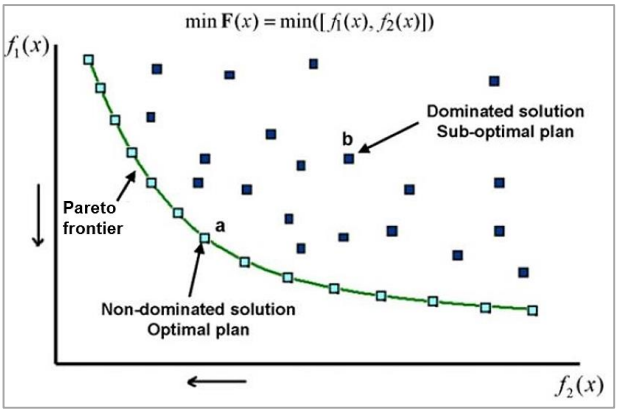

Figure 2.6. Example of a Pareto frontier for a multi-objective optimization problem with two objective functions [16].

objective optimization process is shown in Figure 2.7. The information contained in the Pareto frontier elucidates compromise solutions between the stakeholders, or trade-offs between incommensurable objectives. As a result, the decision-making process takes place after the multi-objective optimization. Initially, several solutions of the Pareto frontier are found, and the preference is expressed afterwards.

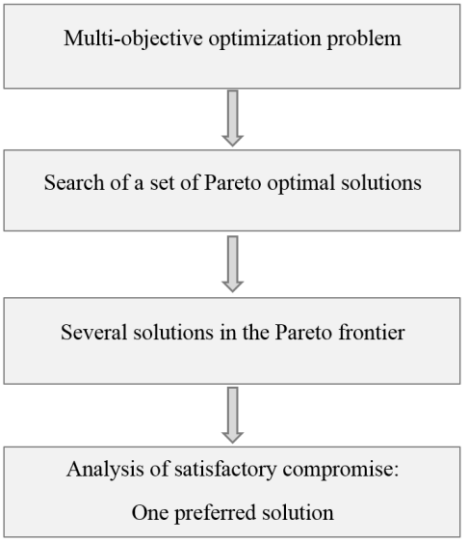

Figure 2.7. General flow-chart of the multi-objective optimization process

Normally, multi-objective optimization problems have a large number of solutions involved in the Pareto frontier. Since finding all the solutions belonging to the Pareto frontier is practically impossible, a subset of the Pareto optimal solutions is usually looked for. Therefore, the multi-objective optimization process is the process of finding as many solutions of the Pareto frontier as possible. Solving a multi-objective optimization problem involves the following three satisfying requirements [20, 21]:

- Accuracy: the set of solutions found has to be as close as possible to the real Pareto frontier;
- Diversity: the set of solutions found has to be as diverse as possible;
- Spread: the set of solutions found has to capture the entire spectrum of the real Pareto frontier.

These requirements are exemplified in Figure 2.8. The first case (Case 1) is able to obtain accurate solutions and to capture the extent of the two objectives. However, the set of solutions found is not diverse. In the second case (Case 2), a diverse set of well-spread solutions is attained, although solutions are not accurate. In the third case (Case 3), the solutions found are accurate and diverse. However, the extreme edges of the Pareto frontier are not explored. The fourth case (Case 4) illustrates the solutions found by an ideal algorithm.

There are several methods to find the Pareto frontier for a multi-objective optimization problem. These methods are divided into two main groups. The first group converts the multi-objective optimization problem into a single-objective optimization problem. Two of the most common methods of this type are the weighted-sum method and the ε-constrained method. The key idea of the weighted-sum method is to change the multi-objective functions into a single-objective function:

$$\min \; F_{obj}(y) = \sum_{i=1}^{m} \omega_i f_i(y) \tag{2.2}$$

where the weights ω_i indicate the relative importance of each objective function f_i. The weight values are assigned so that the summation of weights is equal to 1:

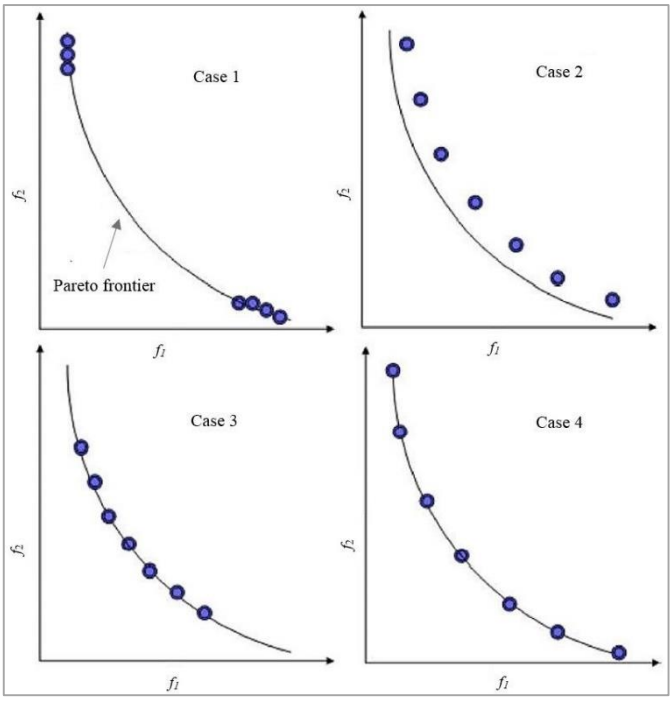

Figure 2.8. Requirements of a multi-objective optimization problem [16]

$$\sum_{i=1}^{m} \omega_i = 1 \tag{2.3}$$

The Pareto frontier can be found by varying the weight in the interval 0 – 1. Generally, objective functions do not have the same order of magnitude, and a normalization is required. This method is simple and easy to implement, and it has been demonstrated that it allows to find all solutions belonging to the Pareto frontier in convex problems [20]. However, this method is not appropriate when a large number of objective functions is involved [22].

The key idea of the ε-constrained method is to keep a single-objective function, f_μ, and to express the other objective functions as inequality constraints. The vector of constraints ε defines upper bounds for these objectives, i,e,

$$\min \ f_\mu(y)$$
$$\text{s.t.} \tag{2.4}$$

$$f_j(y) \leq \varepsilon \quad \text{with } j = 1,2,\ldots,m \text{ and } j \neq \mu$$

The value of the constrained vector represents the trade-off between the objective functions. To obtain a good solution for $f_\mu(y)$, relaxation of the constraints for the rest of the objective functions is required. The Pareto frontier can be found by changing the ε-constrained vector. As for the weighted-sum method, also this method is not appropriate when a large number of objective functions is involved [22].

The second group of multi-objective optimization methods is based on Evolutionary Algorithms [22], which handle sets of possible solutions simultaneously, and, as a result, permit to identify several solutions of the Pareto frontier at once. These methods also have been recognized as an efficient way to solve multi-objective optimization problems.

2.3. Literature review on the optimal planning of Distributed Energy Systems

In the latest years, interest has been intensifying in the development of DESs. Much research has been reported on the optimal planning of DESs, most of which are focused on a specific DES technology, such as Combined Heat and Power (CHP) [23 - 30], or Combined Cooling Heating and Power (CCHP) systems [31 - 38]. However, developing DESs by integrating fossil energy resources with renewable ones is attracting much interest as a new way to attain energy sustainable development worldwide [39]. Several works in literature deal with the optimal planning of DESs, where multiple energy devices convert a set of input energy sources, including renewable ones, to satisfy the user demands, also including energy storage systems. Among them, the integrated optimization of energy devices and energy processes of a small eco-community was carried out in Yan et al. [40] to reduce the total daily energy cost. The solution methodology used was branch-and-cut. A mixed-integer optimization model for the optimal operation planning of multiple energy devices connected to a low energy building was developed in Guan et al. [41] to minimize the overall costs of electricity and natural gas. The problem was also solved by branch-and-cut. A generic energy systems engineering framework toward the optimal design of DESs was presented by Zhou et al [42], with the aim to obtain the optimal combination of technologies to satisfy the given energy user

demands. A mixed-integer linear programming problem was formulated, and the objective function was formulated as the total annual cost to minimize. A mixed-integer linear programming problem was also formulated by Mehleri et al [43], for the optimal design planning of a DES to minimize the total annual cost.

Beyond minimizing costs only, several works addressing the optimal planning of DESs, by using a multi-objective approach, have been found in [44 - 48]. A multi-objective optimization model was developed in Ren et al [49], to analyze the optimal operation strategies of a DES, while combining minimization of energy costs and environmental impacts. The optimization problem was solved by using the compromise programming method. A multi-objective optimization model for the optimal planning of DESs was presented in Buoro et al [50], with the aim to find the optimal structure of the system, as well as the optimal operation strategies, by taking into account minimization of the total annual cost and environmental impacts. The problem was solved by using the compromise programming method. In all the works mentioned above, the multi-objective approach was found to be a powerful tool to increase sustainability of energy supply as compared to conventional energy supply systems.

2.4. Prospects of the spread of Distributed Energy Systems

As discussed in Section 2.1, fossil fuels supply most of the energy to meet the global energy demand, and this scenario is expected to not vary significantly based on the current world energy policies. A change in the energy supply structure is essential to increase the proportion in the usage of other clean energy resources, thereby increasing sustainability of the energy supply. Based on the current research on DESs, these systems may be a powerful instrument to change the energy supply structure, offering a new sustainability-oriented pathway, because of the promising benefits in energetic, economic and environmental aspects. Beyond the research in such context, in the recent years, several policies and specifications have been set up to accelerate the development of DESs, not only in developed countries, but also in emerging economies as China [15]. Interest in developing DESs is also growing, due to the urgent need to improve the power supply security, and reliability. Based on these assessments, DESs will have vast prospects, and the application of DESs will

have an upward tendency worldwide, as also demonstrated by the multiple demonstration projects in most of developed countries and beyond. A fully developed financial incentive system as well as specific technical guidelines and enforcement rules should be set up as a driving force to prompt the market growth of DESs. Through the support of policy instruments, DESs could realize the sustainable development in energy field, becoming the mainstream of future energy supply.

References

[1] Yuan J-H, Kang J-G, Zhao C-H, Hu Z-G. Energy consumption and economic growth: evidence from China at both aggregated and disaggregated levels. Energy Economics 2008;30:3077–94.

[2] Soytas U, Sari R. Energy consumption and income in G-7 countries. Journal of Policy Modeling 2006;28:739–50.

[3] IEA, World Energy Outlook 2013, London, November 2013. Available: http://www.worldenergyoutlook.org/pressmedia/recentpresentations/londonnovember12.pdf.

[4] IEA, CO_2 emissions from fuel combustion, highlights, 2015 Edition. Available:https://www.iea.org/publications/freepublications/publication/CO2EmissionsFromFuelCombustionHighlights2015.pdf.

[5] ECBCS – Annex 49 – Low Exergy Systems for High Performance Buildings and Communities, Available <http://www.ecbcs.org/annexes/annex49.htm.

[6] Lucon O, Ürge-Vorsatz D, Zain Ahmed A, Akbari H, Bertoldi P, Cabeza LF, Eyre N, Gadgil A, Harvey LDD, Jiang Y, Liphoto E, Mirasgedis S, Murakami S, Parikh J, Pyke C, Vilariño MV, 2014, Chapter 9: Buildings. In: Climate Change 2014: Mitigation of Climate Change. Contribution of Working Group III to the Fifth Assessment Report of the Intergovernmental Panel on Climate Change [Edenhofer, O., R. Pichs-Madruga, Y. Sokona, E. Farahani, S. Kadner, K. Seyboth, A. Adler, I. Baum, S. Brunner, P. Eickemeier, B. Kriemann, J. Savolainen, S. Schlömer, C. von Stechow, T.

Zwickel and J.C. Minx (eds.)]. Cambridge University Press, Cambridge, United Kingdom and New York, NY, USA.

[7] Ren H, Gao W, Zhou W, Nakagami, KI. Multi-criteria evaluation for the optimal adoption of distributed residential energy systems in Japan. Energy Policy 2009;37(12):5484-5493.

[8] Bilgen S, Keles S, Kaygusuz A, SarI A, Kaygusuz K. Global warming and renewable energy sources for sustainable development: a case study in Turkey. Renewable and Sustainable Energy Reviews 2008;12:372–96.

[9] Abulfotuh F. Energy efficiency and renewable technologies: the way to sustainable energy future. Desalination 2007;209:275–82.

[10] Resnier M, Wang C, Du P, Chen J. The promotion of sustainable development in China through the optimization of a tax/subsidy plan among HFC and power generation CDM projects. Energy Policy 2007;35:4529–44.

[11] Kari A, Arto S. Distributed energy generation and sustainable development. Renewable and Sustainable Energy Reviews 2006;10:539–58.

[12] Akorede MF, Hizam H, Poresmaeil E. Distributed energy resources and benefits to the environment. Renewable and Sustainable Energy Reviews 2010;14:724–34.

[13] Pepermans G, Driesen J, Haesoldoncklx D, Belmans R, D'haeseleer W. Distributed generation: definition, benefits and issues. Energy Policy 2005;33:787–98.

[14] Söderman J, Pettersson F. Structural and operational optimisation of distributed energy systems. Applied Thermal Engineering 2006;26:1400–8.

[15] Han J, Ouyang L, Xu Y, Zeng R, Kang S, Zhang G. Current status of distributed energy system in China. Renewable and Sustainable Energy Reviews 2016;55:288-297.

[16] Alarcon-Rodriguez A, Ault G, Galloway S. Multi-objective planning of distributed energy resources: A review of the state-of-the-art. Renewable and Sustainable Energy Reviews 2010;14(5):1353-1366.

[17] Luenberg DG, Yinyu Y. L. Linear and Nonlinear Programming, Third Edition 2008, Springer, ISBN: 978-0-387-74502-2.

[18] Alarcon-Rodriguez AD. A Multi-objective Planning Framework for Analysing the Integration of Distributed Energy Resources. PhD Thesis. Institute of Energy and Environment, University of Strathclyde; April 2009.

[19] Celli G, Ghiani E, Mocci S, Pilo F. A multi-objective evolutionary algorithm for the sizing and siting of distributed generation. IEEE Transactions on Power System 2005;20.

[20] Deb K. Multi-objective optimization using evolutionary algorithms. John Wiley and Sons; 2001, ISBN 047187339X.

[21] Konak A, Coit DW, Smith AE. Multi-objective optimization using genetic algorithms: a tutorial. Reliability Engineering and System Safety 2006;91: 992–1007.

[22] Leyland G. Multi-objective Optimization Applied To Industrial Energy Problems. Doctoral Dissertation. Ecole Poly-technique Fédérale de Lausanne; 2002.

[23] Hawkes AD, Leach MA. Cost-effective operating strategy for residential microcombined heat and power. Energy 2007;32(5):711–23.

[24] Houwing M, Ajah AN, Heijnen PW, Bouwmans I, Herder PM. Uncertainties in the design and operation of distributed energy resources: the case of micro-CHP systems. Energy 2008;33(10):1518–36.

[25] Bracco S, Dentici G, Siri S. Economic and environmental optimization model for the design and the operation of a combined heat and power distributed generation system in an urban area. Energy 2013;55:1014-24.

[26] Motevasel M, Seifi AR, Niknam T. Multi-objective energy management of CHP (combined heat and power)-based micro-grid. Energy 2013;51:123-36.

[27] Ren H, Gao W. Economic and environmental evaluation of micro CHP systems with different operating modes for residential buildings in Japan, Energy and Buildings 2010;42:853-861.

[28] Van Schijndel AWM. Optimal operation of a hospital power plant. Energy and Buildings 2002;34(10):1155–65.

[29] Wakui T, Yokoyama R, Shimizu K. Suitable operational strategy for power interchange operation using multiple residential SOFC (solid oxide fuel cell) cogeneration systems. Energy 2010;35(2):740–50.

[30] Mancarella P, Chicco G. Global and local emission impact assessment of distributed cogeneration systems with partial-load models. Applied Energy 2009;86(10):2096–106.

[31] Wang J, Jing Y, Zhang C. Optimization of capacity and operation for CCHP system by genetic algorithm, Applied Energy 2010;87:1325-1335.

[32] Kong XQ, Wang RZ, Huang XH. Energy optimization model for a CCHP system with available gas turbines, Applied Thermal Engineering 2005;25:377:391.

[33] Abdollahi G, Meratizaman M. Multi-objective approach in thermoenvironomic optimization of a small-scale distributed CCHP system with risk analysis. Energy and Buildings 2011;43:3144-3153.

[34] Mago PJ, Chamra LM. Analysis and optimization of CCHP systems based on energy, economical, and environmental considerations, Energy and Buildings 2009;41:1099-1106.

[35] Roque Díaz P, Benito YR, Parise JAR. Thermoeconomic assessment of a multi-engine, multi-heat-pump CCHP (combined cooling, heating and power generation) system a case study. Energy 2010;35:3540-3550.

[36] Chicco G, Mancarella P. Matrix modelling of small-scale trigeneration systems and application to operational optimization. Energy 2009;34:261-273.

[37] Ortiga J, Bruno JC, Coronas A. Selection of typical days for the characterisation of energy demand in cogeneration and trigeneration optimisation models for buildings. Energy Conversion and Management 2011; 52:1934-1942.

[38] Carvalho M, Lozano MA, Serra L.M. Multicriteria synthesis of trigeneration systems considering economic and environmental aspects, Applied Energy 2012;91:245-254.

[39] Chang KH, Lin G. Optimal design of hybrid renewable energy systems using simulation optimization. Simulation Modelling Practice and Theory 2015;52:40–51.

[40] Yan B, Luh PB, Sun B, Song C, Dong C, Gan Z, et al. Energy-efficient management of eco-communities. In: Proceedings of IEEE CASE; Madison, USA, 2013 August 17–20.

[41] Guan X, Xu Z, Jia Q. Energy-efficient buildings facilitated by microgrid. IEEE Trans Smart Grid 2011;1:466–73.

[42] Zhou Z, Liu P, Li Z, Ni W. An engineering approach to the optimal design of distributed energy systems in China. Applied Thermal Engineering 2013;53(2):387-396.

[43] Mehleri ED, Sarimveis H, Markatos NC, Papageorgiou LG. A mathematical programming approach for optimal design of distributed energy systems at the neighbourhood level. Energy 2012;44(1):96-104.

[44] Burer M, Tanaka K, Farrat D, Yamada K. Multi-criteria optimization of a district cogeneration plant integrating a solid oxide fuel cell-gas turbine combined cycle, heat pumps and chillers. Energy 2003;28 (6): 497–518

[45] Cardona E, Piacentino A, Cardona F. Matching economical, energetic and environmental benefits: an analysis for hybrid CHCP-heat pump systems. Energy Conversion and Management 2006;47(20):pp. 3530–3542.

[46] Roque Díaz P, Benito YR, Parise JAR. Thermoeconomic assessment of a multi-engine, multi-heat-pump CCHP (combined cooling, heating and power generation) system – a case study. Energy 2010;35:3540–3550.

[47] Yan B, Luh PB, Bragin MA, Song C, Dong C, Gan Z. Energy-efficient building clusters. In: Proceedings of IEEE CASE Taiwan; Taipei, Taiwan, 2014 August 18–22.

[48] Weber C, Shah N. Optimisation based design of a district energy system for an eco-town in the United Kingdom. Energy 2011;36(2):1292-1308.

[49] Ren H, Zhou W, Nakagami KI, Gao W, Wu Q. Multi-objective optimization for the operation of distributed energy systems considering economic and environmental aspects. Applied Energy 2010;87(12):3642-3651.

[50] Buoro D, Casisi M, De Nardi A, Pinamonti P, Reini M. Multicriteria optimization of a distributed energy supply system for an industrial area. Energy 2013;58:128-137.

"Mathematical models become more realistic if cost and environmental concerns are explicitly considered, by giving them an explicit role as objective functions, rather than aggregating them in a single economic indicator objective function"

Chapter 3

Multi-objective operation planning of a Distributed Energy System through cost and environmental impact assessments

3.1. Introduction

In this chapter, an original tool based on a mathematical programming approach is presented to attain the optimal operation planning of a DES through cost and environmental impact assessments. The DES under consideration involves multiple energy conversion devices as well as thermal storage systems, which provide electricity, heat and cooling to end-users. A Multi-Objective Linear Programming (MOLP) problem is formulated based on the detailed modeling of the energy devices and thermal storage systems, to find the optimized operation strategies, which allow to reduce the energy cost, and the environmental impacts in terms of CO_2 emissions, while satisfying the given time-varying user demands. The economic objective is formulated as the total energy cost to be minimized, whereas the environmental objective is formulated as the total CO_2 emission to be minimized. The Pareto frontier, involving the best possible trade-offs between the economic objective, essential in the short-run, and the environmental objective, crucial in the long-run, is obtained by minimizing a weighted sum of the total energy cost and CO_2 emission, by using branch-and cut. The proposed tool allows to provide decision support to

planners for selecting the operations strategies of the DES, based on their short- and long-run priorities.

As an illustrative example, a large-scale utility customer (a large hotel located in Italy) is considered as end-user. The model is implemented by using IBM ILOG CPLEX Optimization Studio Version 12.5. Results of numerical testing show that the optimized operation strategies of the DES allow to reduce significantly energy costs and environmental impacts, as compared with conventional energy supply systems. In addition, a sensitivity analysis is carried out to analyze the effects of variations in the configuration of the DES on energy costs and environmental impacts.

In the following, the modeling of the DES including the detailed modeling of the energy devices and thermal storage is presented in Section 3.2. The economic and environmental objectives as well as the multi-objective optimization method are presented in Section 3.3. Results of the numerical testing, including results of the sensitivity analysis are presented in Section 3.4.

3.2. Problem formulation

The DES under consideration consists of energy conversion devices, thermal storage systems, and different types of end-user demands (electricity, domestic hot water, space heating and space cooling), interconnected via different energy carriers. The energy devices are chosen among the most commonly used in practical DESs. Figure 3.1 shows the scheme of the DES with the possible routes of energy carriers from energy resources via primary and secondary energy devices, and thermal energy storage systems to meet the user demands. Primary energy devices convert a set of primary input energy carriers into electricity and heat. Secondary energy devices convert electricity and heat for heating and cooling purposes. To allow more efficient use of thermal energy, thermal energy storage systems are also included in the DES confoguration.

The detailed modeling of energy devices and thermal storage, and the energy balances are presented in Subsections 3.2.1. The economic and environmental objectives, as well as the multi-objective optimization method are discussed in Subsection 3.2.2.

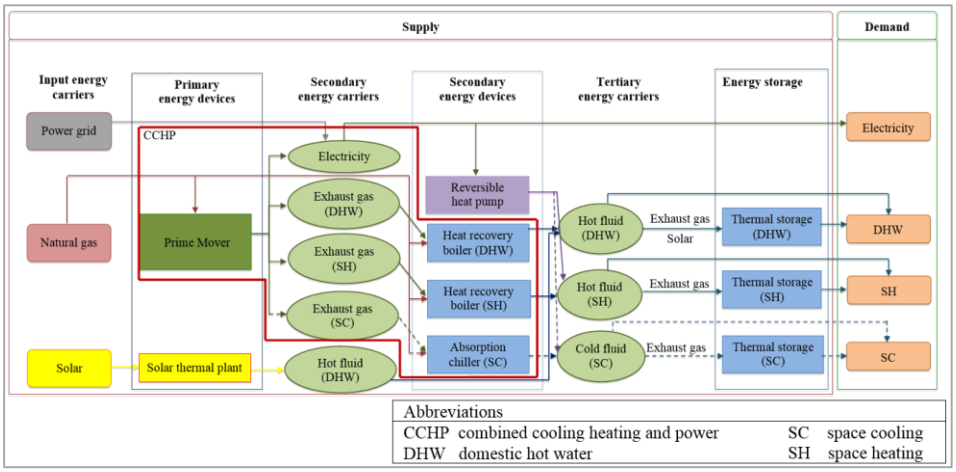

Figure 3.1. Scheme of the DES for the optimization problem

3.2.1. Modeling of energy devices and thermal storage

In this Subsection, the modeling of the CCHP system, solar thermal plant, reversible heat pump, and thermal energy storage is presented. It is assumed that the energy devices involved in the DES have constant efficiencies, although these latter actually depend on partial loads. The constant-efficiency assumption for energy devices is systematically used in the scientific literature for design and operation optimization problems of large-scale DESs, to maintain the problem linearity [1 - 6].

The common constraint for the prime mover in the CCHP, the solar thermal plant, heat recovery boilers, and heat pumps is the capacity constraint, described as follows.

If the energy device, *ED*, is in use, (the on/off binary decision variable, $x_{ED}(t)$ is equal to 1), its generation level, $R_{ED}(t)$ (a continuous decision variable), has to be within the minimum value, $R_{ED}^{\min}$, and the capacity, $R_{ED}^{\max}$:

$$x_{ED}(t)R_{ED}^{\min} \le R_{ED}(t) \le x_{ED}(t)R_{ED}^{\max} \tag{3.1}$$

Additional constraints of each energy device are presented in the following.

3.2.1.1 Modeling of Combined Cooling Heating and Power

The CCHP system consists of a prime mover (e.g., internal combustion engine, gas turbine) to meet the electricity demand; two heat recovery boilers, using high-

temperature exhaust gas to satisfy the demands of space heating and domestic hot water; and an absorption chiller, using also high-temperature exhaust gas to satisfy the space cooling demand [7]. The layout of the CCHP system is sketched inside the bold lines in Figure 3.1. Heating and cooling can be also directly provided by supplementary burning of natural gas in the boilers, and the absorption chiller, respectively. Constraints considered for the CCHP system are presented below.

The CCHP ramp rate constraints limit the variations in the power generation between two successive time steps to be within the ramp-down, DR_{CCHP}, and ramp-up, UR_{CCHP}, [8]:

$$-DR_{CCHP} \le \dot{E}_{CCHP}(t) - \dot{E}_{CCHP}(t-\Delta t) \le UR_{CCHP} \tag{3.2}$$

where $\dot{E}_{CCHP}(t)$ and $\dot{E}_{CCHP}(t-\Delta t)$ are the energy generation levels at time t and (t - Δt), respectively. The ramp-down rate, DR_{CCHP}, and ramp-up rate, UR_{CCHP}, are assumed to be the same [9, 10].

The volumetric flow rate of natural gas, $\dot{G}_{PM}(t)$, required by the prime mover to provide the electricity rate, $\dot{E}_{CCHP}(t)$, is:

$$\dot{G}_{PM}(t) = \dot{E}_{CCHP}(t) / \left(\eta_{e,PM} LHV_{NG}\right) \tag{3.3}$$

where $\eta_{e,PM}$ is the electric efficiency of the prime mover, that represents how much electricity can be obtained by the combustion of the unit volumetric flow rate of natural gas in the prime mover, and LHV_{NG} is the lower heat value of natural gas.

The heat rate made available by the exhaust gas recovered from the prime mover, $\dot{Q}_{PM,ex}(t)$, is:

$$\dot{Q}_{PM,ex}(t) = \dot{E}_{CCHP}(t)\left(1-\eta_{e,PM}-\mu_{PM}\right)/\eta_{e,PM} \tag{3.4}$$

where μ_{PM} is the percent heat loss of the prime mover which cannot be recovered.

The exhaust gas can be subdivided among the heat recovery boilers and the absorption chiller to supply heating for domestic hot water and space heating demands, as well as cooling for space cooling demand, respectively. The heat rate

delivered by the exhaust gas to the heat recovery boiler for the domestic hot water demand, $\dot{H}_{ex}^{DHW}(t)$, is:

$$\dot{H}_{ex}^{DHW}(t) = \dot{Q}_{PM,ex}(t)\xi_{DHW}(t)\eta_{HR,boil} \tag{3.5}$$

where $\eta_{HR,boil}$ is the waste heat recovery efficiency of the boiler, and the continuous decision variable $\xi_{DHW}(t)$ is the percentage of exhaust gas supplied to the heat recovery boiler for the domestic hot water demand.

Heating can be also directly provided by supplementary burning of natural gas in the boiler. The volumetric flow rate of natural gas, $\dot{G}_{boil}^{DHW}(t)$, required by the boiler to directly provide the heat rate $\dot{H}_{di}^{DHW}(t)$ is:

$$\dot{G}_{boil}^{DHW}(t) = \dot{H}_{di}^{DHW}(t) / \left(\eta_{boil} LHV_{gas}\right) \tag{3.6}$$

where η_{boil} is the combustion efficiency of the boiler.

Therefore, the total generation level of the heat recovery boiler for the domestic hot water demand, $\dot{H}_{CCHP}^{DHW}(t)$, is formulated as the sum of the heat rate obtained by exhaust gas, $\dot{H}_{ex}^{DHW}(t)$, and the heat rate directly provided by the supplementary burning of natural gas in the boiler, $\dot{H}_{di}^{DHW}(t)$:

$$\dot{H}_{CCHP}^{DHW}(t) = \dot{H}_{ex}^{DHW}(t) + \dot{H}_{di}^{DHW}(t) \tag{3.7}$$

Modeling of heating by the CCHP system for the space heating demand is similar to that described above.

The cooling rate delivered by the exhaust gas to the absorption chiller, $\dot{C}_{ex}(t)$, is:

$$\dot{C}_{ex}(t) = \dot{Q}_{PM,ex}(t)\xi_{SC}(t)\eta_{HR,abs}COP_{abs} \tag{3.8}$$

where $\eta_{HR,abs}$ is the waste heat recovery efficiency of the absorption chiller, and COP_{abs} is its coefficient of performance. The continuous decision variable $\xi_{SC}(t)$ is the percentage of exhaust gas supplied to the absorption chiller.

As for the domestic hot water and space heating demands, cooling can be also directly provided by supplementary burning of natural gas in the absorption chiller. The volumetric flow rate of natural gas, $\dot{G}_{abs}(t)$, required by the absorption chiller to directly provide the cooling rate $\dot{C}_{di}(t)$ is:

$$\dot{G}_{abs}(t) = \dot{C}_{di}(t) / \left(COP_{abs} \eta_{abs} LHV_{gas} \right) \tag{3.9}$$

where η_{abs} is the efficiency of the absorption chiller combustor. Therefore, the total generation level of the absorption chiller, $\dot{C}_{CCHP}(t)$, is formulated as the sum of the cooling rate obtained by exhaust gas, $\dot{C}_{ex}(t)$, and the cooling rate directly provided by supplementary burning of natural gas in the absorption chiller, $\dot{C}_{di}(t)$:

$$\dot{C}_{CCHP}(t) = \dot{C}_{ex}(t) + \dot{C}_{di}(t) \tag{3.10}$$

The sum of gas turbine exhaust fractions for domestic hot water, $\xi_{DHW}(t)$, for space heating, $\xi_{SH}(t)$, in heat recovery boilers, and for space cooling, $\xi_{SC}(t)$, in the absorption chiller, has to be one:

$$\xi_{DHW}(t) + \xi_{SH}(t) + \xi_{SC}(t) = 1 \tag{3.11}$$

The overall volumetric flow rate of natural gas consumed by the CCHP system, $\dot{G}_{CCHP}(t)$, is:

$$\dot{G}_{CCHP}(t) = \dot{G}_{PM}(t) + \dot{G}_{boil}^{DHW}(t) + \dot{G}_{boil}^{SH}(t) + \dot{G}_{abs}(t) \tag{3.12}$$

where $\dot{G}_{boil}^{SH}(t)$ is the volumetric flow rate of natural gas required by the boiler to directly provide heating for the space heating demand.

3.2.1.2 Modeling of the solar thermal plant

The solar thermal plant is used to meet the domestic hot water demand. The heat rate provided by the solar plant, $\dot{H}_{ST}(t)$, depends on the collector area, A_{coll}, the thermal efficiency, η_{coll}, and the total solar irradiance, $\dot{I}_T(t)$, and it is expressed as [5]:

$$\dot{H}_{ST}(t) = \eta_{coll} A_{coll} \dot{I}_T(t) \tag{3.13}$$

where the collector area is assumed to be known, since the optimal design of the DES is not the aim of this study.

3.2.1.3 Modeling of the reversible heat pump

A reversible heat pump is used to meet the space heating and cooling demands in the heating and cooling modes, respectively. In the heating mode, the electricity consumption of the heat pump, $\dot{E}_{HP}(t)$, to provide the heat rate, $\dot{H}_{HP}(t)$, is given by:

$$\dot{E}_{HP}(t) = \dot{H}_{HP}(t) / COP_{HP} \tag{3.14}$$

where COP_{HP} is the coefficient of performance of the heat pump in the heating mode. Modeling of cooling mode is similar to that described above.

3.2.1.4 Modeling of thermal energy storage

The energy stored in the domestic hot water tank at the time t, $H_{sto}(t)$, depends on the non-dissipated energy stored at the previous time step ($t - \Delta t$); the heat rate input to the storage, $\dot{H}_{sto}^{in}(t)$ (a continuous decision variable); and the heat rate released by the storage, $\dot{H}_{sto}^{out}(t)$ (a continuous decision variable). It can be expressed as follows [11]:

$$H_{sto}(t) = H_{sto}(t - \Delta t)(1 - \varphi_{sto}(\Delta t)) + \left(\dot{H}_{sto}^{in}(t) - \dot{H}_{sto}^{out}(t)\right)\Delta t \tag{3.15}$$

where the loss fraction $\varphi_{sto}(\Delta t)$ accounts for the heat losses through the tank walls during the time interval, Δt. Modeling of thermal storage systems for space heating and cooling is similar to that described above.

3.2.2. Energy balances

In order to satisfy the given time-varying user demands, electricity and thermal energy balances are formulated by matching supply and demand.

3.2.2.1 Electricity balance

The electricity rate demand, $\dot{E}_{dem}(t)$, and the electricity rate required by the heat pump, $\dot{E}_{HP}(t)$, must be covered by the sum of the electricity rate provided by the CCHP system, $\dot{E}_{CCHP}(t)$, and the electricity rate bought from the grid (a continuous decision variable), $\dot{E}_{buy}(t)$:

$$\dot{E}_{dem}(t) + \dot{E}_{HP}(t) = \dot{E}_{CCHP}(t) + \dot{E}_{buy}(t) \tag{3.16}$$

3.2.2.2 Domestic hot water energy balance

The heat rate demand for domestic hot water, $\dot{H}_{dem}^{DHW}(t)$, must be satisfied by the sum of the heat rate provided by the CCHP system, $\dot{H}_{CCHP}^{DHW}(t)$, which is the sum of the heat rate provided by the exhaust gas and the heat rate directly provided by the supplementary burning of natural gas in the boiler; the heat rate provided by the solar thermal plant, $\dot{H}_{ST}(t)$; and the heat rate provided by the thermal storage, $\dot{H}_{sto}^{out}(t) - \dot{H}_{sto}^{in}(t)$:

$$\dot{H}_{dem}^{DHW}(t) = \dot{H}_{CCHP}^{DHW}(t) + \dot{H}_{ST}(t) + \dot{H}_{sto}^{out}(t) - \dot{H}_{sto}^{in}(t) \tag{3.17}$$

The space heating and cooling energy balances can be expressed in a similar way.

3.3. Multi-objective optimization: energy costs and environmental impacts

In order to consider the economic priority, crucial in the short-run, and the environmental impacts, essential in the long-run, two objectives, i.e., economic and environmental, are involved in the optimization problem, as presented in Subsection 3.3.1. The multi-objective optimization method is discussed in Subsection 3.3.2.

3.3.1 Economic and environmental objectives

The economic objective is to minimize the total energy cost, *Cost*, which is the sum of two terms: cost of buying electricity from the power grid, and cost of natural gas, as follows:

$$Cost = \sum_t \left(P_{grid}(t) \dot{E}_{buy}(t) + P_{NG} \dot{G}_{buy}(t) \right) \Delta t \tag{3.18}$$

where $P_{grid}(t)$ is the time-of-day unit price of electricity from the power grid at time t, P_{NG} is the constant unit price of natural gas, and Δt is the length of the time interval. In Eq. (3.15), the volumetric flow rate of natural gas bought, $\dot{G}_{buy}(t)$, corresponds to the total energy consumption requirement of the CCHP system, $\dot{G}_{CCHP}(t)$.

The environmental objective is to minimize the environmental impact, *Env*, in terms of CO_2 emission from the power grid and the consumed fuels. The CO_2 emission due to the use of electricity from the power grid is evaluated by multiplying the carbon intensity of the power grid, E_{cin}, and the total amount of electricity taken from the power grid, $\dot{E}_{buy}(t)$. The carbon intensity of the power grid that the DES is connected to, is the amount of CO_2 emission per unity of electricity generated, which depends on the fuel mix. The CO_2 emission due to the natural gas consumption is evaluated by multiplying the carbon intensity of the fuel, G_{cin}, and the total amount of fuel consumed by the CCHP, $\dot{G}_{CCHP}(t)$, which corresponds to the volumetric flow rate of natural gas bought, $\dot{G}_{buy}(t)$ [12]. Therefore, the environmental objective function is expressed as:

$$Env = \sum_t \left(E_{cin} \dot{E}_{buy}(t) + G_{cin} \dot{G}_{buy}(t) \right) \Delta t \tag{3.19}$$

3.3.2 Multi-objective optimization method

With the economic objective function (Eq. 3.18) and the environmental one (Eq. 3.19), the problem has two objective functions to be minimized. To solve this multi-objective problem, the weighted-sum method is used. Therefore, a single objective function is formulated as a weighted sum of the total energy cost, *Cost*, and the environmental impact, *Env*, to be minimized:

$$F_{obj} = c\omega Cost + (1-\omega) Env \tag{3.20}$$

where the constant c is a scaling factor, chosen such that c *Cost* and *Env* have the same order of magnitude. For $\omega = 1$, the economic optimization is carried out and the

solution that minimizes the total energy cost can be found. For ω = 0, the environmental impact optimization is carried out, and the solution that minimizes the total CO_2 emission can be found. Then, the scaling factor c is calculated as the ratio of the maximum total CO_2 emission obtained by the economic optimization to the maximum total energy cost obtained by the environmental impact optimization. With the constant c, the Pareto frontier involving the best possible trade-offs between the two objectives can be found by varying the weight ω in between the interval 0 and 1. The problem formulated in Sections 3.2 and 3.3 is linear, and involves both discrete and continues variables, so this mixed integer linear programming problem is to be solved by branch-and-cut. Figure 3.2 shows the flow-chart to find the optimized operation strategies of the DES, with both the economic and environmental objectives. Given the input data, by solving the above optimization problem, the Pareto frontier, consisting of the best possible trade-offs between the two objectives can be found. Each point on the Pareto frontier corresponds to a different operation strategy of the DES, thereby providing decision support to planners for selecting the operations strategy, based on their short- and long-run priorities.

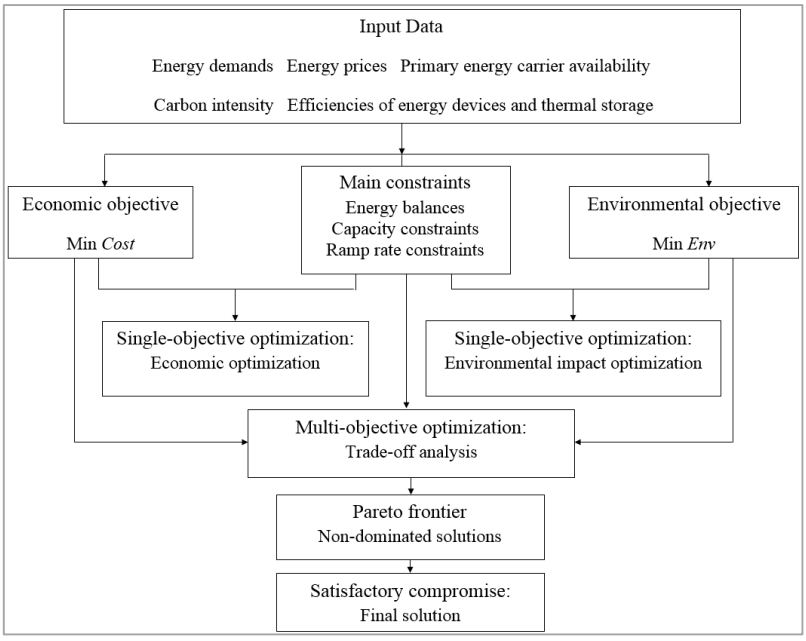

Figure 3.2. Flow-chart of the multi-objective optimization problem.

3.4. Numerical testing: an Italian case study

The method developed above is implemented by using IBM ILOG CPLEX Optimization Studio Version 12.5. Branch-and-cut is powerful for mixed-integer linear optimization problems, and easy to code by using commercial solvers. CPLEX, a popular solver where branch-and-cut is implemented with flexibility and high-performance, is therefore used to solve the optimization problem. As an illustrative example, a hypothetic large hotel of 16,000 m^2 located in Italy (D climatic zone [13]) is selected as the targeted end-user. In Europe, hotel facilities have ranked among the top five in terms of energy consumption in the tertiary building sector [14]. Moreover, in Italy, interest has been intensifying in promoting DESs, as demonstrated by several research and demonstration projects [15 - 18]. A typical winter day is chosen, with one hour as time-step. The configuration of the DES, including the sizes of energy devices and thermal energy storage systems, is sketched in Figure 3.3. Since a winter day is chosen, the energy devices and thermal storage for meeting the space cooling demand are not represented in Figure 3.3.

In the following, the input data for the optimization model are presented in Subsection 3.4.1. Results of the multi-objective optimization problem are presented and discussed in Subsection 3.4.2. To show the effects of variations in the configuration of the DES on energy costs and environmental impacts, results of the

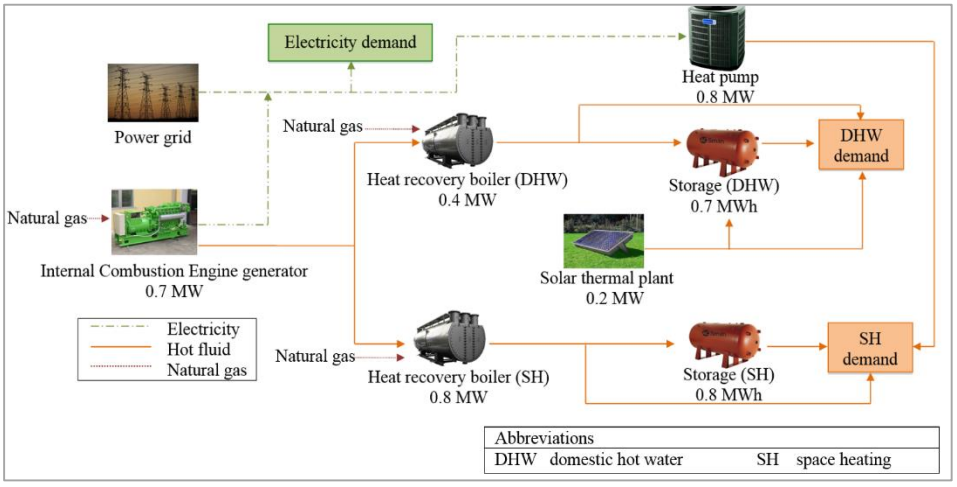

Figure 3.3. DES configuration analyzed for the hypothetic hotel in Italy.

sensitivity analysis are presented and discussed in Subsection 3.4.3.

3.4.1 Input data

The required input data include building energy demands, energy prices, primary energy carriers availability, carbon intensity, and efficiencies of energy devices and thermal storage as discussed below.

3.4.1.1 Building energy demands

The hourly electricity, domestic hot water, and space heating demands are taken from a comprehensive investigation about energy demands of hotels in Italy [19 -21], and the energy rate demand profiles for a typical winter day are chosen as shown in Figure 3.4.

3.4.1.2 Energy prices

The time-of-day unit price of electricity from the power grid and the unit price of natural gas are chosen according to the current Italian market scenario. With reference to the Italian BTA6 tariff [22] for industrial use of electricity from the power grid, the unit price (€/kWh) accounts for the sum of the energy and dispatching prices, the power distribution and transmission quotas, the equalization component,

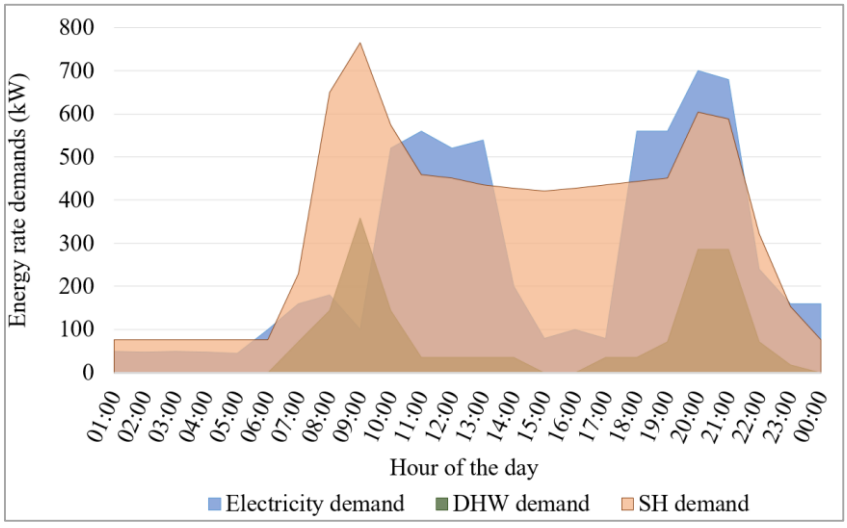

Figure 3.4. Energy rate demands of a hypothetic hotel in Italy for a representative winter day.

and the excise fee. The time-of-day grid price considered in this study is shown in Figure 3.5. For the natural gas, the tariff for industrial use is adopted [23]. Reference is made to a unit price (€/Nm^3) consisting of the energy quotas (energy unit price and additional charges), the other variable quotas as distribution and transport sale quotas, and the excise fee.

3.4.1.3 Primary energy carriers availability

The energy carriers input to the DES are electricity from the power grid, natural gas and solar energy. The first two are assumed unlimited, whereas the heat rate provided by the solar thermal plant is derived by the solar energy input taken from meteorological data for the considered location [24]. The hourly solar irradiance of a representative winter day is evaluated as the average of the solar irradiance in the corresponding hours of all winter days.

3.4.1.4 Carbon intensity

The carbon intensities of electricity from the power grid and natural gas are needed to evaluate the total amount of CO_2 emission related to the operation of the DES. The carbon intensity of the power grid is taken from [25] equal to 0.354 kg/kWh, as the averaged value in the years 2009-2011 for Europe. The carbon intensity of natural gas is taken from [12] equal to 0.202 kg/kWh.

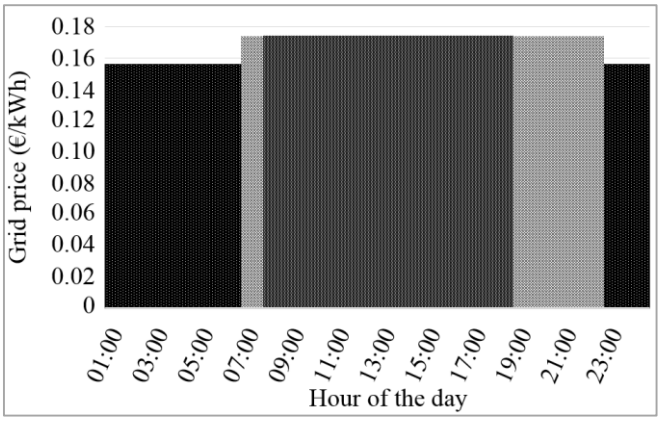

Figure 3.5. Time-of-day grid price for industrial use.

3.4.1.5 Efficiency of energy devices and thermal storage

In the following, reference is made to a gas-fired internal combustion engine as the prime mover of the CCHP system with an actual nominal peak output of 700 kW, and an exhaust gas temperature of 623.15 K. It operates at a 35% gas-to-electric efficiency, with a 15% heat loss fraction [26]. An efficiency of 90% is chosen for the natural gas boiler. The exhaust gas temperature of the heat recovery boiler can be safely brought down to 363.15 K [12]. The heat recovery efficiency of the boiler is defined as the ratio of difference between the exhaust gas temperature from the prime mover and the exhaust gas temperature out of the heat recovery boiler to the difference between the exhaust gas temperature from the prime mover and the ambient temperature [7]. The thermal efficiency of the solar collectors is assumed to be 40%. A typical value of the coefficient of performance of heat pumps in Italy is used. The loss fractions of thermal storage systems are assumed equal to 0.10. The above mentioned data are listed in Table 3.1.

3.4.2 Results of the multi-objective optimization problem

With the input data described above, the optimization problem can be solved within several seconds with a mixed integer gap 0.1%. The Pareto frontiers obtained without and with the discount on the excise fee of natural gas applicable to high-efficiency cogeneration systems are presented in Subsection 3.4.2.1. The optimized operation strategies obtained at various trade-off points are discussed in Subsection 3.4.2.2.

Table 3.1 Efficiency of energy devices and thermal storage systems.

Primary energy devices	**Efficiency**	
	Electrical	Thermal
Internal combustion engine	0.35	0.50
Solar thermal plant		0.40
Secondary energy devices	**Efficiency**	
Heat pump	$COP_{HP} = 3.0$	
Heat recovery boiler	$\eta_{HR,boil} = 0.75$	$\eta_{boil} = 0.90$
Thermal energy storage	**Storage loss fraction**	
DHW and SH storage	$\phi_{sto} = 0.10$	

3.4.2.1 Pareto frontier

Figure 3.6 shows the Pareto frontiers obtained without and with the discount on the excise fee of natural gas applicable to high-efficiency cogeneration systems with a Primary Energy Saving (PES) > 0 [27]. In the first case, the natural gas tariff for industrial use described in Subsection 3.4.1.2 is adopted, considering the excise fee for industrial use for all the natural gas consumed by the CCHP system [28]. In the second case, the discount on the excise fee for natural gas is involved, since the CCHP system has a PES > 0. According to [28], this discount is applied to a 0.25 Nm^3 volumetric flow rate of natural gas consumed by the CCHP system for each kWh of electricity provided. The additional consumption of natural gas, which occurs when the CCHP system has an electrical efficiency less than 42%, is subjected to the industrial excise fee. Also the natural gas consumed by the boilers to directly provide heating for the domestic hot water and space heating demands is subjected to the industrial excise fee [28].

In the first case (without discount on the excise fee of natural gas), the point marked with *a* is obtained by minimizing the daily energy cost, and the daily energy cost is 1,260 €/d, whereas the daily CO_2 emission is 4,160 kg/d. The point marked with *b* is obtained by minimizing the environmental impacts (the daily CO_2 emission), and the daily energy cost is 1,594 €/d, whereas the daily CO_2 emission is 3,448 kg/d. The points between the extreme points are found by equally subdividing the weight interval into 100 spaces.

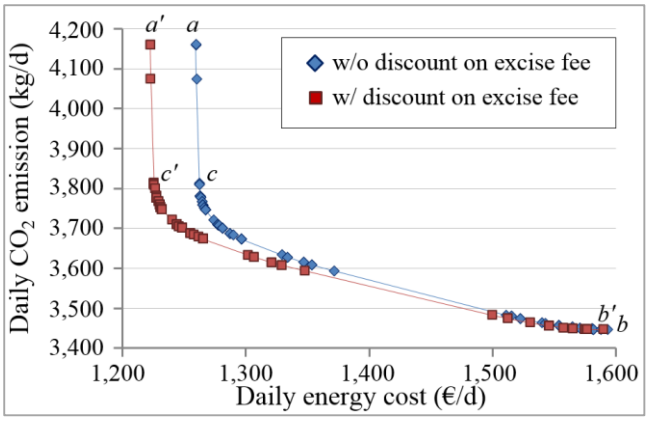

Figure 3.6. Pareto frontiers obtained without and with the discount on the excise fee of natural gas

In the second case (with discount on the excise fee of natural gas), the Pareto frontier is obtained in the same way, where the points marked with *a'* and *b'* are obtained by minimizing the daily energy cost and the daily CO_2 emission, respectively. In both cases, a significant reduction, 8%, in the CO_2 emission is gained from solution points *a* and *a'* (obtained for $\omega = 1$) to the solution points *c* and *c'* (obtained for $\omega = 0.9$) with a negligible 0.25% increase in the energy cost. The differences between the two Pareto frontiers become more significant when the weight for the economic objective increases (left side). Under the economic optimization, at the point *a'*, the daily energy cost is 1,223 €/d and it is reduced by about 3% as compared with the energy cost at the point *a*. The total CO_2 emission is the same as those at the point *a*. When the weight for the environmental objective increases, the sensitivity of the DES operation to the energy prices reduces, therefore the difference between the Pareto frontiers also reduces (right side). Under the environmental impact optimization, at the point *b'*, the daily energy cost is 1,589 €/d and the daily CO_2 emission is the same as those at the point *b*, since, when the environmental objective is minimized, the operation of the DES is not sensitive to the energy prices. Under the environmental impact optimization, the daily energy cost at the point *b'* is almost equal to that at the point *b*, because of the very small difference between the discounted excise and the full excise prices for industrial use.

3.4.2.2 Optimized operation strategies at various trade-off points

Each point on the Pareto frontier corresponds to a different operation strategy of the DES. To understand how the operation strategies of the DES affect the energy cost and the CO_2 emission under different weight values, the results at various trade-off points are shown in Figure 3.7. These trade-off points belong to the Pareto frontier obtained when the discount on the excise fee is involved (red Pareto frontier in Figure 3.6).

Figure 3.7a points out that, as ω increases from 0 to 1 (from the environmental impact optimization the economic optimization), the share of the electricity load (the sum of electricity demand and electricity rate required by the heat pump) satisfied by the CCHP significantly increases (5% to 59%), highlighting that the CCHP system allows to reduce the total energy cost. The opposite occurs to the share of electricity load covered by the grid power. The maximum value is obtained when the

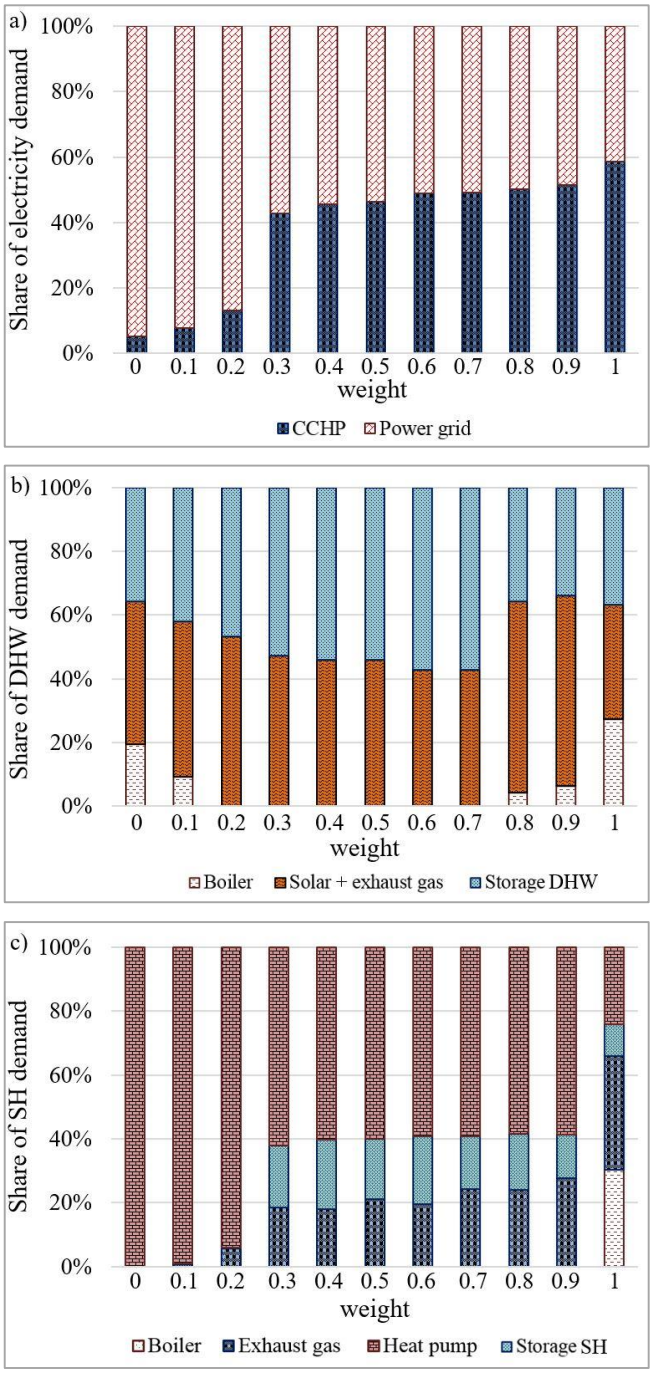

Figure 3.7. Optimized operation strategies of the DES at various trade-off points for a) electricity; b) domestic hot water; c) space heating.

environmental impact is minimized, since the space heating demand is fully satisfied by the heat pump, as shown in Figure 3.7c. As ω increases from 0 to 1, the share of the space heating demand satisfied by the heat pump decreases, whereas the share covered by the heat recovery boiler driven by exhaust gas increases because of the increase in the use of the CCHP system as shown in Figure 3.7a. Under the economic optimization, the operation of the DES is only sensitive to energy prices, and the CCHP system instead of the power grid is mostly used to provide electricity.

It is also worth noting that Figures 3.7a, 3.7b and 3.7c are strongly related. For instance, the CCHP system is rarely used when the environmental impact is minimized, since the space heating demand is fully satisfied by the heat pump. Correspondingly, the heat rates from exhaust gas and the solar thermal plant do not completely satisfy the domestic hot water demand, and the integration with the boiler driven by natural gas is needed. As the use of the CCHP system increases and the use of the heat pump reduces, the amount of exhaust gas increases, and the integration with the boiler driven by natural gas is not needed. When the weight of the economic objective is close to 1 (ω = 0.8 and ω = 0.9), the natural gas boiler is used to satisfy a small share (3 - 5%) of the domestic hot water demand. Although under the economic optimization the use of the CCHP system reaches the maximum value, exhaust gas are not enough to satisfy the domestic hot water and space heating demands. Therefore, the use of natural gas boilers significantly increases consistently with the reduction in the use of the heat pump. The remarkable difference in the operation of the DES from ω = 1 to ω = 0.9 corresponds to the big jump from *a'* to *c'* shown in Figure 3.6.

3.4.3 Sensitivity analysis

A sensitivity analysis is carried out to investigate the effects of variations in the configuration of the DES on energy cost and environmental impacts. The configurations analyzed are listed in Table 3.2. For each configuration, one, two or three energy devices are taken out of the DES configuration shown in Figure 3.3 (considered as the reference case), including the thermal storage systems, the solar thermal plant, the heat pump, the prime mover in the CCHP system. In Configuration 8, the prime mover (i.e., the gas-fired internal combustion engine), is substituted with a gas turbine generator of the same capacity.

Table 3.2. Configurations investigated in the sensitivity analysis

Configuration	Energy devices excluded from the reference case (Configuration 1)
2	without SH storage
3	without solar thermal plant
4	without solar thermal plant and DHW storage
5	without solar thermal plant, DHW/SH storage
6	without heat pump
7	without internal combustion engine
Configuration	**Other cases**
8	Gas turbine instead of internal combustion engine
9	Conventional energy supply system

In order to show the contribution of each energy device and thermal storage in reducing energy costs and CO_2 emission separately, the single-objective optimization is carried out for the different configurations of the DES. Moreover, the daily energy cost and CO_2 emission are also evaluated for one of the most common conventional energy supply systems, consisting of the power grid used to meet the electricity demand, and natural gas boilers used to meet the domestic hot water and space heating demands.

Results of the single-objective optimization for the different configurations analyzed are presented and discussed in Subsection 3.4.3.1. In addition, the multi-objective optimization is carried out for the most significant configurations, to compare the related Pareto frontiers with that obtained in the reference case. The related results are presented in Subsection 3.4.3.2.

3.4.3.1 Single-objective optimization for different configurations of the DES

The daily energy cost obtained by the economic optimization and the daily CO_2 emission obtained by the environmental impact optimization are shown in Figures 3.8a and b, respectively. Configuration 1 is the reference case, where the minimum energy cost and minimum CO_2 emission are obtained by the economic and environmental impact optimizations, respectively. For Configuration 2, there is a negligible increase in the energy cost and no change in CO_2 emission, compared with those of the reference case. This highlights the small impact of the space heating

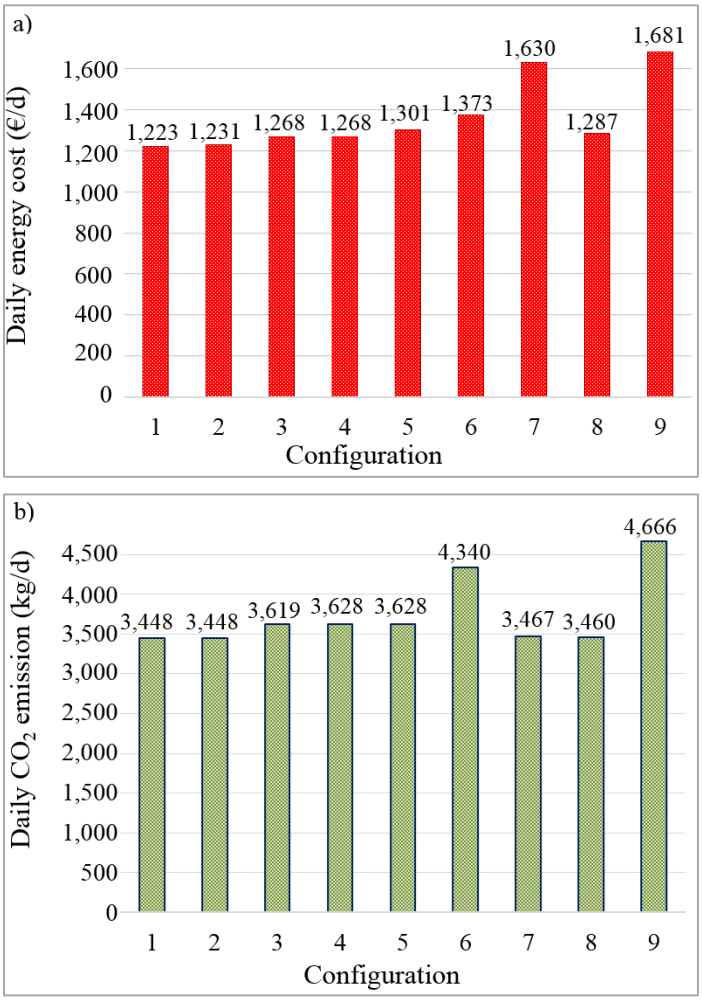

Figure 3.8. a) Daily energy cost for Configurations 1-9 under the economic optimization; b) Daily CO_2 emission for Configurations 1-9 under the environmental impact optimization.

storage on both the objectives.

Configuration 3 excludes the solar thermal plant. A 3% increase in the energy cost, and a 5% increase in the CO_2 emission compared with those of the reference case, respectively, confirm the importance of this energy device for both the economic and environmental objectives. Besides the solar thermal plant, Configurations 4 and 5 exclude the domestic hot water storage and both the thermal

storage systems respectively, and results are similar to those obtained for Configuration 3.

Configuration 6 excludes the heat pump. The daily energy cost is 11% higher than that in the reference case. The daily CO_2 emission is 21% higher than that in the reference case. Therefore, the heat pump affects the environmental impacts more than the energy costs, as also shown in Figure 3.7c. Under the environmental impact optimization, the space heating demand is fully satisfied by the heat pump, whereas under the economic optimization, the share of space heating demand satisfied by the heat pump reaches the minimum value.

Configuration 7 excludes the gas-fired internal combustion engine. The electricity load is fully satisfied by the power grid, and without exhaust gas, the heat recovery boilers are fuelled by natural gas. The opposite trends of energy costs and CO_2 emission as compared with those of Configuration 6 are exhibited. The daily energy cost is 25% higher than that in the reference case. However, the daily CO_2 emission is only 0.5% higher than that in the reference case. This result is also remarkable in Figure 3.7a, since under the environmental impact optimization, only 5% of the electricity load is satisfied by the CCHP system.

In Configuration 8, the energy cost is increased by 5% and the CO_2 emission is increased by 0.3%, as compared with those in the reference case, respectively. This confirms that the gas-fired internal combustion engine is a better solution as prime mover in terms of costs and environmental impacts than the gas turbine generator, due to the higher total energy conversion efficiency of the CCHP system with the gas-fired internal combustion engine than that of the CCHP system with the gas turbine. It can be noticed that the effect of the prime mover change has larger effects on energy costs than environmental impacts.

Finally, for the conventional energy supply system, the daily energy cost and the daily CO_2 emission are 27% and 26% higher than those in the reference case, respectively. This latter result show that the energy cost and the environmental impacts are strongly reduced by the optimized operation of the DES.

3.4.3.2 Multi-objective optimization for different configurations of the DES

The Pareto frontiers obtained by the multi-objective optimization for Configurations 3, 6, 8, as well as for the reference case are presented in Figure 3.9.

For Configuration 3 (without solar thermal plant), the Pareto frontier is similar to that in the reference case, especially in the left side (ω is close to 1). The CO_2 emission is highly reduced (10%) when ω varies from 1 to 0.9, with a negligible increase in the energy cost (0.31%). When the weight of the environmental objective increases over that of the economic one (right side), the slope of the Pareto frontier is lower than that of the reference case. This means that when more attention is paid to the environmental performance, the energy cost increase is larger than the CO_2 emission reduction, as compared with the reference case. The daily energy costs obtained by the economic and environmental impact optimizations are 24% and 22% lower than those obtained with the conventional energy supply system (Configuration 9), respectively.

For Configuration 6 (without heat pump), very few trade-offs points are obtained. The difference between the maximum and minimum daily energy cost obtained by the environmental impact and economic optimization, respectively, is only 1.5%. The difference between the maximum and minimum daily CO_2 emission obtained by the economic and environmental impact optimizations is only 0.34%. This is because of the flat shape of the Pareto frontier, which implies a negligible reduction in CO_2 emission with a significant increase in the energy cost. Daily energy costs obtained by the economic and environmental impact optimization are 18% and 7% lower than those obtained with the conventional energy supply system (Configuration 9), respectively.

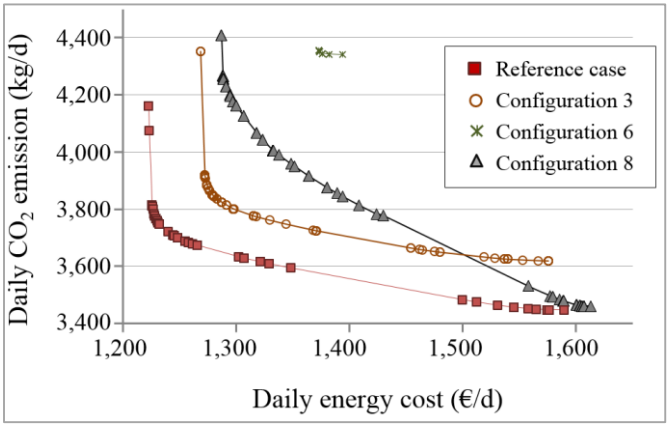

Figure 3.9. Pareto frontiers for Configurations 3, 6, 8 and Reference case.

For Configuration 8 (gas turbine generator instead of gas-fired internal combustion engine as prime mover), the shape of the Pareto frontier is different from that in the reference case. The slope of the Pareto frontier changes more quickly than that of the Pareto frontier in the reference case. When ω varies from 1 to 0.9, there is a negligible increase in the energy cost (0.12%), and the reduction in the CO_2 emission is about 3.4%. The daily energy costs obtained by the economic and environmental impact optimizations are 23% and 26% lower than those obtained with the conventional energy supply system (Configuration 9), respectively.

References

[1] Söderman J, Pettersson F. Structural and operational optimisation of distributed energy systems. Applied Thermal Engineering 2006;26:1400–8.

[2] Ren H, Weisheng Z, Ken'ichi N, Weijun G, Qiong W. Multi-objective optimization for the operation of distributed energy systems considering economic and environmental problems. Applied Energy 2010;87:3642–51.

[3] Hawkes AD, Leach MA. Modelling high level system design and unit commitment for a microgrid. Applied Energy 2009;86:1253–65.

[4] Mehleri ED, Sarimveis H, Markatos NC, Papageorgiou LG. A mathematical programming approach for optimal design of distributed energy systems at the neighbourhood level. Energy 2012;44:96–104.

[5] Weber C, Shah N. Optimisation based design of a district energy system for an eco-town in the United Kingdom. Energy 2011;36:1292–308.

[6] Zhou Z, Liu P, Li Z, Ni W. An engineering approach to the optimal design of distributed energy systems in China. Applied Thermal Engineering 2013;53:387–96.

[7] Kong XQ, Wang RZ, Huang XH. Energy optimization for a CCHP system with available gas turbines. Applied Thermal Engineering 2005;25:377–91.

[8] Aiying R, Risto L. An effective heuristic for combined heat-and-power production planning with power ramp constraints. Applied Energy 2007;84:307–25.

[9] Kriett P, Salani M. Optimal control of a residential microgrid. Energy 2012;42(1):321–30.

[10] Brahman F, Jadid, S. Optimal energy management of hybrid CCHP and PV in a residential building. In: Proceedings of 19th IEEE Conference on Electrical Power Distribution Networks, 2014 May 6–7:19–24.

[11] Ren H, Gao W. A MILP model for integrated plan and evaluation of distributed energy systems. Applied Energy 2010;87(3):1001-1014.

[12] Educogen. The European Educational Tool on Cogeneration, Second Edition, December 2001. Available online: < http://citeseerx.ist.psu.edu/viewdoc/download?doi=10.1.1.618.8470&rep=rep1&type=pdf.>

[13] EPBD buildings platform. Country reports; 2008 [ISBN 2-930471-29-8]. Available online: http://www.epbdca.org/Medias/Pdf/EPBD_BuPLa_Country_reports.pdf.

[14] Hotel Energy Solutions (2011), Analysis on Energy Use by European Hotels: Online Survey and Desk Research, Hotel Energy Solutions project publications, Available online: http://hes.unwto.org/sites/all/files/docpdf/analysisonenergyusebyeuropeanhotelsonlinesurveyanddeskresearch2382011-1.pdf.

[15] RESILIENT Project, FP7 RESILIENT Project Consortium, Grant Number #314671, Available online: http://www.resilient-project.eu/.

[16] Dispositivi, tecniche e tecnologie abilitanti per le Fonti Energetiche Rinnovabili verso la Green Economy, FERGE PON Campania, PON03PE_00177_1, funded by Ministry of Education, University and Research.

[17] Smart grid con sistemi di poligenerazione distribuita, POLIGRID POR Campania FSE 2007/2013.

[18] Rivarolo M, Greco A, Massardo AF. Thermo-economic optimization of the impact of renewable generators on poly-generation smart-grids including hot thermal storage. Energy Conversion and Management 2013;65:75–83.

[19] Aprile M. Caratterizzazione del settore alberghiero in Italia. Report ENEA RSE/2009/162, 2009.

[20] Beccali M, La Gennusa M, Lo Coco L, Rizzo G. An empirical approach for ranking environmental and energy savings measures in the hotel sector. Renewable Energy 2009;34:82-90.

[21] Mongibello L, Bianco N, Caliano M, Graditi G, Musto M. Optimal operation of micro-CHP systems for a single-family house in Italy. Applied Mechanics and Materials 2014;492:467-472.

[22] Delibera Autorità per l'Energia Elettrica e per il Gas 119/11. Available online: <http://www.autorita.energia.it/allegati/docs/11/119-11arg.pdf.>

[23] Autorità per l'Energia Elettrica e per il Gas. Available online: <http://www.autorita.energia.it/it/prezzi.htm.>

[24] ASHRAE International Weather files for Energy Calculations (IWEC weather files). Users manual and CD- ROM, American Society of Heating, Refrigerating and Air-Conditioning Engineers, Atlanta, GA, USA, 2001.

[25] IPCC. Guidelines for national greenhouse gas inventories - CO2 emissions from fuel combustion, highlights, 2013 Edition, IEA (2013).

[26] Catalog of CHP Technologies. U.S. Environmental Protection Agency Combined Heat and Power Partnership. March 2015. Available online: http://www.epa.gov/sites/production/files/2015-07/documents/catalog_of_chp_technologies.pdf.

[27] Guida alla Cogenerazione ad Alto Rendimento CAR, 1st Edition, GSE 2012.

[28] Delibera Autorità per l'Energia Elettrica e per il Gas 16/98 http://www.autorita.energia.it/allegati/docs/98/016-98.pdf.

"Exergy analysis adds information to conventional energy analysis: the supply of high quality exergy in buildings for thermal purposes needs to be minimized. This implies avoiding burning processes in building supply systems and substituting them by low-temperature systems and sources."

Chapter 4

Optimal operation planning of a Distributed Energy System considering energy costs and exergy efficiency

4.1. Introduction

In this chapter, the exergy analysis is involved in the operation planning of a DES through a multi-objective approach to take into account also the economic factor, represented by energy costs, as a crucial priority in the short-run. The exergy analysis in DESs promotes the matching of energy quality levels of supply and demand, by covering, if possible, low-quality thermal demands with low exergy sources, e.g., solar thermal or waste heat of power generation processes, and electricity demands with high exergy sources. As a direct consequence, sustainability of energy supply is improved by an efficient use of energy resources, thereby reducing the fossil fuels consumption with the related GHG emissions. To demonstrate the effectiveness of the exergy analysis in the operation planning of DESs to attain long-run sustainability of the energy supply, an innovative tool for the exergy-based operation planning of a DES is presented. A Multi-Objective Linear Programming (MOLP) problem is formulated to find the optimized operation strategies of the DES to reduce the energy cost, and increase the overall exergy efficiency. The DES under consideration involves multiple energy conversion devices: Combined Cooling Heating and Power (CCHP) system, biomass boiler, solar thermal plant, reversible heat pumps, as well

as thermal energy storage systems. A set of primary energy carriers with different energy quality levels are converted to meet given time-varying user demands with different energy quality levels. The economic objective is formulated as the total energy cost to be minimized. The exergetic objective is to maximize the overall exergy efficiency of the DES. Since energy demands are assumed known, the total exergy required to meet the demands is also known, and the overall exergy efficiency can be increased by reducing the exergy input to the DES. Therefore, the exergetic objective is formulated as the total primary exergy input to be minimized. The Pareto frontier consisting of the best possible trade-offs between the energy costs, essential in the short run, and the overall exergy efficiency crucial in the long run, is obtained by minimizing a weighted sum of the total energy cost and primary exergy input, by using branch-and cut.

As an illustrative example, a large hotel located in Beijing is considered as targeted end-user. The model is implemented by using IBM ILOG CPLEX Optimization Studio Version 12.5. Results of numerical testing show that the minimization of primary exergy input to the DES promotes an efficient energy supply system where all the energy resources, including renewable ones, are used in an efficient way. The optimized operation allows reducing energy costs and primary exergy input as compared with conventional energy supply systems. A sensitivity analysis is carried out to show the contribution of each energy device in reduction of energy costs and primary exergy input. In addition, the influence of the exergy analysis on CO_2 emissions evaluated under the optimized operation strategies of the DES attained in the multi-objective optimization is also investigated. Results show that by increasing the overall exergy efficiency of the DES, further sustainability of the energy supply is attained, not only better exploiting the potential of energy resources, but also reducing the environmental impact.

In the following, the modeling of the DES is presented in Section 4.2. The economic and exergetic objectives as well as the multi-objective optimization method are presented in Section 4.3. Results of the numerical testing, including results of the sensitivity analysis are presented in Section 4.4. The analysis of the influence of the exergy analysis on CO_2 emissions in the optimal operation planning of the DES is addressed in Section 4.5.

4.2. Problem formulation

Figure 4.1 shows the scheme of the DES with the possible routes of energy carriers from energy resources via primary and secondary energy devices, and thermal energy storage systems to meet the user demands. The energy devices and thermal storage systems are the same as those presented and modelled in Chapter 3. A biomass boiler is added as primary energy device to meet the demand of domestic hot water. Modeling of energy devices and thermal storage, and energy balances are presented in Subsection 4.2.1 and 4.2.2, respectively.

4.2.1. Modeling of energy devices and thermal storage

The MOLP problem formulated is based on the detailed modeling of energy devices and thermal storage presented in Subsection 3.2.1 of Chapter 3, with the related ramp constraints, capacity constraints and assumptions. As for the multi-objective operation planning of a DES through cost and environmental impact assessments, also in this case the constant-efficiency assumption for energy devices is made. The detailed modeling of energy devices and thermal storage is omitted in this chapter, except for the modeling of the biomass boiler, presented below.

4.2.1.1. Modeling of the biomass boiler

A biomass boiler is used to meet the domestic hot water demand. The mass flow

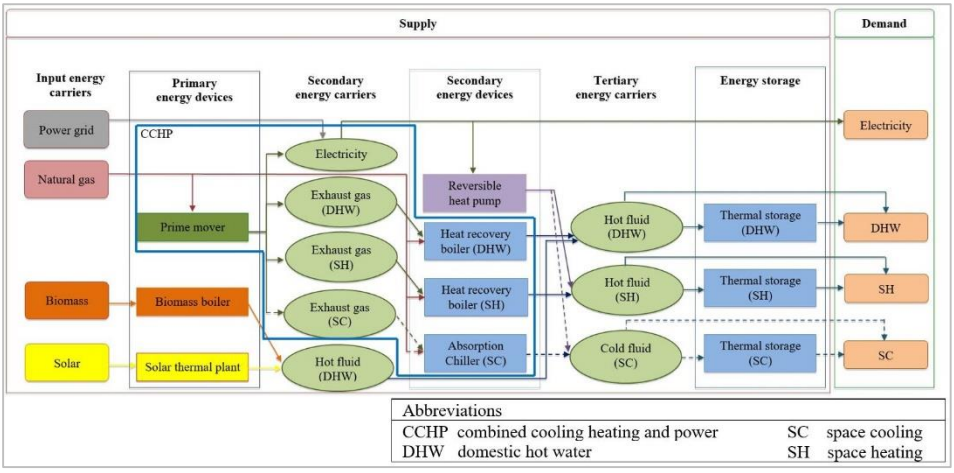

Figure 4.1. Scheme of the DES for the optimization problem.

rate required by the biomass boiler, $\dot{B}_{bioboil}(t)$, is given by:

$$\dot{B}_{bioboil}(t) = \dot{H}_{bioboil}(t) / \left(\eta_{bioboil} LHV_{bio} \right) \tag{4.1}$$

where $\dot{H}_{bioboil}(t)$ is the heat rate provided by the biomass boiler, $\eta_{bioboil}$ is the combustion efficiency of the biomass boiler, and LHV_{bio} is the lower heat value of the biomass.

4.2.2. Energy balances

In order to satisfy the given time-varying user demands, electricity and thermal energy balances are formulated by matching supply and demand. The electricity balance is the same as that presented in Subsection 3.2.2.1 of Chapter 3, and it is omitted in this chapter.

4.2.2.1 Domestic hot water energy balance

The heat rate demand for domestic hot water, $\dot{H}_{dem}^{DHW}(t)$, must be satisfied by the sum of the heat rate provided by the CCHP system, $\dot{H}_{CCHP}^{DHW}(t)$, which is the sum of the heat rate provided by the exhaust gas and the heat rate directly provided by the supplementary burning of natural gas in the boiler; the heat rate provided by the solar thermal plant, $\dot{H}_{ST}(t)$; the heat rate provided by the biomass boiler, $\dot{H}_{bioboil}(t)$; and the heat rate provided by the thermal storage, $\dot{H}_{sto}^{out}(t) - \dot{H}_{sto}^{in}(t)$:

$$\dot{H}_{dem}^{DHW}(t) = \dot{H}_{CCHP}^{DHW}(t) + \dot{H}_{ST}(t) + \dot{H}_{bioboil}(t) + \dot{H}_{sto}^{out}(t) - \dot{H}_{sto}^{in}(t) \tag{4.2}$$

The space heating and cooling energy balances can be expressed in a similar way.

4.3. Multi-objective optimization: energy costs and overall exergy efficiency

In order to attain a rational use of the energy resources by considering both short- and long-run priorities, two objectives, i.e., economic and exergetic, are involved in

the optimization problem, as presented in Subsection 4.3.1 and 4.3.2, respectively. To solve the multi-objective optimization problem, the multi-objective optimization method is discussed in Subsection 4.3.3.

4.3.1 Economic objective

The economic objective is to minimize the total energy cost, *Cost*, which is the sum of three terms: cost of buying electricity from the power grid, cost of natural gas, and cost of biomass as follows:

$$Cost = \sum_{t} \left(P_{grid}(t)\dot{E}_{buy}(t) + P_{NG}\dot{G}_{buy}(t) + P_{bio}\dot{B}_{buy}(t) \right) \Delta t \tag{4.3}$$

where $P_{grid}(t)$ is the time-of-day unit price of electricity from the power grid at time t, P_{NG} and P_{bio} are the constant unit price of natural gas and biomass, respectively, and Δt is the length of the time interval. In Eq. (4.3), the volumetric flow rate of natural gas bought, $\dot{G}_{buy}(t)$, corresponds to the total energy consumption requirement of the CCHP system, and the mass flow rate of biomass bought, $\dot{B}_{buy}(t)$, corresponds to the energy consumption requirement of the biomass boiler.

4.3.2 Exergy analysis and exergetic objective

In buildings, energy demands are characterized by different energy quality levels [1 - 4]. For electrical appliances and lighting, the highest possible quality of energy is needed since electricity is theoretically fully convertible into useful work. The exergy rate required by the building to meet the electricity demand, $\dot{E}x^{e}_{dem}(t)$, can be evaluated as [4]:

$$\dot{E}x^{e}_{dem}(t) = \dot{E}_{dem}(t) \tag{4.4}$$

For thermal demands, exergy is directly related to the temperature required for the demand under consideration – the higher the temperature required, the higher the exergy. The exergy rate required by the building to meet the domestic hot water demand, $\dot{E}x^{DHW}_{dem}(t)$, can be evaluated as [4]:

$$\dot{E}x_{dem}^{DHW}(t) = F_q(t)\dot{H}_{dem}^{DHW}(t) \tag{4.5}$$

with the Carnot factor, $F_q(t)$, expressed as:

$$F_q(t) = 1 - T_0(t)/T_{req} \tag{4.6}$$

which depends on the temperature required, T_{req}, and the reference temperature, $T_0(t)$. By a dynamic exergy analysis, the hourly ambient temperatures are considered as the reference temperatures [5]. The exergy required by the building to meet the space heating and cooling demands can be evaluated in a similar way.

The total exergy output, Ex_{out}, is the total exergy required to meet the given user energy demands, as formulated in the following:

$$Ex_{out} = \sum_t \left(\dot{E}x_{dem}^{e}(t) + \dot{E}x_{dem}^{DHW}(t) + \dot{E}x_{dem}^{SH}(t) + \dot{E}x_{dem}^{SC}(t)\right)\Delta t \tag{4.7}$$

At the supply side, input energy carriers are characterized by different energy quality levels as well. The energy carriers input to the DES under consideration include electricity, natural gas, biomass and solar energy, as discussed in the following.

Electricity from the power grid is an energy carrier provided by power generation plants, and their exergy efficiency, ε_{gen}, is based on the technologies used in the plants. The exergy rate of the electricity from the power grid is formulated as [6, 7]:

$$\dot{E}x_e(t) = \dot{E}_{buy}(t)/\varepsilon_{gen} \tag{4.8}$$

For natural gas, its specific chemical exergy is the maximum work that can be obtained from the substance, by taking it to the chemical equilibrium with the reference environment at the constant temperature and pressure [8]. The exergy input rate of natural gas, $\dot{E}x_{NG}(t)$, corresponds to the exergy input rate to the CCHP system, and it is the overall natural gas volumetric flow rate consumed by the CCHP system, $\dot{G}_{CCHP}(t)$, multiplied by the specific chemical exergy of natural gas, ex_{NG}:

$$\dot{E}x_{NG}(t) = ex_{NG}\dot{G}_{CCHP}(t) \tag{4.9}$$

The specific chemical exergy of natural gas, ex_{NG}, can be evaluated by multiplying the exergy factor, ς_{NG}, and the lower heat value, LHV_{NG}:

$$ex_{NG} = \varsigma_{NG} LHV_{NG} \tag{4.10}$$

According to [8], the exergy factor for natural gas is equal to 1.04 ± 0.5%.

Similar to natural gas, the exergy input rate of the biomass fuel, $\dot{E}x_{bio}(t)$, is the exergy input rate to the biomass boiler. It is the product of the biomass mass flow rate consumed by the biomass boiler, $\dot{B}_{bioboil}(t)$, and the specific chemical exergy of biomass, ex_{bio}:

$$\dot{E}x_{bio}(t) = ex_{bio}\dot{B}_{bioboil}(t) \tag{4.11}$$

The specific chemical exergy of biomass, ex_{bio}, can be evaluated as the product of the exergy factor, ς_{bio}, and the lower heat value, LHV_{bio}:

$$ex_{bio} = \varsigma_{bio} LHV_{bio} \tag{4.12}$$

According to [8], the values of the exergy factor for wood, considered as the biomass fuel, are in the range 1.15-1.30.

Solar energy input to the solar collectors is considered as a low-exergy source since the solar exergy input rate, $\dot{E}x_{solar}(t)$, is evaluated at the output of the solar collector field [9, 10]:

$$\dot{E}x_{solar}(t) = \dot{H}_{ST}(t)\left(1 - T_0(t)/T_{coll}^{out}\right) \tag{4.13}$$

where T_{coll}^{out} is the temperature of the heat transfer fluid at the exit of the collector.

The total primary exergy input, Ex_{in}, is formulated as the sum of the exergy rates of the primary energy carriers over time, as follows:

$$Ex_{in} = \sum_t \left(\dot{E}x_e(t) + \dot{E}x_{NG}(t) + \dot{E}x_{bio}(t) + \dot{E}x_{solar}(t)\right)\Delta t \tag{4.14}$$

With the exergy output and input defined above, the overall exergy efficiency,

ψ, is the ratio of the total exergy output, Ex_{out}, to the total primary exergy input, Ex_{in}, as follows:

$$\psi = Ex_{out} / Ex_{in} \tag{4.15}$$

As mentioned earlier, the total exergy required to meet the given energy demands is known, and the overall exergy efficiency in Eq.(4.15) can be increased by reducing the exergy input to the DES. Therefore, the exergetic objective is formulated as the total primary exergy input, Ex_{in}, as in Eq. (4.14), to be minimized.

4.3.3 Multi-objective optimization method

With the economic objective function (Eq. 4.3) and the exergetic one (Eq. 4.14), the problem has two objective functions to be minimized. To solve this multi-objective problem, the weighted-sum method is used. Therefore, a single objective function is formulated as a weighted sum of the total energy cost, *Cost*, and the total primary exergy input, Ex_{in}, to be minimized:

$$F_{obj} = c\omega Cost + (1-\omega)Ex_{in} \tag{4.16}$$

where the constant c is a scaling factor, chosen such that c *Cos*t and Ex_{in} have the same order of magnitude. For $\omega = 1$, the economic optimization is carried out and the solution that minimizes the total energy cost can be found. For $\omega = 0$, the exergetic optimization is carried out, and the solution that minimizes the total primary exergy input can be found. Then the scaling factor c is calculated as the ratio of the total exergy input obtained by the economic optimization to the total energy cost obtained by the exergetic optimization. With the constant c, the best possible trade-offs between the two objectives, appertaining to the Pareto frontier, are obtained by solving the problem with values of ω varying in-between 0 and 1. The problem formulated in Sections 4.2 (including the detailed modeling of energy devices and thermal storage presented in Subsection 3.2.1 of Chapter 3, with the related ramp constraints, capacity constraints and assumptions), and 4.3 is linear and involves both discrete and continues variables, so this mixed integer linear programming problem is to be solved by branch-and-cut.

4.4. Numerical testing: a Chinese case study

The method developed above is implemented by using IBM ILOG CPLEX Optimization Studio Version 12.5. As an illustrative example, a hypothetic large hotel located in Beijing with a 30,000 m^2 area is selected as the targeted end-user. Worldwide, China is ranked third in energy consumption in commercial building sector [11], and the application of DESs has increased rapidly in recent years because of the supportive government policies and financial incentives [12]. A typical winter day of January and a typical summer day of July are chosen with one hour as time-step. The configuration of the DES analyzed, including the sizes of energy devices, is shown in Figure 4.2.

In the following, the input data for the optimization model are described in Subsection 4.4.1. The Pareto frontiers obtained for the winter and summer cases are presented and discussed in Subsection 4.4.2. The optimized operation of the DES is also discussed for a trade-off point on the Pareto frontier to show how the operation strategy affects the energy costs and primary exergy input under different weights for the two objectives. To show how the constant-efficiency assumption affects the optimized operation strategies, the performance of the heat pump and the variation of the electric efficiency of the prime mover in the CCHP at partial loads are considered in the multi-objective optimization in Subsection 4.4.3. In addition, to show the effects of variations in the configuration of the DES on energy costs and primary

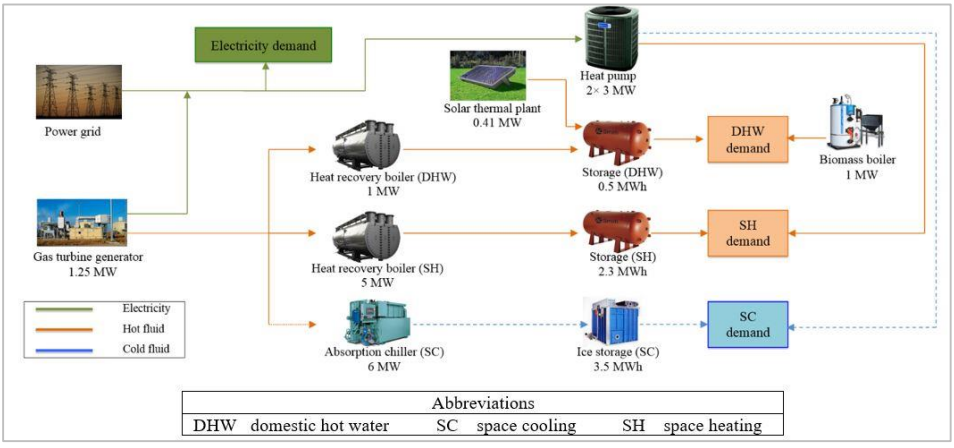

Figure 4.2. DES configuration analyzed for the hypothetic hotel in Beijing.

exergy input, results of the sensitivity analysis are presented and discussed in Subsection 4.4.4.

4.4.1 Input data

The required input data include building energy demands, prices and exergy factors of primary energy carriers, and efficiencies of energy devices as discussed below.

4.4.1.1 Building energy demands

The hourly electricity, domestic hot water, space heating and cooling demands are taken from a comprehensive investigation about energy demands of hotels in Beijing [13], and the energy rate demand profiles for a typical winter day of January and of July, respectively, are chosen as shown in Figure 4.3a and b, respectively. The exergy of thermal demands for each day is evaluated by assuming the reference temperatures as the hourly ambient temperatures of the corresponding day, taken from meteorological data in Beijing [14]. The temperatures required for domestic hot water, space heating and cooling demands, T_{req}, are set to be 333.15 K, 293.15 K and 299.15 K, respectively [15].

4.4.1.2 Prices and exergy of primary energy carriers

As mentioned earlier, power grid, natural gas, biomass, and solar energy, are the

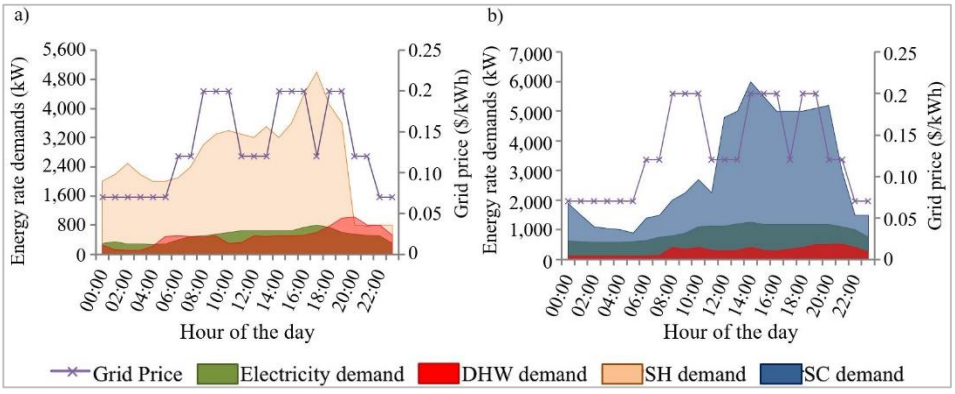

Figure 4.3. Energy rate demands of a hypothetic hotel in Beijing
a) representative winter day of January; b) representative summer day of July.

energy carriers input to the DES. The first three are assumed unlimited in this study. The grid power price is time-varying as shown in Figure 4.3 [16], and the exergy efficiency of the power generation plant is assumed equal to 0.32 [17], a typical value when electricity is mostly generated by coal-fired thermal power plants as in China [18]. The price of natural gas is assumed equal to 0.38 \$/Nm^3 [16], and the fuel of the biomass boiler is assumed to be wood pellet with a price of 70 \$/t [19]. Their exergy factors are assumed equal to 1.04 and 1.16 [8], respectively. To evaluate the heat rate provided by the solar collector field, for each hour of the representative winter day of January, the solar irradiance has been evaluated as the average of the hourly mean values of the solar irradiance in the corresponding hour of all January days. The same has been done for a representative summer day of July [14]. In the evaluation of the Carnot factor for the solar exergy input rate (Eq. (4.13)), the temperature of the heat transfer fluid at the exit of the collector field is assumed constant and equal to 353.15 K.

4.4.1.3 Efficiency of energy devices and thermal storage

In the following reference is made to a gas turbine as the prime mover of the CCHP system with an actual nominal peak output of 1,250 kW and an exhaust gas temperature of 785.15 K. It operates at a 24% gas-to-electric turbine efficiency with an 8% heat loss efficiency [20]. A gas-fired absorption chiller that can be indirectly fired by the gas turbine exhaust gas is chosen for the system. The COP of the chiller unit is 1.2 with an exhaust gas temperature of 443.15 K and its combustion efficiency is 85% [21]. The heat recovery efficiency of the absorption chiller is defined as the ratio of difference between the exhaust gas temperature from the prime mover and the exhaust gas temperature out of the absorption chiller to the difference between the exhaust gas temperature from the prime mover and the ambient temperature. The thermal efficiency of the wood pellet biomass boiler is assumed to be 80%. Typical values of the coefficient of performance of heat pumps in Beijing have been used. As to the other energy devices and thermal storage systems, values of their efficiencies are the same as those presented in Subsection 3.4.1.5 of Chapter 3. The above mentioned data are listed in Table 4.1.

Table 4.1 Efficiency of energy devices and thermal storage systems.

Primary energy devices	**Efficiency**	
	Electrical	Thermal
Gas turbine	0.24	0.68
Biomass boiler		0.80
Solar thermal		0.40
Secondary energy devices	**Efficiency**	
	Heating mode	Cooling mode
Heat pump	$COP = 3.0$	$COP = 3.2$
Heat recovery boiler	$\eta_{boil} = 0.90$	
	$\eta_{HR,boil} = 0.74$	
Absorption chiller		$COP_{abs} = 1.2$
		$\eta_{abs} = 0.85$
		$\eta_{HR,abs} = 0.70$
Thermal energy storage	**Storage loss fraction**	
DHW and SH storage	$\phi_{sto} = 0.10$	

4.4.2 Pareto frontier

With the input data described above, the optimization problem can be solved within several seconds with a mixed integer gap 0.1%. The Pareto frontiers obtained for the winter and summer cases are shown in Figure 4.4. For the winter case, the point marked with *a* is obtained by minimizing the total daily energy cost, and the

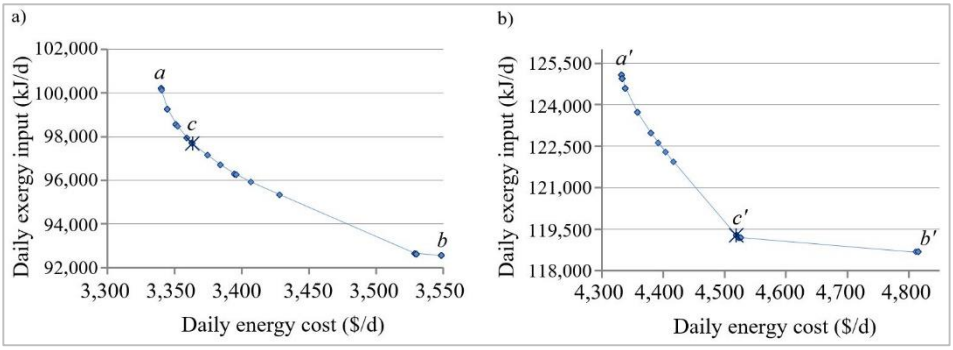

Figure 4.4. Pareto frontier for a) winter case; b) summer case.

daily energy cost is 3,340 $/d whereas the daily exergy input is 100,210 kJ/d. The point marked with *b* is obtained by minimizing the total daily exergy input. The daily energy cost is 3,549 $/d whereas the daily exergy input is 92,548 kJ/d. The points between the extreme points are found by subdividing the weight interval into 100 equally-spaced points. There are 17 points since some solutions have been found under more than one weight values. For the summer case, the Pareto frontier with 13 points is obtained in the same way, where the points marked *a'* and *b'* are obtained by the economic and exergetic optimizations, respectively. The planners of the DES can choose the operation strategy from the Pareto frontier based on their cost and exergy preference and priorities. For the illustration purpose, the point marked with *c* in the winter case is chosen to show the optimized operation of the DES under a higher weight of 0.7 for the economic objective. The point marked with *c'* in the summer case is chosen to show the optimized operation of the DES under a higher weight of 0.62 for the exergetic objective.

Figure 4.5 shows the hourly grid power price, electricity rate demand, electricity rate required by the heat pump, electricity rate provided by the CCHP system, and electricity rate bought from the power grid, for point *c* of the winter day and point *c'* of the summer day. In the winter case, electricity is bought from the power grid when its price is low, e.g., from 0:00 to 5:00, and it is used to meet the electricity demand and to drive the heat pump. Conversely, when the grid power price increases, the CCHP system is used to meet the electricity demand and to drive the heat pump, for

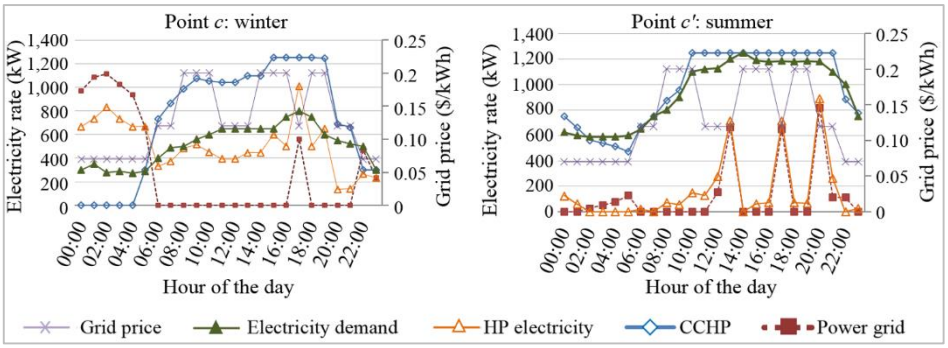

Figure 4.5. Hourly grid price, electricity rate demand, electricity rate required by the heat pump, electricity rates provided by the CCHP and the power grid, for points *c* and *c'*.

example, at 15:00, 16:00, 18:00 and 19:00. In the summer case, the operation of the DES is less sensitive to the grid power price variation. For instance, from 0:00 to 5:00, despite the low grid power price, electricity from the CCHP system is mostly used to meet the electricity demand and to drive the heat pump. With less electricity bought from the power grid, the total daily exergy input would be lower.

The hourly domestic hot water rate demand, the hourly heat rates provided by the CCHP system, by the biomass boiler, by the solar thermal, and the thermal energy stored, are reported in Figure 4.6. The figure points out the differences in the operation of the DES under different weights for the economic and exergetic objectives. For point *c* in the winter case, the biomass boiler, instead of the gas-fired boiler, is used to meet the domestic hot water demand, because of its lower price. In addition, since the solar thermal plant is sized to almost totally satisfy the hot water demand in the winter day during the insolation hours, thermal energy is never stored during the insolation hours. Conversely, for point *c'* in the summer case, the biomass boiler is never used to meet the domestic hot water demand. This is due to the fact that biomass is a high-quality renewable energy resource, and it should not be used to meet the low-quality thermal demand. This result agrees with those presented in [1], where different energy supply systems for space heating and domestic hot water demands (i.e., natural gas boiler, wood pellet boiler, ground source heat pump, and waste district heat), were compared through exergy analysis. It was shown that the exergy input of the wood-fuelled boiler is the largest among the four options, since

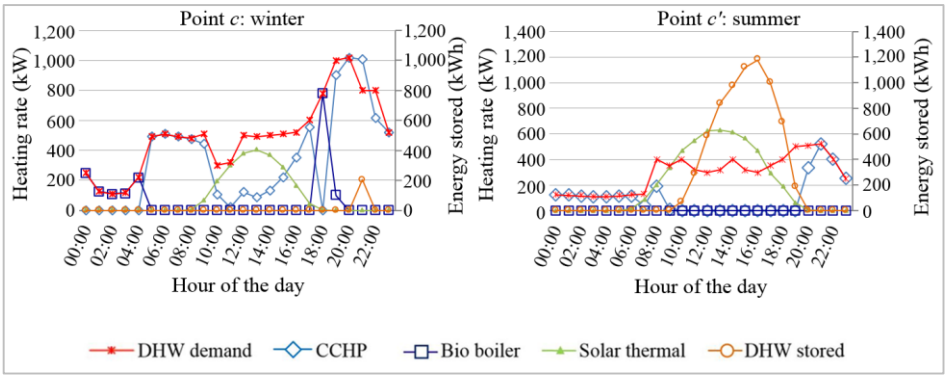

Figure 4.6. Hourly domestic hot water rate demand, hourly heat rates provided by CCHP, biomass boiler, solar thermal plant, thermal energy stored, for points *c* and *c'*.

wood is a renewable and high-quality energy resource, but the conversion efficiencies of wood boilers are usually not as high as those of conventional natural gas boilers. The fact that the exergy input is the largest indicates that such an energy supply does not promote an efficient use of the potential of the energy sources used. In addition, in the summer case, thermal energy is mostly stored during the insolation hours because of the higher solar irradiation and the lower hot water demand, and the stored energy is recovered for the evening hours.

The hourly grid prices, hourly space heating and cooling rate demands, hourly heat and cooling rates provided by the CCHP system and by the heat pump, and thermal energy stored, are reported in Figure 4.7. Results are similar to those shown in Figure 4.5. In the winter case, the operation of the DES is more sensitive to the grid price variation, and in the summer case, the operation of the DES is less sensitive to that.

4.4.3 Effect of partial loads performance of heat pump and prime mover in the CCHP system on the optimized operation strategies of the DES

To show how the constant efficiency assumption affects the optimized operation strategies of the DES, while maintaining the problem linearity, the performance of the heat pump and the prime mover in the CCHP system at partial loads is analyzed for the winter case in this Subsection.

Unlike the other energy devices, the partial load performance of the heat pump

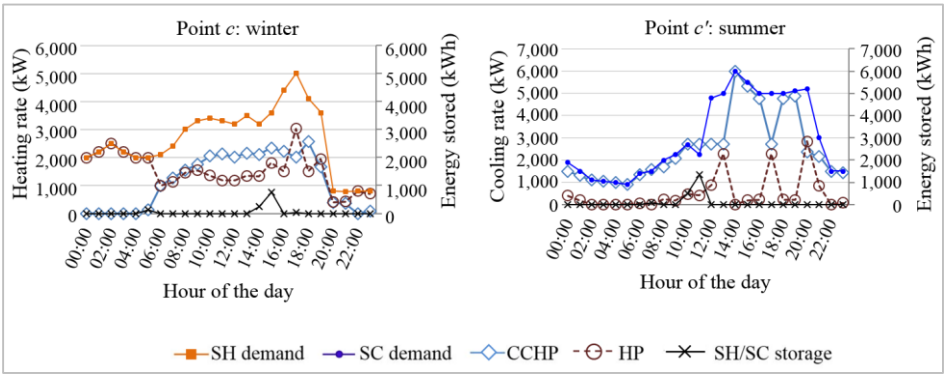

Figure 4.7. Hourly space heating/cooling rate demands, hourly heat/cooling rates provided by the CCHP system and by the heat pump, thermal energy stored, for points *c* and *c′*.

can be deduced from the full load value [22] and the problem linearity is maintained.

However, the electric efficiency of the gas turbine generator is a nonlinear function of the generation level (a continuous decision variable), which makes the problem nonlinear. Therefore, to maintain the problem linear, the effects of the variation of the gas turbine electric efficiency at partial loads on the optimized operation strategies of the DES are evaluated through a heuristic iterative approach. This approach consists of iterating the following steps till convergence:

(1) Solve the optimization problem including the partial load performance of the heat pump and considering the gas turbine electric efficiency as a vector of 24 components.
(2) For each hour of the day, evaluate the gas turbine electric efficiency from the gas turbine efficiency-load curve [23] by entering the curve with the electricity provided by the gas turbine coming from step 1, expressed in percentage of the full load.
(3) If convergence is not reached, update the turbine electric efficiency vector, and then return to step 1.

At the beginning, step 1 has to be performed considering for all 24 hours the gas turbine electric efficiency equal to the one at full load.

The optimized operation strategies (shares of the energy provided by each energy device normalized on the total energy provided to meet the corresponding energy demand in the winter day), under different weight values, are compared in the following. Results for the summer case are similar. Figures 4.8 and 4.9 show the optimized operation strategies to meet the electricity load (sum of the electricity demand and electricity required by the heat pump) and thermal demands, respectively, obtained by varying the weight ω from 0 to 1, with a 0.1 increase: a) considering constant efficiencies for all the energy devices, b) considering the performance of the heat pump and the variation of the gas turbine electric efficiency at partial loads, while maintaining constant efficiencies of the other energy devices. From the comparison between a) and b) of the two figures, it can be seen that the trends of the operation strategies are almost the same when ω varies from 1 to 0 (from the economic to the exergetic optimization).

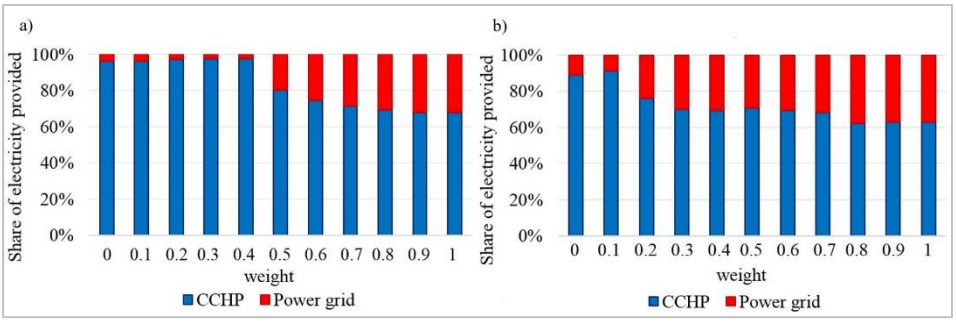

Figure 4.8. Share of electricity provided by CCHP system and power grid in the winter day:
a) Considering constant efficiencies of all the energy devices;
b) Considering the performance of the heat pump and the variation of the gas turbine electric efficiency at partial loads and constant efficiencies of other energy devices.

Figure 4.8 shows that for both the cases, when ω varies from 1 to 0, the share of the electricity provided by the CCHP system increases, highlighting the importance of this energy device for the exergetic optimization. However, the CCHP system is less used when the performance of the heat pump and the variation of the gas turbine electric efficiency at partial loads are taken into account. In this case, the CCHP system is mostly used at high loads, since its electric efficiency reduces at low loads.

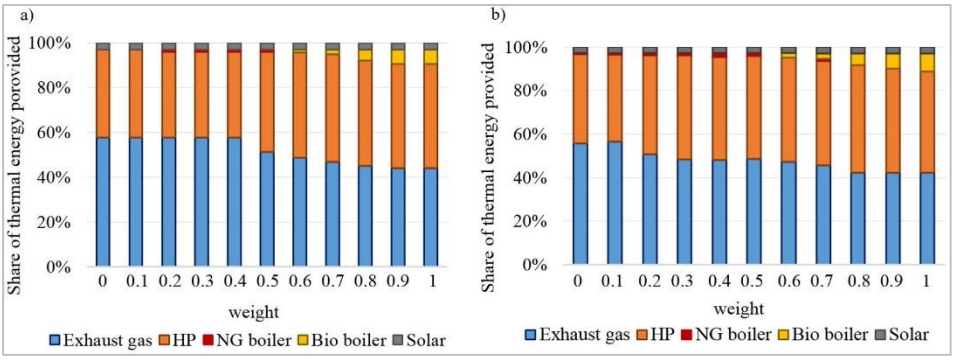

Figure 4.9. Share of thermal energy provided by energy devices in the DES in the winter day:
a) Considering constant efficiencies of all the energy devices;
b) Considering the performance of the heat pump and the variation of the gas turbine electric efficiency at partial loads and constant efficiencies of other energy devices.

Conversely, when a constant efficiency is assumed, the CCHP system is used also at lower loads, resulting in the higher use of the CCHP system and the lower use of grid power, as shown in Figure 4.8a. The share of the electricity provided by the power grid is generally slightly higher when the performance of the heat pump and the variation of the gas turbine electric efficiency at partial loads are taken into account. In this case, the heat pump is mainly off or operates at full load, since its efficiency is the highest under full load condition. Conversely, if a constant efficiency is assumed, the heat pump is used mostly at partial loads, resulting in the higher use of the CCHP system and the lower use of grid power, as shown in Figure 4.8a.

Figure 4.9 shows that for both the cases, when ω varies from 1 to 0, the use of exhaust gas for thermal purposes increases, coherent with the increasing use of CCHP, highlighting the importance of waste heat recovery for the exergetic purpose. In addition, the use of the heat pump slightly reduces, showing that the heat pump is important for both the objectives, and its contribution in reducing energy costs is higher than that in reducing primary exergy input. Also the use of the biomass boiler reduces, highlighting the importance of this energy device for energy costs. However, when the performance of the heat pump and the variation of the gas turbine electric efficiency at partial loads are taken into account, the use of the exhaust gas for thermal purposes is slightly lower, coherent with the lower use of CCHP system. Conversely, the use of the heat pump is slightly higher when the performance of the heat pump at partial loads is considered, since in this case, the heat pump is off or it is used at full load with the maximum efficiency.

4.4.4 Sensitivity analysis

A sensitivity analysis is carried out to investigate the effects of variations in the configuration of the DES on energy cost and primary exergy input. In detail, the single-objective optimization is carried out in the winter case, for the configurations listed in Table 4.2, to show how each energy device contributes to the reduction of energy costs and primary exergy input. For each configuration, one energy device or thermal storage is taken out of the DES configuration shown in Figure 4.2 (considered as the reference case), including the biomass boiler, thermal storage system, the solar thermal plant, the heat pump, the gas turbine in the CCHP system, and the entire CCHP system. Moreover, the total daily energy cost and primary exergy input are

Table 4.2. Configurations investigated in the sensitivity analysis.

Configuration	**Energy devices excluded from the reference case (Configuration 1)**
2	without biomass boiler
3	without DHW/SH storage
4	without solar thermal plant
5	without heat pump
6	without the gas turbine in the CCHP
7	without CCHP
Configuration	**Other cases**
8	Conventional energy supply system

also evaluated for a conventional energy supply system, where all types of the building energy demands are satisfied by the grid power. The daily energy cost obtained by the economic optimization and the daily primary exergy input obtained by the exergetic optimization are shown in Figures 4.10a and b, respectively. Results for the summer case are similar.

Configuration 1 is the reference case, where the minimum energy cost and minimum primary exergy input are attained by the economic and exergetic optimizations, respectively. Configuration 2 excludes the biomass boiler from the reference case. Under the economic optimization, results show a higher total daily energy cost than that of the reference case, due to the low price of biomass. Under the exergetic optimization, the daily exergy input is the same as that in the reference case, since the biomass boiler is not used to meet the low-quality domestic hot water demand. This is due to the fact that biomass is a high-quality renewable energy resource, and should be used to supply high exergy demands such as electricity. This result agrees with those presented in [24], where it was shown that when the biomass is used as fuel of boilers for thermal purposes, a lower exergy efficiency is attained as compared with when the biomass is used as fuel of CHP plants. Minimization of not only fossil but also renewable energy input promotes efficient use of all energy resources.

Configuration 3 excludes the thermal energy storage systems from the reference case. Under the economic optimization, the total daily energy cost is higher than that of the reference case. Under the exergetic optimization, the total daily exergy input

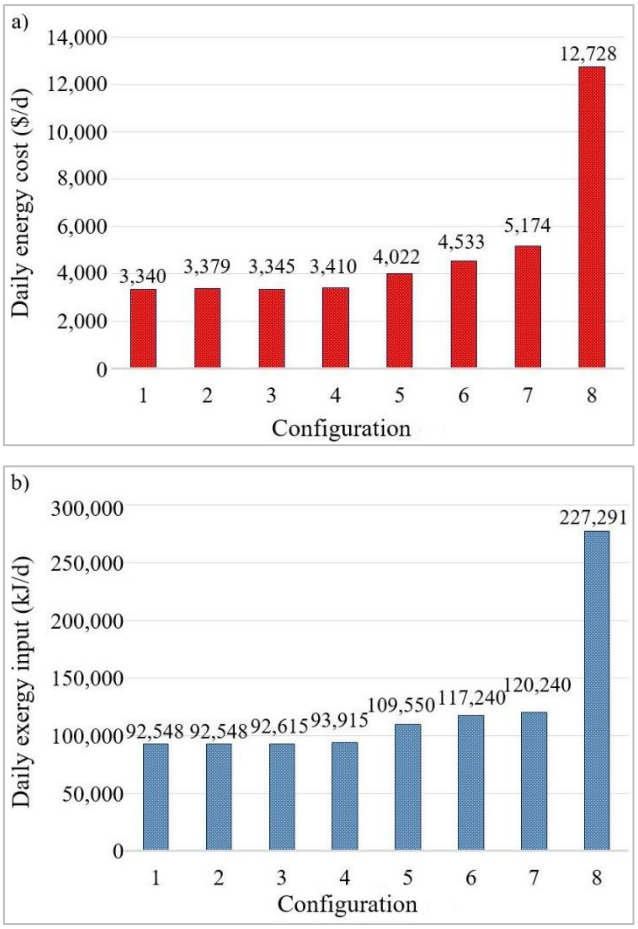

Figure 4.10. a) Daily energy cost for Configurations 1-8 under the economic optimization; b) Daily exergy input for Configurations 1-8 under the exergetic optimization.

is higher than that of the reference case. This confirms that the use of thermal storage systems increases economic savings and improves the efficiency of energy resource use.

Configuration 4 excludes the solar thermal plant, and the results are similar to those for Configuration 3. In the reference case, the solar thermal plant is used to meet the low-quality domestic hot water demand. When the solar thermal plant is excluded, other energy devices are used to meet the domestic hot water demand with a higher total primary exergy input. The absence of the free solar energy resource

also increases the energy costs. For Configuration 5, the significant increase in the energy cost and exergy input when the heat pump is excluded demonstrates the essential role of the heat pump for both the objectives, because of its high conversion efficiency.

Configuration 6 excludes the gas turbine generator of the CCHP system. Without exhaust gas, the heat recovery boilers are driven by natural gas. Results underline the important role of the prime mover in the reduction of both the energy cost and primary exergy input. Under the economic optimization, the increase in the energy cost is mainly due to the fact that the electricity demand is now fully satisfied by the grid power even when its price is high. Under the exergetic optimization, the domestic hot water demand is satisfied by the gas-fired boiler during non-insolation hours, whereas the biomass boiler is not used although it is cheaper than natural gas. Both wood and natural gas are high-quality energy resources, but the efficiency of the biomass boiler is lower than that of the conventional gas-fired boiler. Configuration 7 excludes the entire CCHP system. Results show that the energy cost is larger than that of Configuration 6 under the economic optimization, since space heating is fully satisfied by the heat pump driven by electricity from the power grid. The daily exergy input is larger than that in Configuration 6 under the exergetic optimization, because of the high exergy content of the electricity taken from the power grid. The exergy input increase is also because of the use of the biomass boiler to meet the domestic hot water demand.

Results found in this study, related to the usefulness of solar thermal, heat pumps and waste heat recovery from an exergy perspective, agree with those presented in [25, 26]. In [25], four options (i.e., heat pump, condensing boiler, conventional boiler and solar collector) were analyzed and compared to meet the space heating demand of a building through energy and exergy analysis, and it was shown that the heat pump and the solar thermal collectors have the best performance in terms of exergy efficiency. In [26], it was shown that, among different energy supply systems for heating and cooling purposes, the highest overall exergy efficiencies are achieved by solutions employing waste heat from a cogeneration plant, followed by highly efficient electrical heat pumps.

Finally, the daily energy cost and exergy input are evaluated for the conventional

energy supply system represented by Configuration 9. The grid power is used to meet the electricity demand and the electricity required by an electric heater (100% energy conversion efficiency) and by an electric boiler (98% energy conversion efficiency) to satisfy the space heating and domestic hot water demands, respectively. With all types of demands satisfied by the grid power, the total energy cost is 12,728 $/d, and it is 3.8 times of the cost for the reference case (3,340 $/d) obtained by the economic optimization. The total exergy input is 277,291 kJ/d, and it is nearly 3 times of the exergy input for the reference case (92,548 kJ/d) obtained by the exergetic optimization. It can be seen that by the optimized operation of the DES, the energy cost and primary exergy input are much reduced.

4.5. Influence of the exergy analysis on CO_2 emissions in the optimal operation planning of the Distributed Energy System

In this Section, the influence of the exergy analysis on the environmental impact in the optimal operation planning of the DES is investigated. The total CO_2 emission are evaluated under the optimized operation strategies obtained by the multi-objective optimization in the winter case, for the configuration of the DES shown in Figure 4.2. In this way, a decision support is provided to planners for selecting the operations strategies of the DES, based on their short- and long-run priorities, also aware of the effects on CO_2 emissions.

The environmental impact in terms of total CO_2 emission is evaluated as:

$$Env = \sum_t \left(E_{cin} \dot{E}_{buy}(t) + G_{cin} \dot{G}_{buy}(t) + B_{cin} \dot{B}_{buy}(t) \right) \Delta t \tag{4.17}$$

where E_{cin}, G_{cin}, and B_{cin} are the carbon intensities of the power grid, natural gas, and biomass respectively. The carbon intensity of the power grid is assumed equal to 0.771 kg/kWh that is the averaged value in the years 2009-2011 for China [27]. The carbon intensity of natural gas and biomass fuels are assumed equal to 0.202 kg/kWh and 0.320 kg/kWh, respectively [28, 29].

Figure 4.11 shows the total CO_2 emission evaluated under the optimized operation strategies of the DES obtained by varying the weight ω from 0 to 1, with a 0.1 increase. When ω varies from 1 to 0 (from the economic optimization to the exergetic

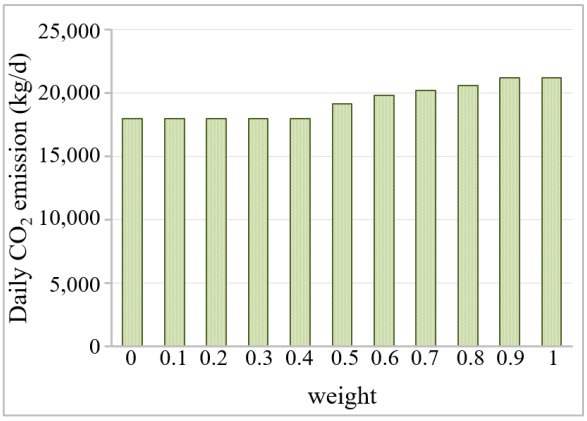

Figure 4.11. Total daily CO_2 emission evaluated under the optimized operation strategies at various trade-off points

optimization), the total daily CO_2 emission decreases. For weight values going from 0 to 0.4, the daily CO_2 emission is around 15% lower than the maximum CO_2 emission evaluated under the optimized operation strategies attained by the economic optimization. This is because of the maximum use of grid power and biomass, as shown in Figures 4.8a and 4.9a. By increasing the overall exergy efficiency of the DES, a reduced use of high-quality energy resources as well as a reduced environmental impact are obtained.

The total daily CO_2 emission is also evaluated under the optimized operation strategies attained by the economic and exergetic optimizations in the winter case for Configurations listed in Table 4.2, as shown in Figure 4.12. In addition, the total daily CO_2 emission is evaluated for the conventional energy supply system represented by Configuration 9. It can be noted that for configurations 1-6, the total CO_2 emission evaluated under the exergetic optimization are always lower than those evaluated under the economic optimization, except for Configuration 7, where they are the same. In fact, when the entire CCHP is excluded, there are no other choices to meet the energy demands. This means that the operation strategies of the DES are the same for all the weights in the range 0 - 1. Moreover, from the comparison between Figures 4.12 and 4.10b, the influence of the overall exergy efficiency of the DES on CO_2 emission is noticeable. For Configurations 3-7, as compared with the reference case,

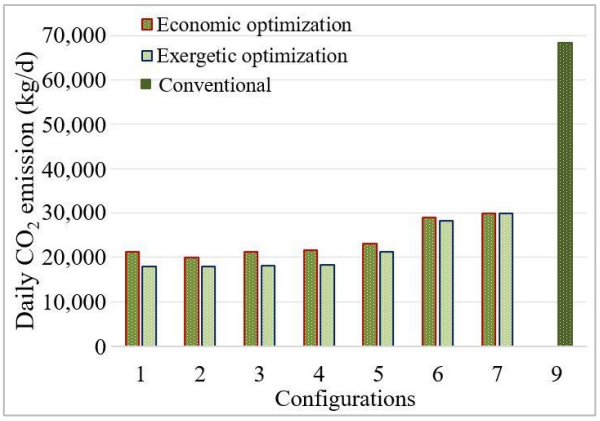

Figure 4.12. Total daily CO_2 emission under the optimized operation strategies obtained by the economic and exergetic optimizations for Configurations 1-9.

the increase in the daily exergy input (reduction of the overall exergy efficiency) corresponds to the increase of CO_2 emission related to the exergetic optimization.The influence of the overall exergy efficiency on CO_2 emissions is also noticeable for the conventional energy supply system. For Configuration 9, as compared with the reference case, the daily exergy input is increased by 64% and the daily CO_2 emission is increased by 74%. Thus, results show that by increasing the overall exergy efficiency, energy resources are more efficiently used, and CO_2 emissions are reduced through the optimized operation of the DES, as compared with conventional energy supply systems.

References

[1] ECBCS – Annex 49 – Low Exergy Systems for High Performance Buildings and Communities, homepage. Available: http://www.ecbcs.org/annexes/annex49.htm.

[2] Szargut J. International progress in second law analysis. Energy 1980;5:709–18.

[3] Rosen MA, Dinçer I, Kanoglu M. Role of exergy in increasing efficiency and sustainability and reducing environmental impact. Energy Policy 2008;36:128–37.

[4] Lu H, Alanne K, Martinac I. Energy quality management for building clusters and districts (BCDs) though multi-objective optimization. Energy Conversion and Management 2014;79:525-33.

[5] Angelotti A, Caputo P. The exergy approach for the evaluation of heating and cooling technologies, first results comparing steady state and dynamic simulations. Proceedings of the 2nd PALENC and 28th AIVC Conference, vol I; 2007 September 27-29; Crete Island, Greece; p. 59-64.

[6] Ramirez-Elizondo LM, Paap GC, Ammerlaan R, Negenborn RR, Toonssen R. On the energy, exergy and cost optimization of multi-energy-carrier power systems. International Journal of Exergy 2013;13:364-385.

[7] Krause T, Kienzle F, Art S, Andersson G. Maximizing exergy efficiency in multi-carrier energy systems. Proceedings of IEEE Power and Energy Society General Meeting; 2010 June 25-29; Minneapolis, USA.

[8] Kotas YJ. The exergy method for thermal plant analysis, reprint ed. Malabar, FL: Krieger; 1995.

[9] Torìo H, Angelotti A, Schmidt D. Exergy analysis of renewable energy-based climatisation systems for buildings: A critical view. Energy and Buildings 2009;41:248-71.

[10] Torìo H, Schmidt D. Framework for analysis of solar energy systems in the built environment from an exergy perspective. Renewable Energy 2010;35:2689-97.

[11] Pacific Northwest National Laboratory, China's Building Energy Use: A Long-Term Perspective based on a Detailed Assessment, January 2012, Available: http://www.pnnl.gov/main/publications/external/technical_reports/PNNL-21073.pdf.

[12] Han J, Ouyang L, Xu Y, Zeng R, Kang S, Zhang G. Current status of distributed energy system in China. Renewable and Sustainable Energy Reviews 2016;55:288-297.

[13] Zhou Z, Liu P, Li Z, Ni W. An engineering approach to the optimal design of distributed energy systems in China. Applied Thermal Engineering 2013;53:387-96.

[14] ASHRAE International Weather files for Energy Calculations (IWEC weather files). Users manual and CD-ROM, American Society of Heating, Refrigerating and Air-Conditioning Engineers, Atlanta, GA, USA, 2001.

[15] ANSI/ASHRAE Standard 55. Thermal Environmental Conditions for Human Occupancy; 2013; Available online from http://www.techstreet.com/products/1868610.

[16] Beijing Municipal Commission of Development & Reform, Current prices for Public commodities; Available online from http://www.bjpc.gov.cn/english/.

[17] Kaushik SC, Reddy VS, Tyagi SK. Energy and exergy analyses of thermal power plants: A review. Renewable and Sustainable Energy Reviews 2011;15:1857-1872.

[18] Forum - Oxford Institute for Energy Studies, Issue 95, February 2014. Available online from: http://www.oxfordenergy.org/wpcms/wp-content/uploads/2014/04/OEF-95.pdf.

[19] Chau J, Sowlati T, Sokhansanj S, Preto F, Melin S, Bi S. Techno-economic analysis of wood biomass boilers for the greenhouse industry. Applied Energy 2009;86:364-71.

[20] Emerson DB, Whitworth BA. Summary of micro-turbine technology. Orlando, Florida: Summit;1998.

[21] Broad Air Conditioning Company. Available online from: www.broad.com/english/product1.htm.

[22] Kinab E, Marchio D, Rivière P, Zoughaib A. Reversible heat pump model for seasonal performance optimization. Energy and Buildings 2010;42:2269-2280.

[23] Catalog of CHP technologies, U.S. Environmental Protection Agency Combined Heat and Power Partnership, Available online from: http://www.epa.gov/chp/documents/catalog_chptech_5.pdf.

[24] Kranzl L, Müller A, Kalt G. The trade-off between exergy-output and capital costs: the example of bioenergy utilization paths. In: 11th Symposium Energy Innovation, 2010 February 10-12, Graz, Austria.

[25] Tolga Balta A, Dincer I, Hepbasli A. Performance and sustainability assessment of energy options for building HVAC applications. Energy and Buildings 2010;42:1320-28.

[26] Angelotti A, Caputo P. Energy and Exergy Analysis of Heating and Cooling Systems in the Italian Context; Proceedings of Climamed 843-854; 2007 5-7 September, Genova, Italy.

[27] IPCC. Guidelines for national greenhouse gas inventories - CO2 emissions from fuel combustion, highlights, 2013 Edition, IEA (2013).

[28] Educogen. The European Educational Tool on Cogeneration, Second Edition, December 2001. Available online: < http://citeseerx.ist.psu.edu/viewdoc/download?doi=10.1.1.618.8470&rep=rep1&type=pdf.>

[29] Chau J, Sowlati T, Sokhansanj S, Preto F, Melin S, Bi S. Techno-economic analysis of wood biomass boilers for the greenhouse industry. Applied Energy 2009;86:364-371.

"Exergy modeling explicitly exposes the irreversibility aspect of energy use, and exergy-based optimization allows increasing world's sustainability, through efficient use of energy resources, while considering energy quality."

Chapter 5

Exergy-based operation planning of a Distributed Energy System through the energy-supply chain considering energy costs and exergy losses

5.1. Introduction

In this chapter, the exergy-based operation planning of a DES is presented by considering the whole energy-supply chain from energy resources to user demands, through the detailed analysis of the energy system components for conversion, storage, distribution and emission for space heating. Instead of considering the overall exergy efficiency as in Chapter 4, exergy losses are modeled for the system components at the energy conversion step. To consider the energy costs as well, a multi-objective optimization problem is formulated to find the optimized operation strategies of the DES to reduce the total energy cost and the total exergy loss occurring at the energy conversion step, which accounts for the largest part of the total exergy loss in the whole energy-supply chain [1 - 3].

The DES under consideration consists of multiple energy conversion devices, and thermal energy storage systems, which convert a set of input energy carriers, such as natural gas, electricity and solar energy, to meet the given time-varying user demands, i.e., electricity, space heating and domestic hot water demands. Energy networks are established from energy resources to user demands, based on the

physical structure of the energy-supply chain. Exergy losses are then modeled for the system components at the energy conversion step, to make visible how much exergy is lost at the related step. The economic objective is formulated as the total energy cost to be minimized, whereas the exergetic objective is formulated as the total exergy loss occurring at the energy conversion step to be minimized. The multi-objective mixed-integer programming problem formulated is nonlinear, and it is efficiently solved by integrating the surrogate Lagrangian Relaxation method and branch-and-cut. The Pareto frontier, including the best possible trade-offs between the economic and exergetic objectives, is obtained by minimizing a weighted sum of the total energy cost and total exergy loss occurring at the energy conversion step.

The targeted end-user considered is the large hotel located in Beijing, as in Chapter 4. The model is implemented by using IBM ILOG CPLEX Optimization Studio Version 12.6. Results demonstrate the usefulness of the exergy analysis applied to the energy supply-chain to reduce the waste of high-quality energy resources through the reduction of exergy losses, thereby leading to a further sustainability of the energy supply. The optimized operation strategies allow reducing energy costs and exergy losses as compared with conventional energy supply systems. Moreover, a sensitivity analysis is carried out to show the contribution of each energy device in reduction of energy costs and exergy losses, through a single-objective optimization performed for various configurations of the DES.

In the following, the detailed modeling of the DES through the energy-supply chain is presented in Section 5.2. The economic and exergetic objectives as well as the multi-objective optimization method are presented in Section 5.3. The solution methodology is discussed in Subsection 5.4, whereas results of the numerical testing, including results of the sensitivity analysis are presented in Section 5.5.

5.2. Problem formulation

The energy-supply chain of the DES under consideration consists of energy conversion devices, including the Combined Heat and Power (CHP) system, solar thermal plant, auxiliary natural gas boilers, and heat pump; thermal energy storage systems; distribution components (e.g., water pipes) as well as terminal devices (e.g., fan coils for the space heating demand) as shown in Figure 5.1.

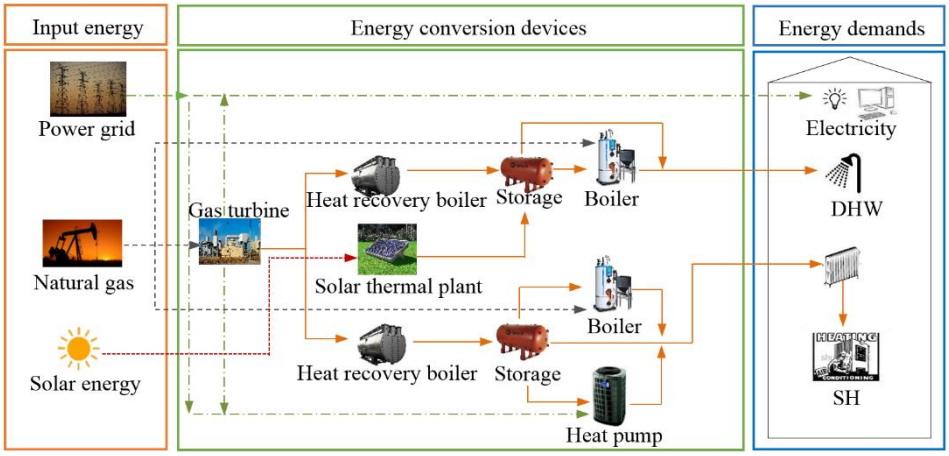

Figure 5.1. Scheme of the DES for the optimization problem.

The common constraint for all the energy devices is the capacity constraint, already presented in Eq. (3.1) of Chapter 3. The exergy loss rate of each energy device at the energy conversion step is formulated by following the input-output approach [4, 5], based on the difference of the input exergy rate and the output exergy rate of the corresponding energy device.

Modeling of the electricity network, and energy networks for space heating and domestic hot water, including the detailed energy and exergy modeling of the system components and energy balances are presented in Subsections 5.2.1, 5.2.2 and 5.2.3, respectively.

5.2.1 Modeling of the energy network for electricity

The system components providing electricity to the end-users are the power grid and the prime mover in the CHP system.

As regards the power grid, the exergy loss rate is formulated as:

$$\dot{E}xloss_{grid}(t) = \dot{E}_{buy}(t)/\varepsilon_{gen} - \dot{E}_{buy}(t) \tag{5.1}$$

where $\dot{E}_{buy}(t)$ is a continuous decision variable, representing the electricity rate bought from the power grid to meet the electricity load. To account for all the exergy losses occurring at the energy conversion step, the exergy losses occurring in the

power generation plants are also included, through their exergy efficiency, ε_{gen}.

Modeling of the prime mover in the CHP system is presented in Subsection 5.2.1.1, whereas the electricity balance is presented in Subsection 5.2.1.2.

5.2.1.1. Modeling of the prime mover in the CHP system

The CHP system consists of a a gas turbine as the prime mover to meet the electricity demand, and two heat recovery boilers, using high-temperature exhaust gas to satisfy the demands of space heating and domestic hot water. Constraints considered for the gas turbine are presented below.

The CHP ramp rate constraint is formulated as:

$$-DR_{CHP} \le \dot{E}_{CHP}(t) - \dot{E}_{CHP}(t-\Delta t) \le UR_{CHP} \tag{5.1}$$

where $\dot{E}_{CHP}(t)$ and $\dot{E}_{CHP}(t-\Delta t)$ are the energy generation levels at time t and (t - Δt), respectively. The ramp-down rate, DR_{CHP}, and ramp-up rate, UR_{CHP}, are assumed to be the same [6, 7].

The volumetric flow rate of natural gas, $\dot{G}_{PM}(t)$, required by the prime mover to provide the electricity rate, $\dot{E}_{CHP}(t)$, is formulated as:

$$\dot{G}_{PM}(t) = \dot{E}_{CHP}(t) / \left(\eta_{e,PM} LHV_{NG}\right) \tag{5.2}$$

The heat rate of the exhaust gas recovered from the prime mover, $\dot{Q}_{PM,ex}(t)$, is given by:

$$\dot{Q}_{PM,ex}(t) = \dot{E}_{CHP}(t)\left(1-\eta_{e,PM}-\mu_{PM}\right)/\eta_{e,PM} \tag{5.3}$$

For the prime mover, the input energy carrier is natural gas. The exergy input rate of natural gas to the gas turbine, $\dot{E}x_{PM}^{NG}(t)$, is the gas volumetric flow rate consumed, $\dot{G}_{PM}(t)$, multiplied by the specific chemical exergy of natural gas, ex_{NG}:

$$\dot{E}x_{PM}^{NG}(t) = ex_{NG}\dot{G}_{PM}(t) \tag{5.4}$$

where the specific chemical exergy of natural gas, ex_{NG}, can be evaluated by multiplying the exergy factor, ς_{NG}, and the lower heat value, LHV_{gas}:

$$ex_{NG} = \varsigma_{NG} LHV_{NG} \tag{5.5}$$

According to [8], the exergy factor for natural gas is equal to 1.04 ± 0.5%.

The electricity provided by the prime mover is theoretically fully convertible into useful work, and the exergy rate of the output electricity is:

$$\dot{E}x^{e}_{PM}(t) = \dot{E}_{CHP}(t) \tag{5.6}$$

The exergy rate of the output exhaust gas, $\dot{E}x^{ex}_{PM}(t)$, is calculated by multiplying the energy rate by the related Carnot factor, since the temperature of the exhaust gas is assumed to be constant [9]:

$$\dot{E}x^{ex}_{PM}(t) = \dot{Q}_{PM,ex}(t) F_q(t) \tag{5.7}$$

with the Carnot factor, $F_q(t)$, expressed as,

$$F_q(t) = 1 - T_0(t)/T^{s}_{ex} \tag{5.8}$$

which depends on both the temperature of exhaust gas, T^{s}_{ex}, and the reference temperature $T_0(t)$. By following the dynamic exergy analysis, hourly ambient temperatures are considered as reference temperatures [10].

The total exergy loss rate in the prime mover is formulated as:

$$\dot{E}xloss_{PM}(t) = \dot{E}x^{NG}_{PM}(t) - \dot{E}_{CHP}(t) - \dot{E}x^{ex}_{PM}(t) \tag{5.9}$$

5.2.1.2. Electricity balance

The electricity balance is formulated in the following. The electricity rate demand, $\dot{E}_{dem}(t)$, and the electricity rate required by the heat pump, $\dot{E}_{HP}(t)$, must be covered by the sum of the electricity rate provided by the CHP system, $\dot{E}_{CHP}(t)$, and the electricity rate from the grid, $\dot{E}_{buy}(t)$:

$$\dot{E}_{dem}(t) + \dot{E}_{HP}(t) = \dot{E}_{CHP}(t) + \dot{E}_{buy}(t) \tag{5.10}$$

5.2.2 Modeling of the energy network for space heating

The energy network for space heating with the related system components is shown in Figure 5.2. The exhaust heat recovered in the heat recovery boiler is stored through the heat exchanger in a water tank, which is used to supply heat rate to buildings through a Heat Transfer Fluid (HTF) with a constant mass flow rate. A fully-mixed tank model is assumed, where the water in the tank has a uniform time-varying temperature, because of the charge and discharge processes with a given efficiency.

As to the water temperature in the tank, there are two cases. If the temperature of the water tank is higher than the required (assumed constant) at the terminal devices, the HTF is directly supplied to the buildings and part of it is mixed with the return HTF from buildings in the mixer. After mixing, the temperature of the mixed HTF is brought to the required one, and then the HTF is sent to the terminal devices in buildings. In the second case, if the temperature of the water tank is lower than the requirement, the HTF is sent to the auxiliary natural gas boiler or to the heat pump, and heated to the required temperature.

In the following, modeling of the components of the energy network are presented, as well as the related energy balances.

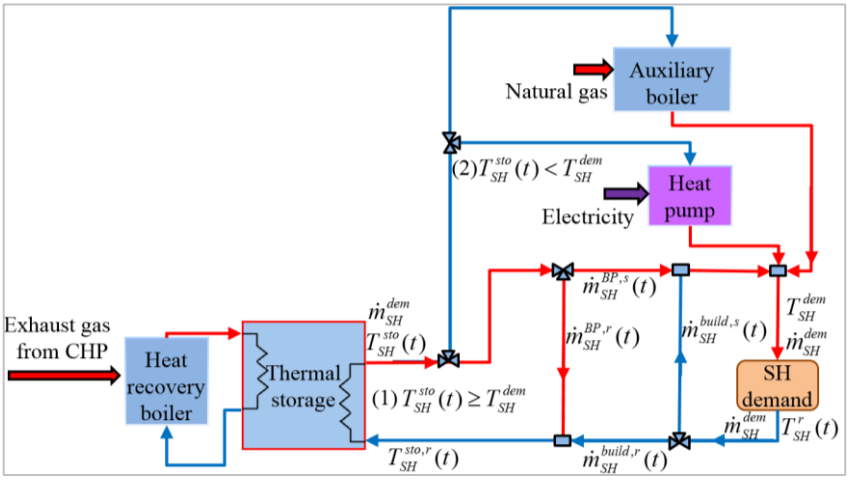

Figure 5.2. Scheme of the energy network for space heating.

5.2.2.1 Modeling of the heat recovery boiler

Heat is recovered from the high-temperature exhaust gas in the heat recovery boiler. The exhaust gas from the prime mover is subdivided between the two heat recovery boilers for the space heating and domestic hot water demands, respectively. The sum of fractions of exhaust gas (continuous decision variable) for space heating, $\xi_{SH}(t)$, and domestic hot water, $\xi_{DHW}(t)$, has to be equal to one:

$$\xi_{SH}(t) + \xi_{DHW}(t) = 1 \tag{5.11}$$

The heat rate delivered by the exhaust gas to the heat recovery boiler for space heating, $\dot{H}_{HRB,SH}(t)$, is:

$$\dot{H}_{HRB,SH}(t) = \xi_{SH}(t)\eta_{HRB}\dot{Q}_{PM,ex}(t) \tag{5.12}$$

where η_{HRB} is the heat recovery efficiency of the boiler. The heat balance equation is:

$$\begin{aligned}\dot{H}_{HRB,SH}(t) &= c_{p,HTF}\,\dot{m}_{HRB,SH}(t)\left(T^{s}_{HRB,SH} - T^{r}_{HRB,SH}(t)\right) = \\ &\eta_{hex}c_{p,HTF}\,\dot{m}_{HRB,SH}(t)\left(T^{s}_{HRB,SH} - T^{sto}_{SH}(t)\right)\end{aligned} \tag{5.13}$$

where $c_{p,HTF}$ is the specific heat of the HTF; $\dot{m}_{HRB,SH}(t)$ is the HTF mass flow rate through the heat exchanger in the storage from the heat recovery boiler, which is a continuous decision variable; $T^{s}_{HRB,SH}$ and $T^{r}_{HRB,SH}(t)$ are the temperatures of the HTF flowing into and out of the heat exchanger, respectively; $T^{sto}_{SH}(t)$ is the temperature of the water in the tank; and η_{hex} is the efficiency of the heat exchanger. The HTF supply temperature, and heat exchanger efficiency are assumed known, and the HTF return temperature is a dependent decision variable.

The exergy input rate to the heat recovery boiler is formulated as the related fraction of exhaust gas multiplied by the exergy rate of exhaust gas. At the output, the exergy rate of the heat provided by the heat recovery boiler, $\dot{E}x^{out}_{HRB,SH}(t)$, is related to the mass flow rate and supply and return temperatures of the HTF, as [9]:

$$\dot{E}x^{out}_{HRB,SH}(t) = c_{p,HTF}\,\dot{m}_{HRB,SH}(t)\left[\left(T^{s}_{HRB,SH} - T^{r}_{HRB,SH}(t)\right) - T_0(t)\ln\left(\frac{T^{s}_{HRB,SH}}{T^{r}_{HRB,SH}(t)}\right)\right] \tag{5.14}$$

Therefore, the exergy loss rate in the heat recovery boiler is formulated as:

$$\dot{E}xloss_{HRB,SH}(t) = \xi_{SH}(t)\dot{E}x^{ex}_{PM}(t) - \dot{E}x^{out}_{HRB,SH}(t) \tag{5.16}$$

5.2.2.2 Modeling of the auxiliary natural gas boiler

The natural gas volumetric flow rate required by the auxiliary boiler to provide the heat rate, $\dot{H}_{boil,SH}(t)$, is given by:

$$\dot{G}_{boil,SH}(t) = \dot{H}_{boil,SH}(t)/\left(\eta_{boil} LHV_{NG}\right) \tag{5.17}$$

where η_{boil} is the combustion efficiency of the boiler. The heat balance equation for the boiler is:

$$\dot{H}_{boil,SH}(t) = c_{p,HTF}\,\dot{m}^{dem}_{SH}\left(T^{s}_{boil,SH}(t) - T^{r}_{boil,SH}(t)\right) \tag{5.18}$$

where $\dot{m}^{dem}_{SH}$ is the HTF mass flow rate (assumed constant) required to satisfy the time-varying space heating demand, and $T^{s}_{boil,SH}(t)$ and $T^{r}_{boil,SH}(t)$ are the temperatures of the HTF flowing out and into of the boiler, respectively, and they are given by:

$$T^{s}_{boil,SH}(t) = T^{dem}_{SH} \quad \text{and} \quad T^{r}_{boil,SH}(t) = T^{sto}_{SH}(t) \tag{5.19}$$

where T^{dem}_{SH} is the temperature required at the terminal devices (assumed constant), and $T^{sto}_{SH}(t)$ is the time-varying water temperature in the tank.

The input energy carrier to the boiler is natural gas. Similarly to the prime mover in the CHP system, the exergy input rate of natural gas to the boiler, $\dot{E}x^{NG}_{boil,SH}(t)$, is the natural gas volumetric flow rate consumed by the boiler multiplied by the specific chemical exergy of natural gas, ex_{NG}. At the output, the exergy rate of the heat provided by the boiler, $\dot{E}x^{out}_{boil,SH}(t)$, is evaluated similarly to that of the heat recovery boiler in Eq. (5.14), based on the mass flow rate and supply and return HTF temperatures [9]. The exergy loss rate in the natural gas boiler is formulated as:

$$\dot{E}xloss_{boil,SH}(t) = \dot{E}x^{NG}_{boil,SH}(t) - \dot{E}x^{out}_{boil,SH}(t) \tag{5.20}$$

5.2.2.3 Modeling of the heat pump

The electricity required by the heat pump, $\dot{E}_{HP}(t)$, to provide the heat rate, $\dot{H}_{HP}(t)$ is:

$$\dot{E}_{HP}(t) = \dot{H}_{HP}(t) / COP_{HP} \tag{5.21}$$

where COP_{HP} is the coefficient of performance. The heat balance equation for the heat pump is:

$$\dot{H}_{HP}(t) = c_{p,HTF}\, \dot{m}_{SH}^{dem}\left(T_{HP}^{s}(t) - T_{HP}^{r}(t)\right) \tag{5.22}$$

where:

$$T_{HP}^{s}(t) = T_{SH}^{dem} \quad \text{and} \quad T_{HP}^{r}(t) = T_{SH}^{sto}(t) \tag{5.23}$$

where $T_{HP}^{s}(t)$ and $T_{HP}^{r}(t)$ are the temperatures of the HTF flowing out and into of the heat pump, respectively.

For the heat pump, electricity is the input energy carrier. The exergy input rate of electricity, $\dot{E}x_{HP}^{e}(t)$, is equal to the electricity consumption of the heat pump. At the output, the exergy rate of the heat provided by the heat pump, $\dot{E}x_{HP}^{out}(t)$, is evaluated similarly to that of the heat recovery and auxiliary natural gas boilers [9]. The exergy loss rate in the heat pump is formulated as:

$$\dot{E}xloss_{HP}(t) = \dot{E}x_{HP}^{e}(t) - \dot{E}x_{HP}^{out}(t) \tag{5.24}$$

5.2.2.4 Modeling of the thermal energy storage

The energy stored in the water tank at time *t* is affected by: the energy stored at time (*t* - Δ*t*), the heat provided by the heat recovery boiler, and the heat supplied:

$$\begin{aligned} c_{p,w} m_{sto,SH} T_{SH}^{sto}(t) = (1 - \varphi_{sto}(\Delta t)) c_{p,w} m_{sto,SH} T_{SH}^{sto}(t - \Delta t) + \\ \left[\dot{H}_{HRB,SH} - c_{p,HTF}\, \dot{m}_{sto,SH}(t)\left(T_{SH}^{sto}(t) - T_{SH}^{sto,r}(t)\right)\right]\Delta t \end{aligned} \tag{5.25}$$

where $c_{p,w}$ is the specific heat of water, $m_{sto,SH}$ is the mass of water in the water tank and $T_{SH}^{sto,r}(t)$ is the temperature of the return HTF to the tank.

5.2.2.5 Space heating energy balance

The components of the energy network for space heating are interconnected by the water network through pipes. As mentioned earlier, there are two cases. In the first one, when the temperature of the water in the tank is higher than the required, T_{SH}^{dem}, the HTF is directly supplied to the buildings, and part of it is mixed with the return HTF from buildings before going to the terminal devices inside the buildings, i.e.,

$$\begin{aligned}\dot{m}_{SH}^{dem} &= \dot{m}_{SH}^{BP,s}(t) + \dot{m}_{SH}^{BP,r}(t) = \dot{m}_{SH}^{BP,s}(t) + \dot{m}_{SH}^{build,s}(t) \\ &= \dot{m}_{SH}^{build,s}(t) + \dot{m}_{SH}^{build,r}(t) = \dot{m}_{SH}^{BP,r}(t) + \dot{m}_{SH}^{build,r}(t)\end{aligned} \tag{5.26}$$

where $\dot{m}_{SH}^{BP,s}(t)$ is the bypass mass flow rate to be supplied to buildings; $\dot{m}_{SH}^{BP,r}(t)$ is the bypass mass flow rate to be returned to the tank; $\dot{m}_{SH}^{build,s}(t)$ is the return mass flow rate from buildings to be mixed with the HTF from the storage; and $\dot{m}_{SH}^{build,r}(t)$ is the return water mass flow rate from buildings to the tank. The energy balance in the mixer is expressed as:

$$c_{p,HTF}\,\dot{m}_{SH}^{dem} T_{SH}^{dem} = c_{p,HTF}\,\dot{m}_{SH}^{BP,s}(t) T_{SH}^{sto}(t) + c_{p,HTF}\,\dot{m}_{SH}^{build,s}(t) T_{SH}^{r}(t) \tag{5.27}$$

where $T_{SH}^{r}(t)$ is the temperature of the return HTF from buildings. After satisfying the space heating demand, the energy balance in the mixer is expressed by:

$$c_{p,HTF}\,\dot{m}_{SH}^{dem} T_{SH}^{sto,r}(t) = c_{p,HTF}\,\dot{m}_{SH}^{BP,s}(t) T_{SH}^{sto}(t) + c_{p,HTF}\,\dot{m}_{SH}^{build,s}(t) T_{SH}^{r}(t) \tag{5.28}$$

where $T_{SH}^{sto,r}(t)$ is the temperature of the return HTF to the water tank.

The energy balance equation at the demand side is:

$$\dot{H}_{SH}^{dem}(t) = c_{p,HTF}\,\dot{m}_{SH}^{dem}\left(T_{SH}^{dem} - T_{SH}^{r}(t)\right) \tag{5.29}$$

where $\dot{H}_{SH}^{dem}(t)$ is the heat rate demand of space heating.

In the second case, when the temperature of the water in the tank is lower than the required, the HTF is sent to the auxiliary natural gas boiler or the heat pump, and heated to the required temperature.

5.2.3 Modeling of the energy network for domestic hot water

The energy network for domestic hot water with the related system components is shown in Figure 5.3. As in the previous subsection, a fully-mixed tank model is assumed. Since the water is used up at the demand side, cold water is continuously supplied to the thermal storage and warmed up by the heat rate provided by the heat recovery boiler and solar collectors through two heat exchangers in the water tank.

When the temperature of the water supplied by the tank is higher than the required (assumed constant), the water is directly supplied to the buildings and mixed with the aqueduct cold water in the mixer to bring down the temperature to the required one before the terminal use. When the temperature of the water in the tank is lower than the required, the water is sent to the auxiliary natural gas boiler, and heated to the required temperature.

The energy and exergy modeling of the heat recovery boiler, auxiliary natural gas boiler, and thermal storage for domestic hot water is similar to the modeling of the corresponding components of the energy network for space heating. Modeling of the solar thermal plant, and the energy balances are presented in the following.

5.2.3.1 Modeling of the solar thermal plant

The heat rate provided by the solar thermal plant, $\dot{H}_{ST}(t)$, is formulated as:

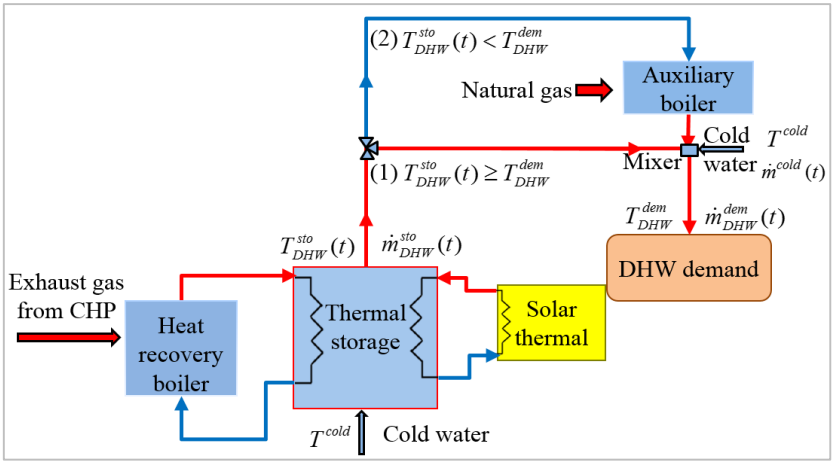

Figure 5.3. Scheme of the energy network for domestic hot water.

$$\dot{H}_{ST}(t) = \eta_{coll} A_{coll} \dot{I}_T(t) \tag{5.30}$$

The energy balance equation for the solar thermal plant is formulated as:

$$\dot{H}_{ST}(t) = c_{p,HTF}\, \dot{m}_{ST}(t)\left(T^{s}_{ST}(t) - T^{r}_{ST}(t)\right) = \eta_{hex} c_{p,HTF}\, \dot{m}_{ST}(t)\left(T^{s}_{ST}(t) - T^{sto}_{DHW}(t)\right) \tag{5.31}$$

where $\dot{m}_{ST}(t)$ is the water mass flow rate from the solar thermal plant through the heat exchanger in the storage; $T^{s}_{ST}(t)$ and $T^{r}_{ST}(t)$ are the temperatures of the water flowing into and out of the heat exchanger, respectively; and η_{hex} is the efficiency of the heat exchanger. The supply temperature is assumed 10 K higher than that of the water in the tank and the return temperature is a dependent variable.

As in Chapter 4, the solar energy input to the collectors is considered as a low-exergy source since the solar exergy input rate is evaluated at the output of the solar collector field [11, 12]. Therefore, by following this approach no exergy loss is taken into account.

5.2.3.2 Domestic hot water energy balance

The components of the energy network for domestic hot water are interconnected by the water network through pipes. Similarly to space heating, when the temperature of the water in the tank, $T^{sto}_{DHW}(t)$, is higher than the required, T^{dem}_{DHW}, the water is directly supplied to the buildings and mixed with the aqueduct cold water before the terminal use:

$$\dot{m}^{dem}_{DHW}(t) = \dot{m}^{sto}_{DHW}(t) + \dot{m}^{cold}(t) \tag{5.32}$$

where $\dot{m}^{dem}_{DHW}(t)$, $\dot{m}^{sto}_{DHW}(t)$, and $\dot{m}^{cold}(t)$ are the water mass flow rates to be supplied to terminal users, the water mass flow rate taken from the storage, and the cold water mass flow rate from the aqueduct, respectively. The energy balance in the mixer is expressed as:

$$c_{p,w}\dot{m}^{dem}_{DHW}(t) T^{dem}_{DHW} = c_{p,w}\dot{m}^{sto}_{DHW}(t) T^{sto}_{DHW}(t) + c_{p,w}\dot{m}^{cold}(t) T^{cold} \tag{5.33}$$

where T^{cold} is the temperature of the cold water from the aqueduct. At the demand

side, it is assumed that the temperature of hot water is brought down to T^{cold} after terminal use, and the energy balance equation is:

$$\dot{H}_{DHW}^{dem}(t) = c_{p,w}\dot{m}_{DHW}^{dem}(t)\left(T_{DHW}^{dem} - T^{cold}\right) \tag{5.34}$$

where $\dot{H}_{DHW}^{dem}(t)$ is the heat rate demand of domestic hot water.

In the second case, when the temperature of the water in the tank, $T_{DHW}^{sto}(t)$, is lower than the required, T_{DHW}^{dem}, the water is sent to the auxiliary natural gas boiler:

$$\dot{m}_{DHW}^{dem}(t) = \dot{m}_{DHW}^{sto}(t) \tag{5.35}$$

The water is heated to the required temperature in the natural gas boiler.

For the overall optimization problem, the coupling across the two water networks is that the sum of exhaust fractions for space heating and domestic hot water has to be one (Eq. 5.11). The coupling across all the three networks is represented by the electricity balance (Eq. 5.10).

5.3. Multi-objective optimization: energy cost and exergy losses at the energy conversion step

The objective is to minimize the total energy cost and the exergy losses occurring at the energy conversion step. The economic and exergetic objective functions are discussed in Subsections 5.3.1 and 5.3.2, respectively. The multi-objective optimization method used to solve the optimization problem is discussed in Subsection 5.3.3.

5.3.1 Economic objective

The economic objective is to minimize the total energy cost, *Cost*, which is the sum of two terms: cost of grid power and cost of natural gas, as follows:

$$Cost = \sum_{t}\left(P_{grid}(t)\dot{E}_{buy}(t) + P_{NG}\dot{G}_{buy}(t)\right)\Delta t \tag{5.36}$$

where $P_{grid}(t)$ is the time-of-day unit price of electricity from the power grid, and P_{NG} is the constant unit price of natural gas. The volumetric flow rate of natural gas

bought, $\dot{G}_{buy}(t)$, corresponds to the total consumption requirement of the CHP system and auxiliary natural gas boilers.

5.3.2 Exergetic objective

As mentioned earlier, the focus of this chapter is on the total exergy loss occurring at the energy conversion step, which accounts for the largest fraction of the total exergy losses in the energy-supply chain from energy resources to user demands. The total exergy loss at the conversion step, $Exloss_{conv}$, is formulated as the sum of the exergy losses of the system components at the conversion step over time:

$$\begin{aligned} Exloss_{conv} = \sum_{t} \Big(& \dot{E}xloss_{PM}(t) + \dot{E}xloss_{grid}(t) + \dot{E}xloss_{HRB,SH}(t) \\ & + \dot{E}xloss_{HRB,DHW}(t) + \dot{E}xloss_{boil,SH}(t) + \dot{E}xloss_{boil,DHW}(t) + \dot{E}xloss_{HP}(t) \Big) \Delta t \end{aligned} \tag{5.37}$$

5.3.3 Multi-objective optimization method

With the economic objective function formulated in Eq. (5.36) and the exergetic objective function formulated in Eq. (5.37), the problem has two objective functions to be minimized. To solve this multi-objective optimization problem, the weighted-sum method is used, and a single objective function is formulated as a weighted sum of the total energy cost, *Cost*, and the total exergy loss at the energy conversion step, $Exloss_{conv}$:

$$F_{obj} = c\omega Cost + (1-\omega) Exloss_{conv} \tag{5.38}$$

where the constant c is chosen such that $c\,Cost$ and $Exloss_{conv}$ have the same order of magnitude. The Pareto frontier involving the best possible trade-offs between the two objectives can be found by varying the weight ω in between the interval 0 and 1. For $\omega = 1$, the economic optimization is carried out, and the solution that minimizes the total energy cost is obtained, whereas for $\omega = 0$, the exergetic optimization is carried out, and the solution that minimizes the total exergy loss at the energy conversion step is obtained. The optimization problem formulated in Sections 5.2 and 5.3 is separable, nonlinear and involves both discrete and continuous variables.

5.4. Solution methodology

The solution methodology used to solve the mixed-integer nonlinear programming problem formulated above is discussed in the following. To coordinate the system components with coupling constraints and solve the optimization problem efficiently, the key idea is to use multipliers as shadow prices in a decomposition and coordination structure. Surrogate Lagrangian relaxation and branch-and-cut are combined for a speedy and near-optimal performance [13 - 15]. After relaxing the coupling constraints, i.e., CHP exhaust gas sharing constraints (Eq. 5.11) by Lagrangian multipliers, the relaxed problem is to minimize the following Lagrangian function, *L*, as:

$$L(\lambda, y) \equiv c\omega Cost(y) + (1-\omega) Exloss_{conv}(y) + \sum_t \lambda(t)\left(\xi_{SH}(t) + \xi_{DHW}(t) - 1\right) \quad (5.39)$$

subject to Eq.s (5.1)-(5.10) and (5.12)-(5.37). In the above, λ represent multipliers relaxing CHP exhaust gas sharing constraints, and *y* represent all the decision variables.

Then, there are two subproblems, e.g., the space heating subproblem and the domestic hot water subproblem (with electricity-related system components). They are solved by branch-and-cut individually.

By solving the relaxed problem, the dual function becomes:

$$q(\lambda) = \min_y L(\lambda, \mathrm{y}) \quad (5.40)$$

Instead of obtaining the dual value (5.40), a surrogate dual value is obtained in the surrogate Lagrangian relaxation as follows:

$$\tilde{L}\left(\lambda^k, y^k\right) = c\omega Cost(y) + (1-\omega) Exloss_{conv}(y) + \lambda^k \tilde{g}(y^k) \quad (5.41)$$

In the above, λ^k and y^k are multipliers and any feasible solution of the relaxed problem at iteration *k*, respectively, and $\tilde{g}(y^k)$ are the surrogate subgradient vectors consisting of:

$$\tilde{g}\left(y^k\right) = \xi_{SH}(t) + \xi_{DHW}(t) - 1 \quad (5.42)$$

Since surrogate Lagrangian relaxation does not require the relaxed problem to be fully optimized, surrogate subgradient directions may not form acute angles with directions toward optimal multipliers, which will cause divergence. To guarantee that surrogate directions form acute angles with directions toward the optimal multipliers, the relaxed problem has to be sufficiently optimized, such that surrogate dual values in Eq. (5.41) satisfy the surrogate optimality condition:

$$\tilde{L}\left(\lambda^k, y^k\right) < \tilde{L}\left(\lambda^k, y^{k-1}\right) \tag{5.43}$$

where y^{k-1} is a feasible solution at the iteration *k-1*. Since the relaxed problem is not fully optimized and subgradient directions do not change much at each iteration, computational requirements and zigzagging of multipliers are much reduced as compared to traditional subgradient methods.

In the method, multipliers are updated as:

$$\lambda^{k+1} = \lambda^k + d^k \tilde{g}(y^k) \tag{5.44}$$

where d^k is the stepsize at iteration *k*. The multipliers converge to the optimum if the stepsizes are updated by using the novel step-sizing formula developed in [13].

To solve subproblems by using branch-and-cut, which is suitable for mixed-integer linear problems, a linear formulation is needed [16, 17]. Usually, the logarithm function can be linearly approximated within a small range. For other nonlinear terms such as the cross product, the linearization is not easy. In the framework of surrogate Lagrangian relaxation, solutions from the previous iteration can be used as input data in the next iteration. Therefore, the nonlinear terms can be linearly approximated by using the values of the previous solution under the monotonic condition as proved in [14]. The resulting linear problem will be optimized and the previous solution will be updated.

5.5. Numerical testing: A Chinese case study

The method developed above is implemented by using IBM ILOG CPLEX Optimization Studio Version 12.6. As in Chapter 4, the hypothetic large hotel located

in Beijing with a 30,000 m^2 area is selected as the targeted end-user. A typical winter day of January is chosen, with one hour as time-step.

The input data for the optimization model are the building energy demands, prices and exergy of primary energy carriers, sizes and efficiencies of energy devices and thermal storage systems. As regards the building energy demands, reference is made to the hourly electricity, domestic hot water, and space heating demands of the hotel for a representative winter day of January [18], shown in Figure 4.3a in Chapter 4. As regards the energy prices used in the numerical testing, the time-of-day unit price of electricity from the power grid is shown in Figure 4.3 in Chapter 4, and the unit price of natural gas is assumed equal 0.38 \$/Nm^3 [19]. To evaluate the exergy loss rate related to the power grid, the exergy efficiency of the power generation plant is assumed equal to 0.32 [20, 21]. The exergy factor of natural gas is assumed equal to 1.04 [8]. To evaluate the heat rate provided by the solar collector field, for each hour of the representative winter day of January, the solar irradiance has been evaluated as the average of the hourly mean values of the solar irradiance in the corresponding hour of all January days [22]. The sizes and efficiencies of the energy devices are listed in Table 5.1. As regards the CHP system, reference is made to a gas turbine as the prime mover with an actual nominal peak output of 1,240 kW and an exhaust gas temperature of 785.15 K. It operates at a 24% gas-to-electric turbine efficiency with an 8% heat loss efficiency [23].

Table 5.1 Sizes and efficiencies of energy devices and thermal storage systems.

Primary energy devices	**Size (MW)**	**Efficiency**	
		Electrical	Thermal
Gas turbine	1.24	0.24	0.68
Solar thermal	0.41		0.40
Secondary energy devices		**Efficiency**	
Heat pump	5.0	3.0	
Heat recovery boiler SH - DHW	2.4 – 1.1	0.74	
Auxiliary natural gas boiler SH - DHW	1.0 - 0.5	0.90	
Thermal energy storage	**Size (MWh)**	**Storage loss fraction**	
SH – DHW storage	3.0 – 2.0	0.10	

In the following, the Pareto frontier and the optimized operation strategies of the DES obtained at various trade-off points are discussed in Subsection 5.5.1. The exergy losses related to the energy system components for conversion and storage in the energy-supply chain obtained by the economic optimization and the exergetic optimization are also presented. In addition, the effects of energy prices on the optimized operation strategies are discussed in Subsection 5.5.2. To show the effects of variations in the configuration of the DES on energy costs and exergy losses, results of the sensitivity analysis are presented and discussed in Subsection 5.5.3.

5.5.1 Pareto frontier and optimized operation strategies of the DES at various trade-off points

Based on the energy network configurations for space heating and domestic hot water shown in Figures 5.2 and 5.3, there are nonlinear logic constraints. The Surrogate Lagrangian relaxation method combined with branch-and-cut is suitable for mixed-integer linear problems. To get a linear problem and test this innovative optimization method, in the numerical testing, temperatures of the water in the tanks are assumed lower than the required temperatures at terminal uses. This assumption is supported by the fact that, in winter days, the average solar irradiance is lower than in summer days, and electricity demand is also lower. As a consequence, water temperature in the storage tanks can be lower than that required for most of the day.

The optimization problem can be solved within several minutes and the Pareto frontier obtained is shown in Figure 5.4. The point marked with *a* is obtained by the economic optimization. The daily energy cost is 3,486 $/d whereas the daily exergy losses at the energy conversion step are 75,459 kJ/d. The point marked with *b* is obtained by minimizing the total exergy loss at the conversion step. The daily energy cost is 3,718 $/d whereas the daily exergy losses are 68,687 kJ/d. The points between the extreme points are found by subdividing the weight interval into 100 equally-spaced points. There are 13 points since some solutions have been found under more than one weight values.

Each point on the Pareto frontier corresponds to a different operation strategy of the DES. In order to understand how the operation strategies vary with the weight, ω, the optimized operation strategies of the DES obtained by varying the weight from 0

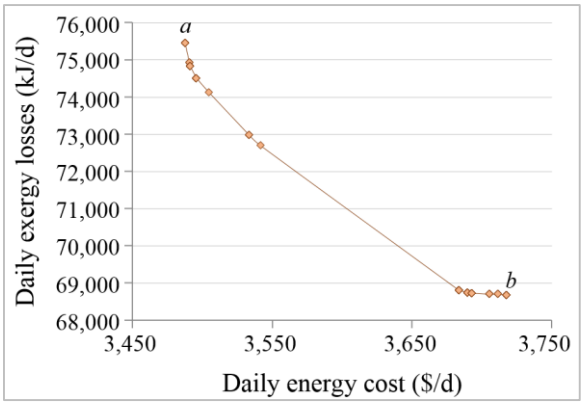

Figure 5.4. Pareto frontier.

to 1, with a 0.1 increase, are presented in Figure 5.5.

Figure 5.5a shows that when ω varies from 1 to 0 (from the economic optimization to the exergetic optimization), the share of electricity load (sum of electricity demand and electricity required by the heat pump) satisfied by the CHP system increases while the exergy losses reduce. This highlights the essential role of the CHP system in the reduction of exergy losses because of the recovery of waste heat for thermal purposes, leading to efficient use of the high-quality energy resource.

Figure 5.5b shows that when ω varies from 1 to 0, the share of the domestic hot water demand satisfied by the heat recovery boiler increases coherently with the increased use of the CHP system (as shown in Figure 5.5a). The use of exhaust gas for low-exergy thermal demands reduces the exergy losses occurring at the energy conversion step. Conversely, the share of domestic hot water demand satisfied by the auxiliary natural gas boiler reduces, highlighting that natural gas as a high-quality energy resource should not be used for low-quality thermal demands, thereby reducing the waste of high-quality energy resources.

Figure 5.5c shows that when ω varies from 1 to 0, the share of space heating demand satisfied by the heat recovery boiler increases, coherently with the increasing use of the CHP, highlighting, as above, the importance of waste heat recovery for the exergetic purpose. When ω varies from 1 to 0, the share of space heating demand met by the heat pump exhibits an opposite trend, decreasing with the reduced use of the grid power, as shown in Figure 5.5a.

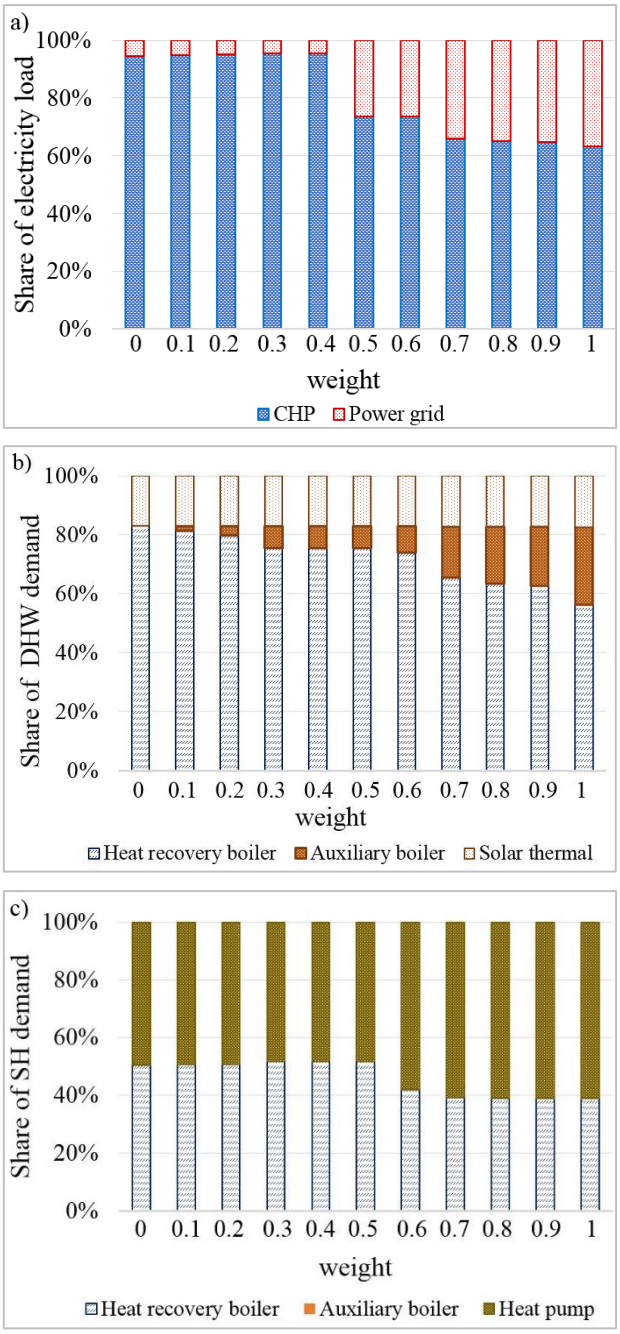

Figure 5.5. Optimized operation strategies of the DES at various trade-off points for a) electricity; b) domestic hot water; c) space heating.

Figure 5.6 shows the exergy losses related to the energy system components for conversion and storage in the energy-supply chain obtained by the economic and the exergetic optimizations. Exergy losses occurring in the thermal storage systems are evaluated according to the ECBCS - Annex 49 [9]. The exergy losses at the energy conversion step attained by the exergetic optimization are about 9% lower than those obtained by the economic optimization. On the other hand, exergy losses evaluated in the thermal storage systems under the exergetic optimization are 22% higher than those evaluated under the economic optimization. This is because, under the exergetic optimization, there is a larger use of heat recovery boilers, which charge the storage tanks, than what occurs under the economic optimization, as shown in Figures 5.5b and 5.5c. This means that the minimization of exergy losses at the energy conversion step does not guarantee the minimization of exergy losses in the other steps of the energy-supply chain.

5.5.2 Effect of energy prices on the optimized operation strategies of the DES

The optimized operation strategies of the DES depend on the prices of primary energy carriers. In the problem under consideration, representing the reference case, the price of natural gas is much cheaper than that of grid power as in the current Chinese market. To show how the relative prices of natural gas and grid power affect the optimized operation strategies, the problem is solved with a natural gas price as 150% of the price considered in the reference case.

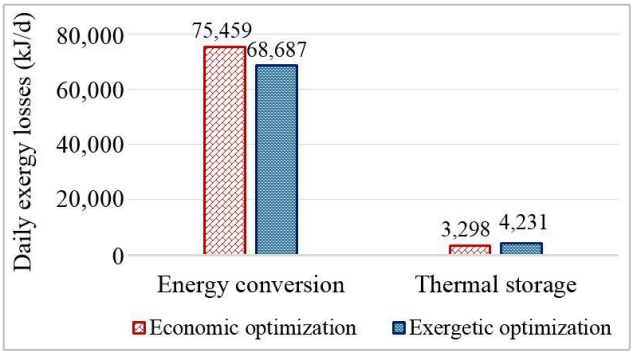

Figure 5.6. Daily exergy losses at the energy conversion and thermal storage steps in the energy-supply chain under the economic and exergetic optimizations.

Figure 5.7 shows the optimized operation strategies for electricity at the various trade-off points with a high natural gas price. It is shown that when ω varies from 1 to 0, the share of the electricity load satisfied by the CHP system increases, as occurs in the reference case, as shown in Figure 5.5a. However, compared to the reference case, the share of electricity load covered by the CHP system is generally lower when the weight of the economic objective is higher than that of the exergetic one, and almost the same when the weight of the economic objective is lower. In particular, when ω = 0.5, 0.7 and 1, the share of the electricity load covered by the CHP system is 69%, 51% and 46% in the new case, respectively, whereas it is 74%. 66% and 63%, in the reference case, respectively, as shown in Figure 5.5a. The lower usage of the CHP system results in lower amount of exhaust gas recovered, and consequent higher usage of auxiliary boilers for thermal purposes. This leads to higher exergy losses at the energy conversion step as compared to the reference case.

5.5.3 Sensitivity analysis

A sensitivity analysis is carried out to show how each energy device contributes to the reduction of energy costs and exergy losses. The single-objective optimization is carried out for the configurations listed in Table 5.2. For each configuration, one energy device is taken out of the DES, including the solar thermal plant, auxiliary natural gas boilers, heat pump, and entire CHP system. In addition, a conventional

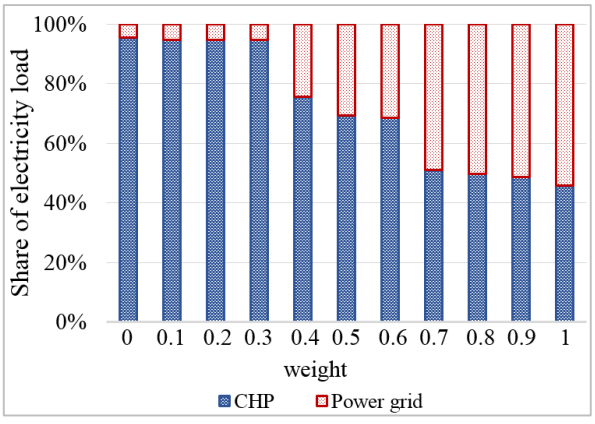

Figure 5.7. Optimized operation strategies of the DES at various trade-off points for electricity with a high natural gas price.

Table 5.2. Configurations investigated in the sensitivity analysis.

Configuration	Energy devices excluded from the reference case (Configuration 1)
2	without solar thermal plant
3	without auxiliary natural gas boilers
4	without heat pump
5	CHP system
Configuration	**Other case**
6	Conventional energy supply system

energy supply system is also analyzed, where the grid power is used to meet the electricity demand, the electricity required by an electric heater to satisfy the space heating demand, and the electricity required by an electric boiler to satisfy the domestic hot water demand.

The daily energy costs obtained by the economic optimization for Configurations 1-6 are compared in Figure 5.8. Configuration 1 is the reference case, consisting of all energy devices and thermal storage systems shown in Figure 5.1. The reference case shows the best performance in terms of the daily energy cost as compared with the other configurations. Configurations 2 and 3 exclude the solar thermal plant and the auxiliary boilers for space heating and domestic hot water from the reference case, respectively. In both the cases, the daily energy cost is about 2% larger than that in

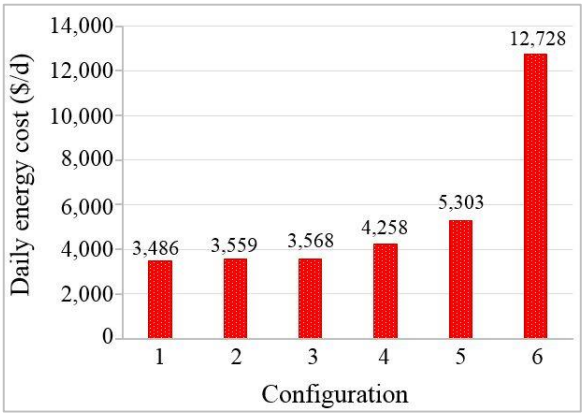

Figure 5.8. Daily energy cost for Configurations 1-6 under the economic optimization.

reference case. Configurations 4 excludes the heat pump from the reference case, and the daily energy cost is 18% larger than that in the reference case, because of the high conversion efficiency of the heat pump. Configuration 5 excludes the CHP system. The daily energy cost is 34% larger than that in the reference case, pointing out the essential role of the CHP system in the reduction of energy costs. The worst case is represented by the conventional energy supply system (Configuration 6). The 73% increase in the daily energy cost, as compared with the reference case, shows that the energy costs can be strongly reduced by the optimized operation of the DES.

Figure 5.9 shows the total daily exergy losses occurring at energy conversion step obtained by the exergetic optimization for Configurations 1-5. The reference case (Configuration 1) shows the best performance, also in terms of minimum exergy losses at the conversion step. For Configuration 2, exergy losses increase by 2% as compared with the reference case. For Configuration 3, the exergy losses are the same as those in the reference case, since under the exergetic optimization, the auxiliary natural gas boilers are never used to satisfy the domestic hot water and space heating demands, as was also shown in Figures 5.5b and 5.5c. For Configuration 4, the exergy losses are 22% larger than those in the reference case, showing the importance of the heat pump not only in the reduction of energy costs but also in the reduction of exergy losses, due to the high energy conversion efficiency. A 28% increase in the exergy losses is found for Configuration 5, as compared with the reference case. Without the

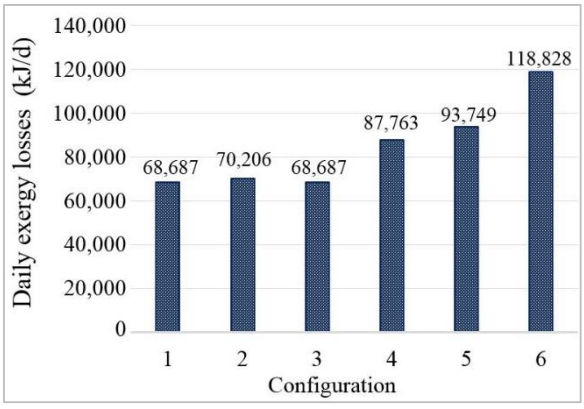

Figure 5.9. Daily exergy losses at the energy conversion step for Configurations 1-6 under the exergetic optimization

CHP system, there is no exhaust gas for thermal purposes, and the use of auxiliary boilers increases the exergy losses because of the combustion processes. Finally, similarly to the energy costs, the worst case is represented by Configuration 6, where the exergy losses are 73% larger than those in the reference case. When all the demands are satisfied by electricity, high exergy losses occur, since a high quality energy carrier, as the electricity from the power grid, is used to satisfy low-quality thermal demands.

Figure 5.10 shows the exergy losses related to the energy system components for conversion and storage in the energy-supply chain for Configurations 1-5 under the exergetic optimization. Exergy losses in thermal storage systems do not reach the minimum value in the reference case. The minimum value is obtained in Configuration 5, where it is 93% lower than that in the reference case. Without the CHP system, the SH storage is not used with consequent zero exergy losses, and the DHW storage is only charged by the solar thermal collectors. Therefore, the total exergy loss is reduced at the storage step. However, the total exergy loss occurring in the whole energy-supply chain reaches the maximum value in Configuration 5, and the minimum in the reference case. In particular, the total exergy loss in the whole energy-supply chain in Configuration 5 are about 22% larger than that in the reference case.

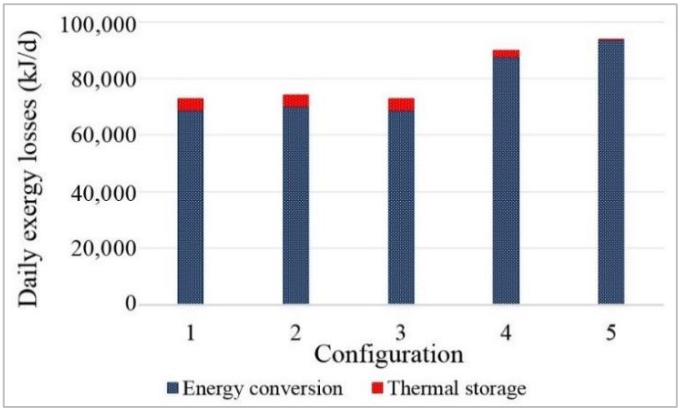

Figure 5.10. Daily exergy losses at the energy conversion and thermal storage steps in the energy-supply chain for Configurations 1-5 under the exergetic optimization.

References

[1] Schmidt D. Low exergy systems for high performance buildings and communities. Energy and Buildings 2009;41:331-336.

[2] Schmidt D. Design of low exergy buildings – method and a pre-design tool. The International Journal of Low Energy and Sustainable Buildings 2004;3:1–2.

[3] Yildiz A, Güngör A. Energy and exergy analyses of space heating in buildings. Applied Energy 2009;86:1939–1948.

[4] Jansen SC, Terès-Zubiaga J, Luscuere PG. The exergy approach for evaluating and developing an energy system for a social dwelling. Energy and Buildings 2012;55:693-703.

[5] Terès-Zubiaga J, Jansen SC, Luscuere P. Dynamic exergy analysis of energy systems for a social dwelling and exergy based system improvement, Energy and Buildings 2013;64:359-371.

[6] Kriett P, Salani M. Optimal control of a residential microgrid. Energy 2012;42(1):321–30.

[7] Brahman F, Jadid S. Optimal energy management of hybrid CCHP and PV in a residential building. In: Proceedings of 19th IEEE Conference on Electrical Power Distribution Networks, 2014 May 6–7:19–24.

[8] Kotas KJ. The exergy method for thermal plant analysis, reprinted. Malabar, FL: Krieger; 1995.

[9] ECBCS - Annex 49 - Low Exergy Systems for High Performance Buildings and Communities, homepage. Available online from: http://www.ecbcs.org/annexes/annex49.htm.

[10] Angelotti A, Caputo P. The exergy approach for the evaluation of heating and cooling technologies, first results comparing steady state and dynamic simulations. Proceedings of the 2nd PALENC and 28th AIVC Conference, vol I; 2007 September 27-29; Crete Island, Greece; p. 59-64.

[11] Torìo H, Angelotti A, Schmidt D. Exergy analysis of renewable energy-based climatisation systems for buildings: A critical view. Energy and Buildings 2009;41:248-71.

[12] Torìo H, Schmidt D. Framework for analysis of solar energy systems in the built environment from an exergy perspective. Renewable Energy 2010;35:2689-97.

[13] Bragin MA, Luh PB, Yan JH, Yu N, Stern GA. Convergence of the Surrogate Lagrangian Relaxation Method. Journal of Optimization Theory and Applications 2015;164 (1):173-201.

[14] Bragin MA, Luh PB, Yan JH, Stern GA. An efficient approach for solving mixed-integer programming problems under the monotonic condition. Journal of Control and Decision 2016;DOI:10.1080/23307706.2015.1129916.

[15] Bragin MA, Luh PB, Yan JH, Stern GA. Novel exploitation of convex hull invariance for solving unit commitment by using surrogate Lagrangian relaxation and branch-and-cut, in Proceedings of the IEEE Power and Energy Society, General Meeting, Denver, Colorado, 2015.

[16] Bixby RE, Fenelon M, Gu Z, Rothberg E, Wunderling R. MIP: Theory and practice – closing the gap, System Modelling and Optimization 2000;46:19-49.

[17] IBM ILOG, IBM ILOG CPLEX Optimization Studio Information Center, 2013. Available online from: http://pic.dhe.ibm.com/infocenter/cosinfoc/v12r5/index.jsp.

[18] Zhou Z, Liu P, Li Z, Ni W. An engineering approach to the optimal design of distributed energy systems in China. Applied Thermal Engineering 2013;53:387-96.

[19] Beijing Municipal Commission of Development & Reform, Current prices for Public commodities; Available online from http://www.bjpc.gov.cn/english/.

[20] Kaushik SC, Reddy VS, Tyagi SK. Energy and exergy analyses of thermal power plants: A review. Renewable and Sustainable Energy Reviews 2011;15:1857-1872.

[21] Forum - Oxford Institute for Energy Studies, Issue 95, February 2014. Available online from: http://www.oxfordenergy.org/wpcms/wp-content/uploads/2014/04/OEF-95.pdf.

[22] ASHRAE International Weather files for Energy Calculations (IWEC weather files). Users manual and CD-ROM, American Society of Heating, Refrigerating and Air-Conditioning Engineers, Atlanta, GA, USA, 2001.

[23] Emerson DB, Whitworth BA. Summary of micro-turbine technology. Orlando, Florida: Summit;1998.

Chapter 6

Conclusions

This thesis focuses on the optimal operation planning of Distributed Energy Systems (DESs) through multi-objective criteria, as an innovative tool for a sustainable energy decision-making process. The proposed mathematical models aim at providing decision support to planners for selecting the operation strategies of a DES throughout the planning period, based on short- and long-run priorities. On the one hand, there are the operators of DESs, whose greatest interest is the economic factor, on the other hand, there is the civil society, ideally represented by the regulator, whose greatest interest is a sustainable future.

The DESs under consideration are complex energy systems, where multiple energy devices, such as Combined Cooling Heating and Power (CCHP) systems or Combined Heat and Power (CHP) systems, natural gas and biomass boilers, solar thermal plants, heat pumps, are involved to satisfy given time-varying user demands at district level. To allow more efficient use of thermal energy, thermal energy storage systems are also included in the DESs configurations.

In order to consider the economic priority, crucial in the short-run, and the environmental impacts, essential in the long-run, in the operation planning of a DES, a multi-objective linear programming problem is formulated to obtain the optimized operation strategies to reduce the energy costs and environmental impacts in terms of CO_2 emissions. The Pareto frontier is obtained by minimizing a weighted sum of the total energy cost and CO_2 emission, by using branch-and-cut. Results of the numerical testing, where a large hotel located in Italy is considered as the targeted end-user, demonstrate the effectiveness of the optimization tool for ensuring both economic and environmental benefits. In fact, the optimized operation allows to reduce significantly energy costs and CO_2 emissions as compared with conventional

energy supply systems. Moreover, the Pareto frontier obtained shows that a significant reduction in the total CO_2 emission can be gained with a negligible increase in the energy cost. The analysis of the optimized operation strategies at various trade-off points highlights that the CCHP system is essential for the energy cost minimization, whereas the heat pumps are crucial for the environmental impact minimization.

The other main contribution of this thesis is to demonstrate the effectiveness of the exergy analysis in the operation planning of DESs to increase sustainability of the energy supply, through a rational use of the energy resources, while considering energy quality. Based on the possibility to integrate different sources in DESs to satisfy different types of end-user demands, the key idea is to apply the exergy analysis in the operation planning of these systems to promote the matching of the energy quality levels of supply and demand. For not neglecting the energy costs, a multi-objective linear programming problem is formulated to attain the optimized operation strategies of a DES to reduce the energy costs and increase the overall exergy efficiency. The Pareto frontier is obtained by minimizing a weighted sum of the total energy cost and primary exergy input, by using branch-and cut. Results of the numerical testing, where a large hotel located in Beijing is considered as the targeted end-user, demonstrate that the minimization of primary exergy input to the DES promotes an efficient energy supply system where all the energy resources, including renewable ones, are used in an efficient way. The optimized operation of the DES allows to reduce significantly energy costs and primary exergy input as compared with conventional energy supply systems. The analysis of the optimized operation strategies at various trade-off points shows that the CCHP system is essential for the exergetic objective, due to the waste heat recovered to meet the low-quality thermal demands. A sensitivity analysis is performed to show the contribution of each energy device in the reduction of energy costs and primary exergy input. Results demonstrate the essential role of the CCHP system, heat pumps and solar thermal from an exergy perspective to increase the overall exergy efficiency. Conversely, the biomass boiler is found to be a good solution for energy costs, due to the low price, but a solution to be avoided for the exergetic objective. This latter result highlights that biomass, as a high-quality energy resource, should not be used

to meet the low-quality thermal demand. Moreover, the influence of the exergy analysis on the environmental impact in the optimal operation planning of the DES is also investigated. Results show that by increasing the overall exergy efficiency of the DES, a reduced use of high-quality energy resources as well as a reduced environmental impact are attained.

The exergy-based operation planning of a DES is also addressed by considering the whole energy-supply chain from energy resources to user demands, through the detailed analysis of the energy system components for conversion, storage, distribution and emission for space heating. Instead of considering the overall exergy efficiency, exergy losses are modeled for the system components at the energy conversion step, which accounts for the largest part of the total exergy loss in the whole energy-supply chain. Therefore, the inefficiencies within the energy supply are pinpointed, quantified and minimized through a multi-objective approach for taking into account also the energy costs. A multi-objective mixed-integer nonlinear programming problem is formulated based on the detailed energy and exergy modeling of the energy system components, to find the optimized operation strategies which reduce energy costs and exergy losses at the energy conversion step. The Pareto frontier is found by minimizing a weighted sum of the total energy cost and exergy loss, by using an innovative solution methodology based on the Surrogate Lagrangian Relaxation combined with branch-and-cut. Results of the numerical testing, where the hotel located in Beijing is considered as the targeted end-user, demonstrate that the exergy-efficient management of the energy-supply chain of the DES allows to reduce the inefficiencies, thereby attaining a further sustainability of the energy supply. The analysis of the optimized operation strategies at various trade-off points shows that under the exergy loss minimization, combustion processes in auxiliary natural gas boiler are avoided for providing low-temperature heat to end-users, and the CHP system is preferred, due to the possibility to recover the waste heat for thermal purposes, thereby increasing the efficiency in the use of the high-quality energy resource.

In the optimization tool proposed, the economic priority, crucial in the short-run, is never neglected, since the optimized operation of DESs allows to reduce the energy costs as compared with conventional energy supply systems. The long-run

sustainability is also achieved, since lower environmental impacts as well as higher efficiency in the energy resource use are attained by the optimized operation of DESs, as compared with conventional energy supply systems. However, the capital investment costs of DESs are generally high as compared with conventional energy supply systems. Remaining issues, objects of study in future work, are related to the planning of DESs for their optimal design, where in the economic objective, also investment and operation and maintenance costs will be involved. As for the optimal operation planning problem, also for the optimal design problem, a multi-objective approach will be used to take into account both short- and long-run priorities.

In conclusion, in this thesis, emphasis is given to the necessity of a strong change in the energy supply structure to address energy-related worldwide problems as depletion of fossil fuels and growing environment protection awareness. If it is true that DESs have been recognized by research and demonstration projects as a powerful instrument to offer a new sustainability-oriented pathway, it is also true that the complex decision-making process related to their optimal planning needs to be guided to account for both short- and long-run priorities. The energy legislations need to be informed on how the optimal planning of DESs can ensure both economic, and environmental benefits as well as a more efficient energy resource use as compared with the conventional energy supply structure. This information could be transformed in incentives and policies to encourage the DESs development with consequent spread. Not only. Results found in this work also demonstrate that the key idea to optimize the operation of a DES through exergy assessments allows to enhance the efficiency in the energy resource use, thereby increasing the time span in which the limited energy resources can be used, and reducing the negative environmental impacts derived from their use. Thus, exergy, recognized in this work and in the scientific literature as a sustainability indicator, should be considered by planners as a crucial benchmark for planning of DESs.